Evaluation of Midwater Trawl Selectivity and its Influence on Acoustic-Based Fish Population Surveys

Kresimir Williams

A dissertation

submitted in partial fulfillment of the

requirements for the degree of

Doctor of Philosophy

University of Washington

2013

Reading Committee:

John K. Horne, Chair

Andre E. Punt

Christopher D. Wilson

Program Authorized to Offer Degree:

School of Aquatic and Fisheries Sciences

University of Washington

Abstract

Evaluation of midwater trawl selectivity and its influence on acoustic-based Fish population surveys

By

Kresimir Williams

Chair of the Supervisory Committee:

Professor Dr. John K. Horne

School of Aquatic and Fisheries Sciences

Trawls are used extensively during fisheries abundance surveys to derive estimates of fish density and, in the case of acoustic-based surveys, to identify acoustically sampled fish populations. However, trawls are selective in what fish they retain, resulting in biased estimates of density, species, and size compositions. Selectivity of the midwater trawl used in acoustic-based surveys of walleye pollock (*Theragra chalcogramma*) was evaluated using multiple methods. The effects of trawl selectivity on the acoustic-based survey abundance estimates and the stock assessment were evaluated for the Gulf of Alaska walleye pollock population. Selectivity was quantified using recapture, or pocket, nets attached to the outside of the trawl. Pocket net catches were modeled using a hierarchical Bayesian model to provide uncertainty in selectivity parameter estimates. Significant under-sampling of juvenile pollock by the midwater

trawl was found, with lengths at 50% retention ranging from 14 – 26 cm over three experiments. Escapement was found to be light dependent, with more fish escaping in dark conditions. Highest escapement rates were observed in the aft of the trawl near to the codend though the bottom panel of the trawl. The behavioral mechanisms involved in the process of herding and escapement were evaluated using stereo-cameras, a DIDSON high frequency imaging sonar, and pocket nets. Fish maintained greater distances from the trawl panel during daylight, suggesting trawl modifications such as increased visibility of netting materials may evoke stronger herding responses and increased retention of fish. Selectivity and catchability of pollock by the midwater trawl was also investigated using acoustic density as an independent estimate of fish abundance to compare with trawl catches. A modeling framework was developed to evaluate potential explanatory factors for selectivity and catchability. Selectivity estimates were dependent on which vessel was used for the survey, and the condition factor of the fish caught. Ambient water temperature, time of day, and the proportion of fish in spawning condition influenced model-derived estimates of catchability. Finally, the effect of trawl selectivity on the acoustic-based survey abundance estimate and Gulf of Alaska pollock assessment was evaluated. Survey biomass estimates were overestimated by up to 40 % as abundance of juvenile fish increased and adult abundance decreased. The increase in uncertainty in survey abundance estimates due to trawl selectivity had a measurable impact on the stock assessment, changing model estimates of fishing mortality, spawning biomass and recruitment by more than 10 %. The studies provide new methods for assessing selectivity, catchability and for observing fish behavior in midwater trawls, which can be used to evaluate midwater trawls used in other surveys.

TABLE OF CONTENTS

LIST OF FIGURES

LIST OF TABLES

ACKNOWLEDGEMENTS

Foremost, I am indebted to my family for their support and patience during the course of this work, during which my wife Vanessa and I welcomed our sons Adrian and Elliot into the world. These events that marked the start of our young family helped put things into proper perspective. I am very grateful to have had the benefit of a very supportive committee, headed by John Horne and including Chris Wilson and Andre Punt. They were all engaged in my research and eager to provide advice and to elevate the level of science by asking the hard questions. I would also like to thank my colleagues Rick Towler, Alex De Robertis, Craig Rose and David King for providing invaluable advice on matters ranging from trawl design to quantitative modeling. Finally, I'd like to thank Martin Dorn for guiding me though the pollock assessment model and for valuable discussions into the implementation of this work.

CHAPTER 1. USE OF TRAWLS AS SCIENTIFIC TOOLS: A GENERAL INTRODUCTION

Fisheries surveys are widely used to derive fishery-independent estimates of abundance for commercially important fish species. For many surveys, trawls are the primary tool used to sample fish populations. Trawl surveys compute fish density by standardizing trawl catch by effort to provide a time-series of catch-based abundance estimates. Surveys that use active acoustics to estimate fish abundance require trawl samples to identify the length and species composition of acoustically detected targets. Despite their extensive use in fisheries surveys, trawls are imperfect sampling tools. Trawls used in surveys are often slightly modified commercial trawls that are designed to most effectively capture larger, market-sized fish. Consequently, when used to sample fish during surveys, trawls can provide biased information due to selective retention of certain species or fish sizes. Despite these shortcomings, trawls are often the only available method for sampling fish populations. Trawl modifications for surveys can improve retention of smaller fish species and sizes. Even with these efforts, the accuracy and precision of trawl catch-based estimates of fish population density, size structure, and species composition have to be quantified to make trawls a valid scientific sampling device.

Acoustic fisheries surveys target pelagic and semi-pelagic fish stocks and primarily use midwater trawls to determine the species and size composition of acoustically detected fish aggregations. Midwater trawls were developed in Europe in the 1970's, evolving

from demersal, or bottom, trawls to target fish aggregations in the water column, such as engraulids, scombrids, clupeids, and pelagic gadoids (Valdemarsen 2001). The mesh openings at the forward end of pelagic trawls are generally much greater than the size of targeted fish. For example, the forward meshes of the Aleutian Wing Trawl (AWT) used by the Alaska Fisheries Science Center for sampling pollock, is 3.25 m (stretch mesh measurement). Trawl capture efficiency relies on herding behavioral, where fish are unwilling to pass through the mesh openings when other pathways are available (Glass and Wardle 1995). When herded, fish move away from the trawl sides and are toward the center of the trawl, and eventually are retained in the aft end of the trawl where they cannot escape. The effectiveness of herding by the trawl is likely to be species and size dependent, leading to selective retention of a subset of the fish that enter the trawl opening.

The objectives of this dissertation are to measure length selectivity of the midwater trawl, describe fish behavior during capture, establish the dependence of selectivity on environmental and other factors, and to evaluate the impact of selective sampling on acoustic survey abundance estimates and stock assessment of walleye pollock (*Theragra chacogramma*; hereafter referred to as pollock) in Alaskan waters. The North Pacific fishery for pollock is one of the world's largest single-species fisheries with reported landings in 2011 exceeding 1.2 million tons (NOAA 2012). The management plan for pollock includes annual acoustic-based abundance estimates carried out by the Nation Oceanic and Atmospheric Administration's (NOAA) Alaska Fisheries Science Center (AFSC). Abundance estimates from acoustic surveys provide a critical fishery-

independent index of size specific abundance to the stock assessment of Pollock in the Gulf of Alaska and the Bering Sea (Dorn *et al*. 2006).

Size and species-selective retention of fish in trawls has been researched extensively for demersal trawl surveys that use catch-per-unit-effort to measure fish density (Godo and Sunnana 1992; Godo and Walsh 1992; Lauth *et al.* 2004). Less is known about selectivity of midwater trawls used in acoustic surveys (Nakashima 1990; Bethke *et al.* 1999). When estimating selectivity of survey trawls, escapement of fish from the entire trawl must be considered (Dremierre *et al.* 1999). Midwater trawls are generally much larger than demersal trawls. For example, the surface area of the pollock midwater survey trawl is ~6000 m^2, compared to ~800 m^2 for the pollock demersal survey trawl. To estimate escapement from the midwater trawl body, a subset of escaping fish can be recaptured, and these samples scaled for the entire trawl surface area. Estimates of total escapement using this approach contain sampling error, which has to be propagated into the estimates of selectivity. In Chapter 2, trawl selectivity is estimated for the pollock midwater trawl by developing recapture devices, incorporating them into a randomized experimental design, and then analyzing the data using a hierarchical Bayesian model to derive selectivity parameters and their uncertainty.

When trawls are used as scientific sampling tools, it becomes critical to understand fish behavior in response to capture by the trawl. Trawl selectivity results from length dependent herding or escaping behaviors in the trawl. Behavioral responses of fish to trawl gear have been studied extensively for a wide variety of fishes (Wardle 1993, Albert *et al.* 2003, Piasente *et al*. 2004, Somerton 2004), including studies of pollock by *in situ* observation (Olla *et al.* 2000) and laboratory trails (Ryer and Olla 2000). Herding

responses result, in part, from the reluctance of fish to penetrate trawl netting even when the mesh openings are sufficiently large for escapement relative to the fish girth (Glass et al. 1993). Behavioral inhibition of passing through meshes is central to the design of the midwater trawl, but may elicit different responses among fish of different size. Chapter 3 investigates *in situ* behavioral responses of pollock during capture, using multiple instruments to gain a comprehensive understanding individual fish movement, position and orientation relative to the trawl.

A fundamental challenge in estimating how well trawl catches represent true fish population density and composition is the lack of independent data to compare to the trawl catch. In acoustic surveys, acoustic data can provide an independent estimate of density, given the assumptions made for converting acoustic backscatter to fish abundance. In Chapter 4, a model-based method for estimating selectivity is applied, combining historic trawl data and concurrent acoustic measurements taken during trawling. This approach allows trawl performance to be evaluated across a variety of environmental and trawling conditions which could influence fish behavior, such as water temperature and the time of day.

The investigation of survey trawl selectivity is part of an effort to understand and reduce acoustic survey observation error. When selectivity-biased catch is used to estimate acoustic-based fish abundance, backscatter from smaller fish that are insonfied but not fully retained by the trawl is erroneously attributed to larger fish that are more effectively retained. The focus of Chapter 5 is to investigate the effects of trawl selectivity on pollock acoustic survey abundance estimates and on the pollock stock assessment

population model that uses acoustic survey data as one index to evaluate of the state of the population.

This series of studies investigates many aspects of trawl sampling, including size selective retention, fish behavior, and influences on trawl performance. The investigative cycle is completed by establishing the relevance of biased trawl sampling to management of the resource. Establishing the accuracy of trawl catch data is an important contribution to improve our ability to assess fish population abundances, and quantifies trawl sampling error relative to other sources of uncertainty in fish surveys. By knowing how trawl catches misrepresent true density and composition of fish in the environment, the accuracy of scientific surveys can be increased, resulting in more effective management of exploited fish populations.

CHAPTER 2. LENGTH-SELECTIVE RETENTION OF WALLEYE POLLOCK, *THERAGRA CHALCOGRAMMA*, BY MIDWATER TRAWLS

2.1. INTRODUCTION

Walleye pollock (*Theragra chalcogramma,* pollock hereafter) stocks in waters off Alaska sustain the world's second largest single-species fishery by catch weight (FAO, 2009). Management of this fishery depends on regular fishery-independent acoustic surveys to estimate age-specific abundance (Karp and Walters, 1994). During these surveys, midwater trawls are used to identify the species and length compositions of acoustically detected fish aggregations. Catch data are then used to scale measurements of acoustic backscatter into abundance (e.g. Honkalehto *et al*., 2009).

It is assumed that catch compositions in trawls accurately represent the source of the backscattering measured by the vessel's acoustic instrumentation. However, all trawl gears are size selective to some degree (Wileman *et al.,* 1996), so that smaller individuals are typically not proportionally represented. This bias may become significant in situations where the insonified population contains a range of sizes. The pollock trawl catches commonly contain a large range of fish lengths (9 – 70 cm). Consequently, trawl gear selectivity is potentially an important source of error in pollock survey abundance estimates.

Trawl selectivity has different functions in commercial and research settings. For commercial fishing operations, it is desirable to minimize bycatch (non-targeted species or undersized target fish) by designing gear that is selective for market-sized individuals

of the target species (MacLennan, 1992). Research in trawl selectivity for commercial gear has focused on estimating escapement of unwanted fish from codends. In contrast, trawls used for stock assessment aim to minimize selectivity to ensure representative sampling of fish populations (Dremiere *et al*., 1999). Establishing the selectivity of research trawl gear requires estimates of escapement from the entire trawl gear, consisting of the trawl body and codend. Codend escapement can be measured directly by recapturing all escaping fish in a codend cover bag (e.g. Wileman *et al*., 1996). Estimating trawl body escapement poses technical challenges, especially for midwater trawls where the surface area of the trawl is very large. For example, a bottom trawl used in Alaskan trawl surveys has a surface area of ~ 550 m^2 compared to ~ 6 500 m^2 area of a midwater trawl.

Escapement of pollock from a midwater trawl was investigated by attaching small recapture bags on the outside of the trawl surface. Previous experiments with pocket nets have shown that fish caught in the pocket nets are smaller compared to those caught in the codend (Suuronen, *et al*., 1997; Nakashima, 1990). To estimate total escapement from the trawl body, pocket net catches have to be expanded to represent the entire trawl surface (Polet, 2000). Extrapolation of pocket net catches does not explicitly incorporate error due to random effects of sampling a small portion of the trawl area. Because of concerns regarding potential errors in scaling, Dremiere *et al*. (1999) used a more conservative approach by limiting expansions to portions of the trawl with similar escape rates, thereby underestimating total escapement. In this study, trawl selectivity was estimated using a modeling approach to incorporate additional uncertainty due to partial sampling of escapement. The model used a hierarchical Bayesian approach (HBA) to

incorporate additional uncertainty in selectivity due to haul-to-haul variability in selectivity.

In this study we introduce a new analytical approach for estimating selectivity, and apply this methodology to assess pollock acoustic survey trawl gear. We aim to outline methodological developments for research groups using similar trawl gear in a scientific setting, but also to provide insight on potential trawl-based error specific to the pollock management process.

2.2. MATERIALS AND METHODS

2.2.1. Midwater trawl characteristics

Pollock acoustic surveys conducted by the Alaskan Fisheries Science Center of the National Marine Fisheries Service use a four seam Aleutian wing trawl (AWT) with a ~ 90 m headrope, a smaller version of the commercial trawl commonly used in the pollock fishery. Trawl mesh sizes range from ~ 3 m (stretch measurement) at the trawl opening to 0.1 m in front of the codend. The codend in the research trawl is constructed of 0.1 m mesh and contains a 12 mm mesh liner assumed to retain all fish > 8 cm in length. The AWT has an approximate 25 m vertical and 35 m horizontal opening while fishing. The trawl diameter at the codend is approximately 1.5 m. Trawl length is ~ 140 m from the trawl opening to the end of the codend. Meshes larger than 0.1 m are constructed of white nylon twine, while the final section of 0.1 m meshes forward of the codend is constructed of orange polypropylene twine.

2.2.2. Fishing operations

Catch and related observations were collected from three sets of eight hauls, each taken within a 24 - 36 hour period during standard stock assessment surveys. Two sets were taken in Shelikof Strait, in the Gulf of Alaska by the NOAA ship "Miller Freeman" in March 2007 (GOA07) and the NOAA ship "Oscar Dyson" in March 2008 (GOA08). A third set was collected in the eastern Bering Sea by the "Oscar Dyson" in July 2007 (EBS07; Fig. 2.1). Locations for each set were selected to sample a wide range of pollock lengths. Acoustic netsondes attached at the headrope were used to monitor trawl performance when fishing. All sets were sampled using the same net with a target trawling speed of 3.5 knots. For each trawl, a Seabird SBE-39 depth and temperature logger and a Wildlife Computers MK-9 light level logger were attached to the trawl headrope. Measurements from the logger were converted to light intensity (μE m^{-2} s^{-1}) using the calibration equation from Kotwicki *et al*. (2009).

For each haul, twelve pocket nets were attached to the outside trawl mesh surface during deployment and removed after retrieval. A stratified-random design was used to determine attachment locations for the pocket nets to control for placement effect. The trawl was subdivided into four sections along its length, referred to as the Forward, Middle 1, Middle 2, and Aft sections. As the net was composed of four panels, each section was further subdivided into a bottom, top, and two side panels. Within each trawl partition, defined by a section and panel, 9 to 14 locations were uniformly distributed and marked for the attachment of pocket nets. Pocket net placement was determined by

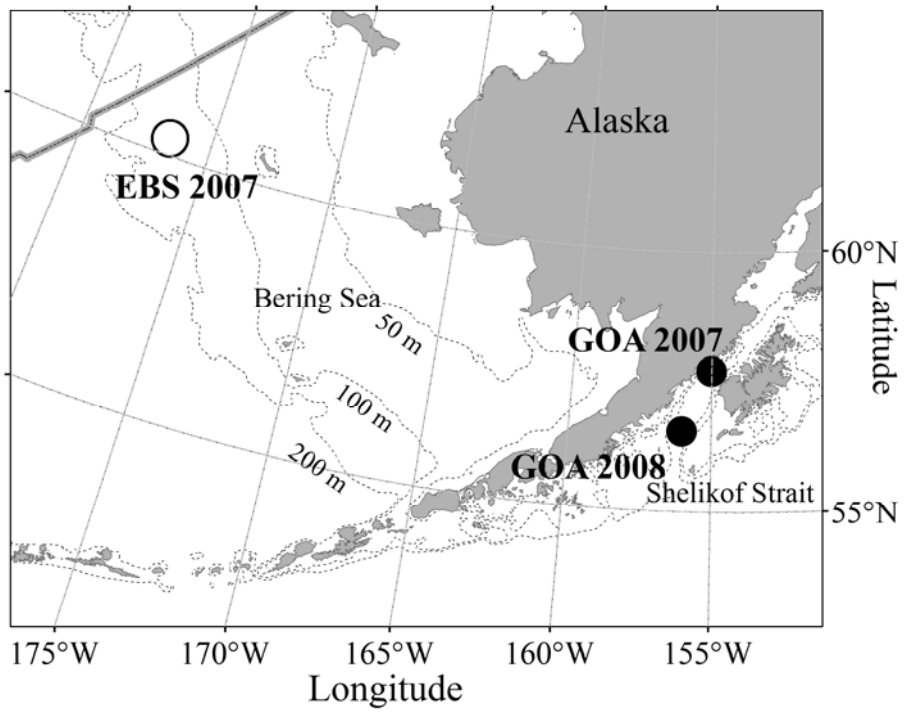

Figure 2.1. Location of midwater trawl selectivity trials. The two Gulf of Alaska (GOA) experimental sets were conducted during the Shelikof Strait acoustic pollock spawning survey during March, and the eastern Bering sea (EBS) set was collected during the EBS pollock summer survey during July.

randomly choosing an attachment point on a trawl partition. A single pocket net was attached to the top, bottom, and one of the side panels, resulting in three nets placed in each section. Pocket nets were attached to the trawl along trawl netting bars, forming a diamond-shaped opening. Two sizes of pocket nets were used; nine with an opening of ~ 2.88 m^2 were placed on the back three sections, and three with an opening of ~ 5.12 m^2 were used on the larger meshes of the forward section (Fig. 2.2). Pocket nets were constructed of ~1.9 cm stretch mesh monofilament netting and were ~ 5 m in length.

Codend catch and the contents of each pocket net were identified to species and weighed. Approximately 300 pollock were measured to the nearest centimeter from a sample taken from the codend catch. All fish caught in pocket nets were identified to species and measured, except for those from a single large catch, for which a random sample of 50 pollock was measured and scaled up for the entire catch using the weight fraction of the sample.

2.2.3. Pocket net model description

Individual haul model

Midwater trawl selectivity was estimated by modeling the pocket net and codend catches. A fish of length i entering the mouth of the net has a length-dependent probability S_i of being retained in the codend, modeled as a logistic selection curve parameterized in terms

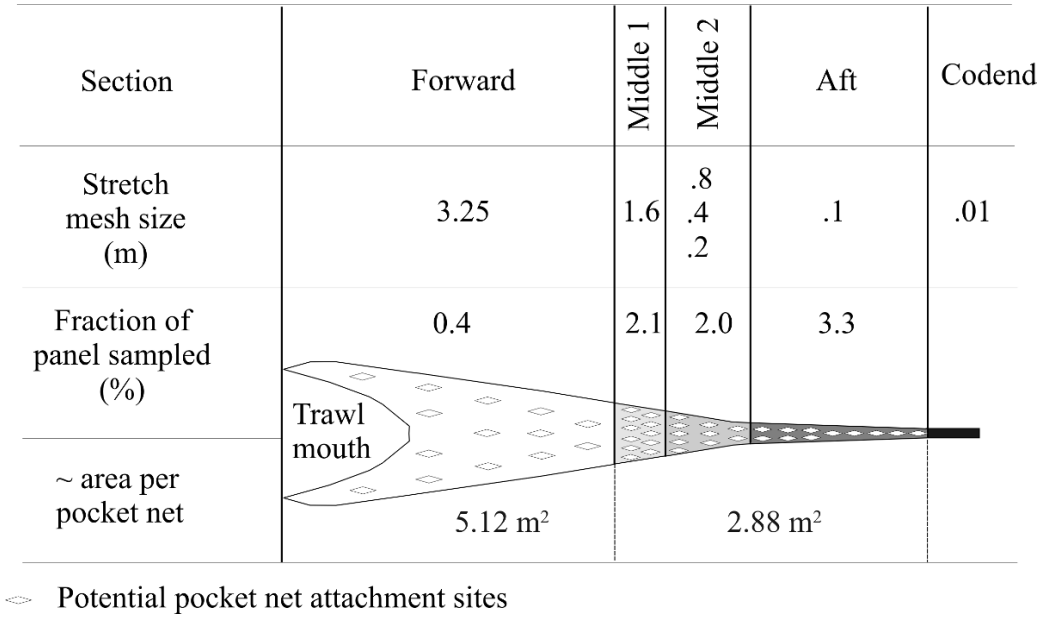

Figure 2.2. Experimental design used in midwater trawl selectivity trials. The figure represents one of four trawl panels (top, bottom, port and starboard sides). A single pocket net was attached to one randomly selected position on each section. The sampling fraction is the ratio of the number of meshes covered by the pocket net to the total meshes in each section/panel.

of the length at 50% retention (L_{50}) and the selection range (length in cm between 25% and 75% retention, *SR*):

$$S_i = \left(1 + e^{\left(\frac{k(L_{50} - i)}{SR} \right)} \right)^{-1} \tag{2.1}$$

where k = 2 log(3) (Millar, 1993). The complementary probability of escapement from the trawl before the codend is (1-S_i). Escaping fish could exit the trawl out of any of the four sections, expressed as a multinomial probability variable P_j, where *j* indicates the section. A fish exiting out of a given section *j* can escape out of the top, side or bottom panels of a section, resulting in an additional multinomial probability conditional of leaving section *j*, $R_{j,k}$, where *k* is the panel conditional on P_j. The total probability of a fish of length *i* being caught in the pocket net in section *j* panel *k* is:

$$H_{i,j,k} = (1 - S_i) P_j R_{j,k} Q_{j,k} \tag{2.2}$$

where $Q_{j,k}$ is the sampling fraction for the pocket nets located in section *j* and panel *k*, calculated as the ratio of the number of meshes covered by the pocket net to the total number of meshes in that trawl partition.

The escapement location parameters *P* and *R* were multinomial logit transformed for computational ease:

$$P_j = \begin{cases} \dfrac{e^{\pi_j}}{1+e^{\pi_1}+e^{\pi_2}+e^{\pi_3}} & for \;\; j = 1 \; to \; 3 \\ 1-(P_1+P_2+P_3) & for \;\; j = 4 \end{cases} \tag{2.3}$$

$$R_{j,k} = \begin{cases} \dfrac{e^{\rho_{j,k}}}{1+e^{\rho_{j,1}}+e^{\rho_{j,2}}} & for \; k = 1,2 \\ (1-[R_{j,1}+R_{j,2}])0.5 & for \; k = 3 \end{cases} \tag{2.4}$$

The estimated proportion of fish exiting from the side, $R_{j,3,}$ is multiplied by 0.5 because the pocket net was placed on one of the two side panels of the net. The probability of being captured in the codend and measured is:

$$h_i = S_i U \tag{2.5}$$

where U is the subsample fraction (sample weight / total catch weight) of the codend catch. While length data from catch samples are often extrapolated to the entire catch using the sampling fraction, using the unscaled measurements results in a more appropriate representation of the overall uncertainty in the model (Millar, 1994). For notational convenience, H and h are combined into a single matrix $F_{i,m}$ with columns m = 1 to 12 for each pocket net and column 13 for the codend retention probability for fish of length i.

Catches of fish by length, conditional on pocket net location, were assumed to be Poisson distributed, as this distribution has been routinely used to model length-dependent fish escapement in selectivity studies (Millar, 1992), and is appropriate for discrete count data. The likelihood function for a single haul is:

$$L(x \mid \theta, \mu) = \prod_i \prod_m \frac{(\mu_i F_{i,m})^{x_{i,m}} e^{-\mu_i F_{i,m}}}{x_{i,m}!} \tag{2.6}$$

where θ is the individual haul parameter vector $\theta = \{L_{50}, SR, \pi, \rho\}$, $x_{i,m}$ is the number of fish of length *i* measured in each pocket (m = 1 to 12) and the codend (m = 13), and μ_i is number of fish of length *i* entering the mouth of the trawl. This variable constitutes a "nuisance" parameter (not being of direct interest) when estimating selectivity, and was handled by marginalization, assuming uniform priors for the μ_i (Appendix A2.1). The negative logarithm of the resulting integral is:

$$-\log \hat{L}(x \mid \theta) \propto \sum_i \left(\sum_m \left[-x_{i,m} \log\{F_{i,m}\} \right] + \log\left[\sum_m F_{i,m} \right] \left[\sum_m x_{i,m} + 1 \right] \right) \tag{2.7}$$

Between-haul variation

Variation between hauls in a set was modeled using the HBA in which individual haul parameters and additional parameters describing the entire set are estimated simultaneously. Hierarchical Bayesian models specify prior distributions from which parameters for individual sampling units are drawn. Priors were applied to hauls within each set. Between-set variation was not modeled; each set was analyzed separately. Priors assigned to haul-specific parameters include $L_{50} \sim N\left(\mu_{L_{50}}, \tau_{L_{50}}\right)$, $SR \sim N\left(\mu_{SR}, \tau_{SR}\right)$, $P \sim \text{Dirichlet}(D)$, $R \sim \text{Dirichlet}(G)$.

L_{50} and *SR* were assumed to be normally distributed, based on independent haul analyses where samples of posterior parameter distributions approximated a normal distribution. Codend selectivity methods for estimating between-haul variation commonly assume normality for selectivity parameters (Fryer, 1991, Wileman *et al*., 1996). Variables *D* and *G* represent Dirichlet distribution parameters that describe escapement proportions in sections (*D*) and among panels within each section *j* (G_j) across all hauls in a set. One prior was applied to escapement among sections *P*, and four priors for escapement among panels in each section (i.e. $G_{1,1}$ is the Dirichlet distribution parameter associated with the proportion of fish escaping out of the top panel in the forward section across all hauls in a set).

Uniform hyper-priors were placed on the selectivity parameters $\mu_{L_{50}}$, $\tau_{L_{50}}$, and μ_{SR}, and Dirichlet escapement location parameters *D* and *G*, while a weakly informative scaled inverse-Chi distributed hyper-prior was placed on the prior τ_{SR}:

$$-\log P(\tau_{SR} \mid \nu_{\tau_{SR}}, \sigma_{\tau_{SR}}) = \frac{\nu_{\tau_{SR}} \sigma^2_{\tau_{SR}}}{2\tau_{SR}} + \left(1 + \frac{\nu_{\tau_{SR}}}{2}\right) \log \tau_{SR} \qquad (2.8)$$

This hyper-prior avoids degenerate solutions in which the maximum posterior density estimate is zero for all of the variance parameters. Values of the hyper-priors were set at $\nu_{\tau_{SR}} = 2$ and $\sigma_{\tau_{SR}} = 3$. Alternative hyper-prior values were explored, but they did not appear to influence posterior selectivity parameter distributions at values $\nu_{\tau_{SR}} > 1$ and $\sigma_{\tau_{SR}} > 1$.

The logarithm of the posterior distribution is proportional to:

$$\log P(\phi,\theta \mid data) \propto \sum_{h=1}^{n} \log L(data_h \mid \theta_h) + \log P(\theta \mid \phi) + \log P(\phi) \qquad (2.9)$$

where ϕ is the parameter vector for the priors $\phi = \{ \mu_{L_{50}}, \tau_{L_{50}}, \mu_{SR}, \tau_{SR}, D, G\}$ and n indicates the haul number within a set. An overview of model components is given in Table 2.1.

2.2.4. Light effect

The HBA assumes that parameter estimates from individual hauls have a common distribution (Gelman *et al*., 2003), and that individual haul observations are exchangeable. Exchangeability implies that the specific location or the order in which hauls were taken does not affect the outcome. This assumption may be inappropriate when factors contributing additional explanatory power to between-haul variance are known. Substantially more fish were caught in pocket nets during the four nighttime tows in the EBS07 set, indicating that hauls within the set may not be exchangeable due to the possibility of a light level effect on selectivity. To account for the potential effect of light on selectivity, an expanded model was fitted with an additional parameter to allow L_{50} to depend on the light intensity. Individual haul estimates of L_{50} were expressed as a log-linear function:

$$L_{50n} = Z_n + \lambda \log(L_n) \qquad (2.10)$$

where Z_n is the haul-specific intercept, λ is a slope parameter, and L_n is the light intensity (μE m^{-2} s^{-1}) for each haul n. In the HBA structure, $\mu_{L_{50}}$ and $\tau_{L_{50}}$ were replaced by μ_Z and

τ_Z. A uniform prior was assumed for λ. The base model (124 parameters; Table 2.1) was compared with the expanded light level model (125 parameters) using the deviance information criterion (DIC; see Appendix A2.2) to evaluate whether the inclusion of ambient light levels in the model was appropriate.

2.2.5. Analysis

Posterior distributions for model parameters were estimated using the MCMC (Markov chain Monte Carlo) algorithm implemented in the package Automatic Differentiation Model Builder (ADMB; Fournier, 2001). For each haul set, 10 million cycles were sampled, with every 2 000th sample retained to reduce the autocorrelation in the MCMC samples. The first 2 500 parameter vectors were then discarded as a "burn in" period, allowing the MCMC sampling algorithm to stabilize. Convergence of the MCMC algorithm was checked by visually inspecting trace plots (value of parameter plotted against ordered sample number) for each parameter and the objective function value (Equation 10), and by computing the Gelman-Rubin statistic from multiple MCMC chains initiated from different starting parameter values (Gelman and Rubin, 1992). The performance of the model was also verified using simulated data with known selectivity.

Posterior predictive distributions for selectivity parameters L_{50} and SR were constructed by taking a random sample from a normal distribution defined by hyper-parameters $\mu_{L_{50}}$, $\tau_{L_{50}}$, μ_{SR}, and τ_{SR}. This process was repeated for all MCMC posterior samples, yielding 2 500 values for L_{50} and SR for an "unknown haul" at each set location and year. For the

Table 2.1. A description of variables and parameters of the midwater trawl selectivity estimation model based on pocket net and codend catches.

Group	Name	Number	Description
Data	x		Observed catches in 12 pocket nets and sampled from the codend
Variables	μ		Number of fish at length entering the trawl mouth.
	H		Proportion of μ escaping through each pocket net
	h		Proportion of μ sampled in the codend
	Q		Panel sampling fraction (pocket net area/panel area)
	U		Codend sub-sampling fraction (weight of subsample/total species weight in haul)
	S		Selectivity – proportion of μ that is retained in the codend
Parameters (θ) - fitted	L_{50}	8	Length at 50 % retention (one parameter per haul in set)
	SR	8	Selection range, difference between the 25% and 75% length-at-retention, in cm
	π	3×8	Parameters used to derive the multinomial variable P (n sections (4) -1)
	ρ	8×8	Parameters used to derive the multinomial variable R
- calculated	P	4×8	Four-way proportional distribution of escapement by section
	R	(3 × 4)×8	Three way proportional distribution of escapement by panel, one per section
Hyper-parameters (φ) - fitted	$\mu_{L_{50}}$, $\tau_{L_{50}}$	2	Two parameters describing the underlying normal distribution from which individual trawl L_{50} belong
	μ_{SR}, τ_{SR}	2	Same as above for SR
	D	4	Four-way Dirichlet distribution parameter for escapement by section
	G	3 × 4	Four separate three-way Dirichlet distributions for escapement by panel, one for each section
Prior distribution parameters -specified	$\nu_{\tau SR}$, $\sigma_{\tau SR}$	1+1	Scaled inverse chi-square prior distribution for τ_{SR} set at $\nu_{\tau SR} = 2$, $\sigma_{\tau SR} = 3$
Total parameters			104 fitted base parameters (for set of eight hauls), 20 hyper-parameters, 4 priors

model including light level, predictive distributions for L_{50} were additionally dependent on light level. These were constructed by repeating the procedure described above for Z in Equation 2.10, and using the posterior sample of λ to generate L_{50} values. Predictive distributions were similarly constructed for the escapement location along the trawl by using the posterior distributions of the Dirichlet distribution parameters to generate realizations of escapement location parameters.

2.3. RESULTS

2.3.1. Haul collections

For inter haul consistency, an attempt was made to keep the fishing duration and gear depth as constant as possible (Table 2.2). However, these had to be varied if fish density dropped as observed on the ship echosounder or if fish aggregations changed depth. Fishing conditions were most constant during the GOA07 set, with little change in fishing duration and depth. Tow durations were longest and most variable in the EBS07 set due to variable fish density, typical of pollock aggregations in the EBS. The GOA08 set varied both in duration and fishing depth, as towing location and direction were altered to avoid commercial fishing traffic.

In the EBS07 set, light intensity at fishing depths ranged from 1.4×10^{-6} μE m^{-2} s^{-1} at night to 4.8×10^{-2} μE m^{-2} s^{-1} during the day. In contrast, average light intensity in the GOA sets was lower than night levels in the EBS (4.0×10^{-7} μE m^{-2} s^{-1}) and was less variable

Table 2.2. Haul conditions and catches during three haul sets taken to estimate midwater trawl selectivity of walleye pollock in the Gulf of Alaska and eastern Bering Sea. Columns 1-4 show means and standard deviations of eight hauls taken in each set, and columns 5 and 6 show catch ranges.

	Gear depth (m)	Haul Duration (min)	Gear temp. (^{o}C)	Light Level (μE m^{-2} s^{-1})	Codend pollock catch range (#)	Combined pocket net catch range (#)
GOA07	262 +/- 4	9.7 +/- 0.7	2.5 +/- 0.2	(4.3 +/- 2.0)×10^{-7}	1605 - 3728	12 - 88
EBS07	126 +/- 4	26.9 +/- 12.5	1.3 +/- 0	(1.6 +/- 2.1)×10^{-2}	1596 - 5072	12 - 325
GOA'08	235 +/- 12	18.9 +/- 7.8	4.5 +/- 0	(3.7 +/- 1.7)×10^{-7}	1639 - 7929	4 - 133

between hauls (CV = 0.45) compared with the EBS set (CV = 1.28). Lower light in the GOA sets was expected due to reduced sunlight in wintertime and greater fishing depths.

Pollock dominated the catch in the EBS07 set, contributing an average of 98.9% by weight. In the GOA sets, catches averaged 57.7% and 67.5% pollock by weight in 2007 and 2008, with an average 95% of the remaining catch comprised of eulachon (*Thaleichthys pacificus*).

2.3.2. Pocket net catch

Catches of pollock in the pocket nets ranged from 0 to 283 fish. The proportion of nets in each haul with no catch varied between 25% and 92 %. The species composition of the pocket net catches consisted primarily of pollock in the EBS (97.4% by weight). In contrast, the GOA sets contained on average 81.3% eulachon in 2007 and 60.9% in 2008 by weight. Length frequency of pollock caught in the pocket nets differed markedly from the codend (Fig. 2.3), consisting predominantly of age-1 (9 – 18 cm) and age-2 (19 - 28 cm) fish (age classification was based on otolith samples taken from previous surveys). Mean length of pollock caught in pocket nets and codend were significantly different (2-way ANOVA by haul, $p < 0.001$ across all sets). Substantial numbers of age-2 pollock were caught in pocket nets in the GOA07 set while the codend contained proportionally fewer age-1 fish compared to other sets. Pollock were captured in all four sections of the trawl in the GOA sets. In contrast, in the EBS07 set no escapement was observed from the two forward sections, and only one pollock was caught in the third

section. Mean pollock lengths from different sections in the GOA sets were not significantly different (Table 2.3), despite large differences in mesh size.

2.3.3. Modeling results

The fit of the model to the observed catches was explored by plotting mean differences between predicted and actual pocket net and codend catches (Fig. 2.4). Model predictions were based on samples from the posterior distributions for the parameters (Appendix A2.3). As expected, residual values were largest near the modes of the length frequencies from the pocket net catches (Fig. 2.3). Residuals showed higher spread for codend catches due to the larger number of fish caught. Model predictions differed from observations most in GOA07 catches of age-2 fish. Mean residuals for this age class were negative for pocket nets, implying that the model predicted more fish in the pocket nets than were observed. The reverse was observed in the model fit to the codend catch, with predicted numbers being less than observed catch. Model fits for the other two haul sets did not show strong length-dependent patterns, meaning the logistic selectivity functional form used in the model captured length-dependent behavior reasonably well.

Selectivity parameters

Posterior predictive distributions for the selectivity parameters L_{50} and SR for an "unknown" haul derived using the HBA represent within-and between-haul uncertainty. Since between-set variation was not included in the model, a comparison of set-level estimates of selectivity is qualitative. The posterior distributions of L_{50} varied between

Table 2.3. Two - way analysis of variance of mean walleye pollock lengths caught in pocket nets placed in four different sections of a midwater trawl. Hauls collected in the Gulf of Alaska (GOA) in 2007 and in 2008 were analyzed separately.

Set	Source	Sum Sq.	d.f.	Mean Sq.	F	Prob>F
GOA07	Sections (4)	85.2	3	28.4	1.71	0.209
	Hauls (8)	335.4	7	47.9	2.88	0.041
	Error	249.8	15	16.7		
	Total	709.6	25			
GOA08	Sections (4)	12.8	3	4.3	0.96	0.432
	Hauls (8)	28.2	7	4.0	0.91	0.520
	Error	84.1	19	4.4		
	Total	124.7	29			

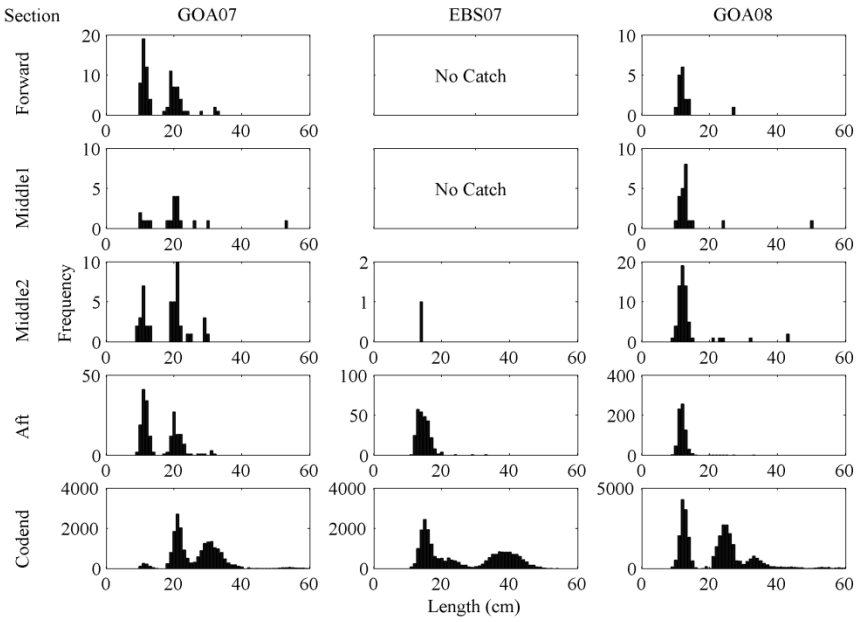

Figure 2.3. Length frequency of walleye pollock from three midwater trawl selectivity experimental sets. Catches in the pocket nets in each section and in the codend were pooled across eight hauls in each set.

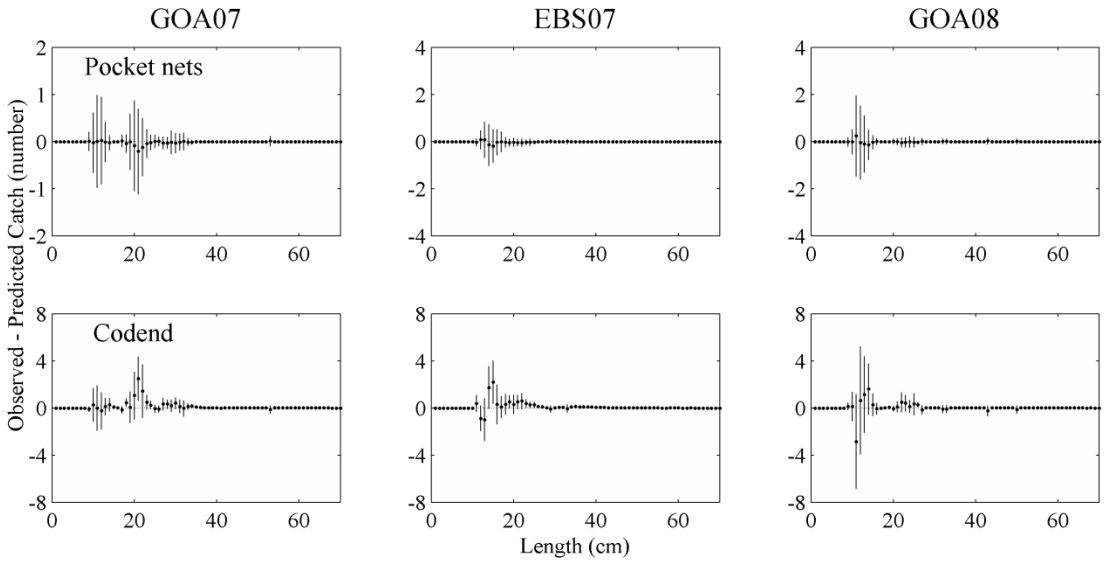

Figure 2.4. Model fits for pocket net catches. Points represent mean residuals between the data and model predicted catches computed by sampling of the posterior distributions of the parameters. The lines represent the standard deviation of the residuals at each length averaged across all hauls and pocket nets.

sets in both modal position and estimation uncertainty (Fig 2.5). The EBS set had the highest uncertainty in L_{50} and *SR* estimates resulting from the larger spread in the modes of the marginal posterior distributions of selectivity parameters for individual hauls. Less between-haul variation was observed within the GOA sets, although the maximum *a posteriori* estimates of L_{50} were different between the two sets (26.4 and 15.2 cm for 2007 and 2008, respectively). Posterior distributions for *SR* were similar between the two GOA sets, with GOA07 being more variable. Individual haul marginal distributions of L_{50} and *SR* show the effect of being "pulled" toward the global mean, as seen by the skew in the distributions furthest from the means of the predictive distributions.

Light effect

The inclusion of light as a covariate in the model for the EBS07 set resulted in a lower DIC value relative to the base model (Δ = 10 log likelihood units), indicating that light levels influenced trawl escapement rates in this experimental set. Figure 2.6 shows the log-linear relationship between selectivity and light level, along with the individual haul estimates of L_{50} plotted against mean light levels. Mean L50 estimates ranged from 10.8 to 20.7 cm between the highest and lowest light intensities encountered during the set.

Escapement distribution

Differences in escapement rates between trawl partitions were analyzed using the posterior predictive distributions (Figure 2.7) derived from hyper-parameters *D* and *G*.

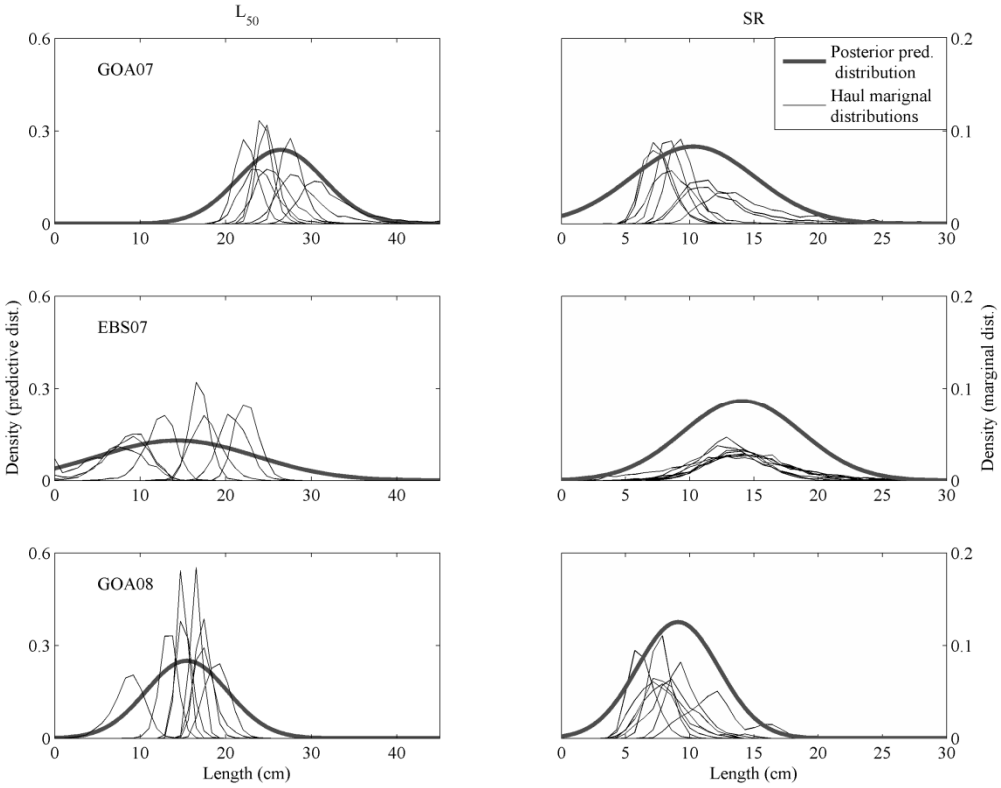

Figure 2.5. Posterior distributions of selectivity parameters. Three data sets were analyzed separately (shown in plot rows). Posterior distributions of L_{50} and SR for each individual haul in a set (n = 8) are shown in thin lines, and the posterior predictive distribution of L_{50} which incorporates within and between-haul variation of each parameter is shown with the thick gray line.

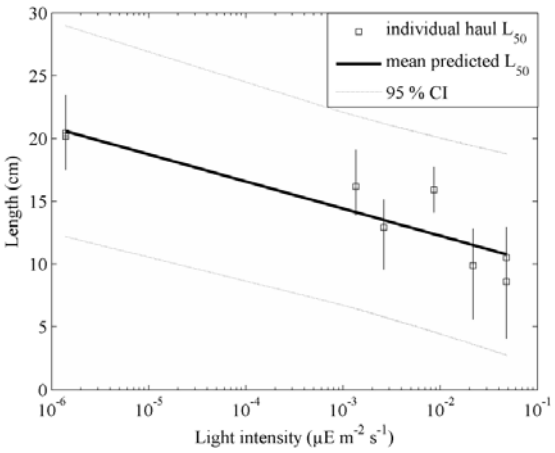

Figure 2.6. Haul estimates of L_{50} plotted as a function of ambient light levels. Points represent the median of the posterior distribution with the 10th and 90th posterior intervals indicated by error bars. The lines represent the mean and variance of the posterior predictive distribution of L_{50} at the given light level.

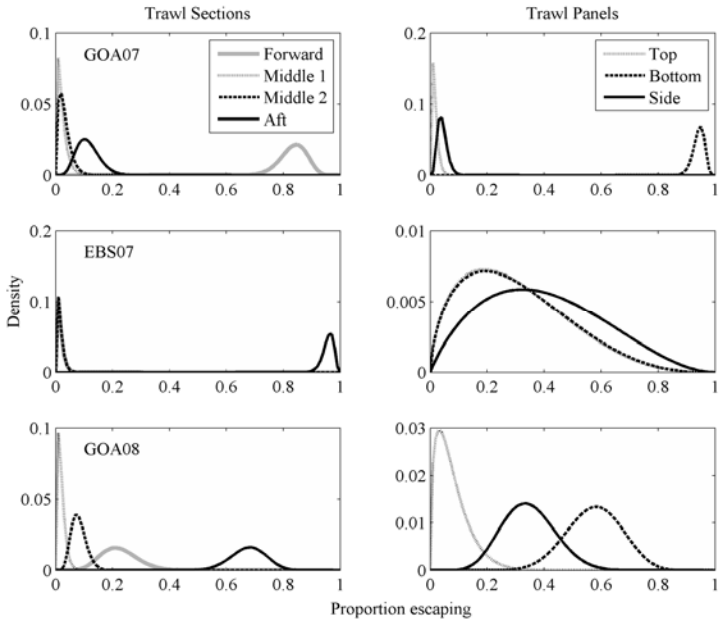

Figure 2.7. Posterior distributions for the proportion of the total escapement of walleye pollock from different areas of the trawl. Results are based on beta distribution fits to samples from the posterior distributions.

Panel escapement distributions were weighted by section escapement and averaged so that panels in sections where little escapement occurred did not disproportionately influence directional trends. The posterior predictive distributions followed patterns in the catch data (Fig. 2.3), providing additional information on variability among hauls in a set. Fish escaped predominantly from the forward section in the GOA07 sets (84.9%, maximum *a posteriori* estimate), and primarily out of the aft section in the other two sets (96.5% - EBS07, 68.2% - GOA 08'). The EBS set was unique in that fish escaped almost exclusively out of the aft section. Moderately narrow posterior predictive distributions show that patterns of escapement by section were consistent among hauls within the sets. Most fish were lost though the bottom panels in the GOA sets, while the direction of fish escapement was more variable in the EBS set, evenly divided among the top, side, and bottom panels.

Selection curves

Selection curves from the posterior distributions for L_{50} and SR are shown in Figure 2.8. Estimates of trawl selectivity were highly uncertain. Uncertainty was highest in the GOA07 set, where the posterior predictive distribution for the retention probability of a 26 cm fish was 0.03 (5^{th} percentile) and 0.96 (95^{th} percentile). Selectivity observed in EBS07 night catches represents an intermediate level between the two GOA sets. The GOA07 was distinct from the other two sets in that full retention (> 0.95%, median curve) was not achieved until a length of 46 cm, compared to 36 cm in EBS07 night samples and 28 cm in GOA08 samples.

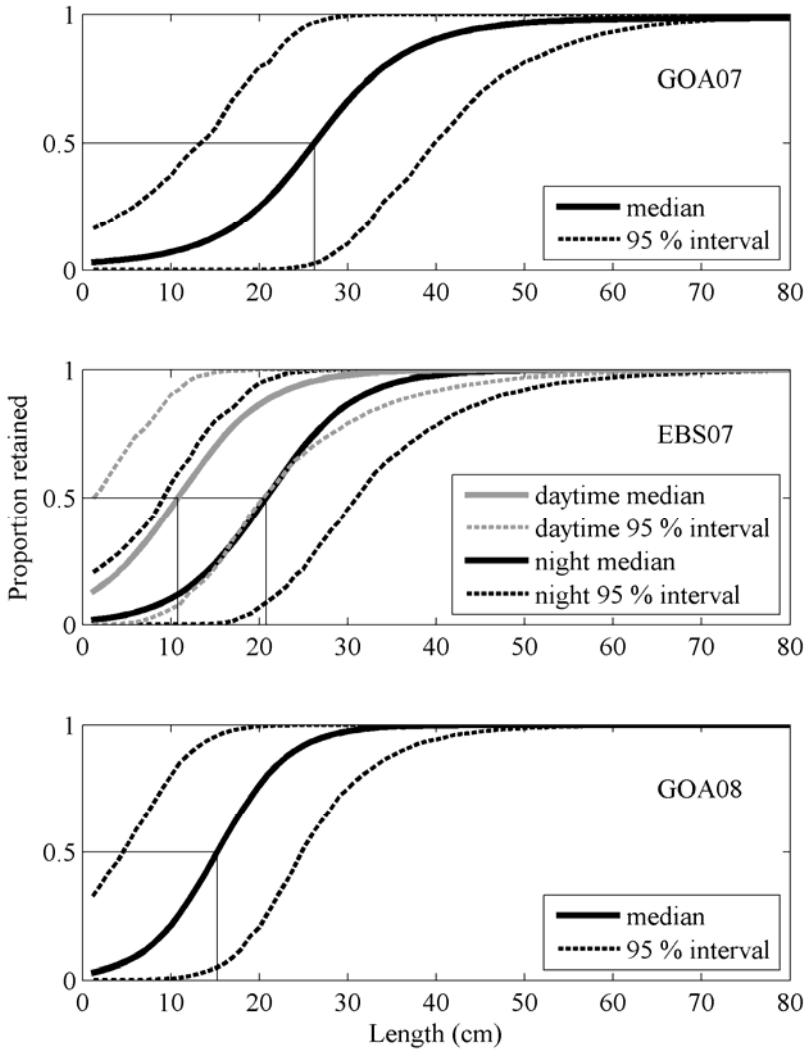

Figure 2.8. Selectivity (proportion of fish entering the net and being caught in the codend) estimates for three haul sets. The EBS set reflects estimates of selectivity at the minimum (night) and maximum (day) light levels observed during data collection. Credibility intervals are based on samples from the posterior distributions for the selectivity parameters.

2.4. DISCUSSION

Our results indicate substantial under sampling of juvenile pollock (< 25 cm) by the survey trawl used in pollock acoustic surveys. Length-dependent escapement varied substantially among the three sets, indicating that retention was influenced by factors not directly related to trawl gear design. Differences in selectivity between surveys (EBS, GOA) were not unexpected as environmental conditions varied. Seasonality has been shown to affect selectivity (Ozbilgin et. al., 2007) by influencing physiological factors such as swimming speed (Slotte et. al., 2007). Differences between the GOA sets were greater than differences among hauls within each set (Fig. 2.5), illustrating that selectivity can differ markedly from year to year within each survey. Higher estimates of L_{50} in GOA07 corresponded to a higher catch of age-2 pollock in the pocket nets, with the majority of escapement occurring out of the front section of the trawl. A closer look at the data suggests several potential causal mechanisms that could explain observed differences in selectivity. For example, age-2 pollock were larger (25.7 cm) in 2008 compared to 2007 (22.2 cm), and averaged 7.7 % greater mean weight per length. These differences indicate that age-2 pollock in 2008 had undergone more rapid growth and may have been in a better condition, which may have positively affected their ability to be herded by the trawl. In addition, a 2 ^{o}C higher gear-depth temperature was observed in 2008. Temperature has been shown to impact swimming ability in pollock (Arimoto *et al*., 1991), with an estimated 80% increase in maximum swimming speed of a 20 cm fish with a temperature increase from 2 to 5 ^{o}C, comparable to the respective temperature levels recorded in the two GOA sets (Table 2.2). Arimoto *et al*. (1991) suggested that changes in maximum swimming speed could increase the ability of pollock to avoid

entering the trawl. Swimming ability could also influence selectivity once fish enter a trawl. The results of this study show that higher temperatures were correlated with a higher retention of juveniles, suggesting that faster swimming may increase retention in midwater trawls by facilitating herding.

Two vessels with different underwater radiated noise signatures were used to sample pollock in the two GOA sets. Ambient noise can impact fish behavior (Popper, 2003) and vessel noise has been demonstrated to impact pollock behavior in some situations (De Robertis and Wilson, 2009). During the latter study, a stronger pollock diving response was observed in acoustic measurements from the older, noisier vessel ("Miller Freeman"), which was used to sample the GOA07 set. Escapement out of the front, bottom portion of the trawl is consistent with a rapid downward movement of fish following the passage of a vessel.

Escapement in other sets conducted with the noise-reduced vessel ("Oscar Dyson") increased with proximity to the codend. This pattern was also observed in midwater trawls fishing capelin (Nakashima, 1990) and in bottom trawls fishing pollock (Matsushita *et al*., 1993). Increased escapement is thought to be linked to increasing fish density within the trawl near the codend. Little or no escapement out of the large forward meshes implies juvenile fish were effectively herded by the front sections of the trawl, even in low light conditions during the GOA08 set or the EBS set night tows. It also suggests that escapement is an active process, as the expectation under passive escapement would be equal escapement over the entire trawl surface, possibly depending on the angle of attack of the mesh.

Fish capture by trawls involves a balance of visual and auditory stimuli (Glass and Wardle, 1989; Engas and Ona, 1990), although vision is thought to be the dominant modality once fish are in the trawl (Wardle, 1993). The effect of light on pollock escapement observed in the EBS further supports the significance of vision during trawl capture. Retention of juvenile pollock by the trawl was positively correlated with ambient light, suggesting that fish escape, in part, because of a failure to detect the trawl netting. Suuronen *et al*. (1997) reported that herring did not escape though trawl body netting during daylight hours, possibly due to stronger herding effects.

Increased total escapement in low light is consistent with several studies on pollock visual behavior. Ryer and Olla (2000) found that juvenile pollock in the laboratory tended to swim closer to and make contact with net panels more frequently at lower light levels. Similarly, Olla *et al*. (1997) reported light levels required for 50% of juvenile pollock to actively swim within a simulated net were 2×10^{-3} μE m^{-2} s^{-1}, a level which separates the night tows from those taken during the day and dusk period in the EBS set (night mean = 1.4×10^{-6} μE m^{-2} s^{-1}, day/transitional mean = 2.2×10^{-2} μE m^{-2} s^{-1}).

Larger fish did not appear in pocket nets regardless of ambient light levels. While no data are available on length-dependent pollock visual thresholds, estimates of pollock length-dependent resolving ability based on eye morphology (Zhang & Arimoto 1993) show that adult pollock (40 cm) have relatively greater sighting distances than juveniles (15 cm). Adults were able to resolve 2 cm diameter netting twine at a distance of 8 m compared with 4 m for juveniles under adequate lighting. It is also possible that non-visual herding may be more important in adults than in juveniles, resulting in effective herding

regardless of ambient light levels. Field observations of adult pollock behavior in trawls by Olla *et al*. (2000) showed that orientation was much more variable under low light (6×10^{-4} μE m^{-2} s^{-1}), and that swimming appeared to be reduced, suggesting that fish may be more likely to strike the net (Glass and Wardle, 1989). Fish reactions after striking the net may result in either retention or escapement, and if the distribution of these reactions is length-dependent with larger fish having a greater probability of being retained, it would provide a non-visual mechanism to explain observed selectivity patterns. Resolving whether escapement though meshes of the midwater trawl body results from a passive failure to herd or by an active directed movement though the meshes will require direct observations of the escapement process using acoustic or optical instruments.

Pocket nets were shown to be a viable method to empirically assess trawl body escapement, despite only covering small areas of the trawl. In an analysis using simulated data, the maximum *a posteriori* estimates of the posterior predictive distributions for selectivity parameters did not vary substantially from those used to generate data until the sampling ratio of the pocket nets (pocket net mouth area / trawl panel area) was reduced below 0.1%. The pocket net coverage in this study averaged ~0.83%. While simulation results cannot fully replicate field conditions and other influences on retention, this result indicates that while increasing the number of pocket nets would potentially reduce uncertainty, an increase is unlikely to improve mean selectivity estimates.

This study provides insight into appropriate sampling efforts for determining between-haul variance. Results from the EBS set showed higher between-haul variability relative to the GOA sets, linked to changing light conditions within the set. In the EBS case,

increasing the number of hauls sampled might have further reduced uncertainty when covariates such as light were added to the model. In the GOA sets haul-to-haul variation was substantially lower, suggesting uncertainty may not be greatly improved by increasing the number of hauls taken. This study sought to validate the pocket net method in determining trawl selectivity, as well as to provide specific estimates of selectivity for pollock surveys. To evaluate the method, it was desirable to collect hauls under as similar conditions as possible, thus allowing an assessment of variability inherent in pocket net sampling of escapement. A more dispersed sampling effort with fewer hauls in more locations would broaden inferences that can be made regarding the entire survey area, and would likely result in much higher variance.

The HBA approach provided a straightforward method to assess uncertainty in selectivity estimates across multiple haul samples. HBA achieves a balance between pooling data within sets and making independent estimates for each haul (Gelman el al., 2003). Bayesian methods, and specifically HBA, have been successfully applied in fisheries stock assessment modeling and meta-analyses (e.g. Harley and Myers, 2001). Although the need to incorporate variance across multiple sampling units is commonly encountered in fisheries gear research, few applications exist in the literature (Askey *et al*., 2007). The HBA methodology provides a straightforward framework for many problems in fishing gear research. MCMC-based analyses can be computationally demanding, but improvements in computer processing power and availability of software have expanded the applicability of these methods to a wider research community.

The impact of biased trawl catches on the accuracy of acoustic abundance estimates depends on several factors. Acoustic surveys where adult and juvenile fish commonly

co-occur in trawl catches will be more affected by selectivity-induced biases, because catch-derived length frequency estimates will be less representative of the sampled population than cases where the sampled fish population is more uniform. In situations where fish aggregate by size, even significant trawl selectivity may not greatly influence abundance estimation, because the estimate of the length distribution from the catch will be representative of the population. Even with substantial under-retention of juvenile fish, acoustic-based abundance estimates are strongly affected because they depend on strength of acoustic returns rather than on catch-per-unit-effort. In mixed size populations, the expected effect of selectivity-induced error on abundance-at-age estimates will underestimate juvenile abundance and, to a lesser degree, overestimate adult abundance, as a portion of the backscatter from juveniles would be erroneously attributed to adult fish.

This study presented a new method of estimating selectivity of midwater trawls and its uncertainty. A greater difference was observed between sets, rather than within sets, suggesting that fish retention by the trawl was dependent on environmental factors present at the locations and times where the samples were collected, or perhaps features of fish populations themselves. Despite relatively high uncertainty in selectivity estimates, significant under-sampling of juveniles was found, potentially resulting in biased survey abundance estimates.

CHAPTER 3. WALLEYE POLLOCK (*THERAGRA CHALCOGRAMMA*) BEHAVIOR IN MIDWATER TRAWLS

3.1. INTRODUCTION

Trawls are selective in what sizes and species of fish they retain. When trawls are used as sampling tools during fisheries abundance surveys, selectivity is a source of error, as the catch is not representative of the size and species composition in the environment. In acoustic-trawl fisheries abundance surveys, midwater trawls are used to identify the length and species composition of acoustically detected fish aggregations (Simmonds and Maclennan, 2005). Selectivity-induced sampling error in both species and length composition can bias abundance estimates and misrepresent the length composition of fished populations, which negatively affect fisheries management efforts (Godo et al., 1998). Consequently, it is important to understand fish behavioral mechanisms that cause selective retention in trawls, and how these behaviors may be influenced to improve both bycatch reduction and survey accuracy.

Trawls exploit fish behavior by utilizing predator avoidance responses (Ryer, 2008) to herd fish into the trawl opening (Wardle, 1993). Midwater trawls differ from demersal trawls in that the trawl mouth opening is typically larger, often 10's of meters in both vertical and horizontal dimensions. After entering the trawl mouth, fish are continually herded as they pass through the trawl towards the codend, effectively capturing fish which occur in low densities in the water column. Mesh sizes in the forward portion of a midwater trawl greatly exceed fish size. Retention in this portion of the trawl exploits

avoidance behavior and the reluctance of fish to pass through open meshes (Valdemarsen, 2001; Glass et. al. 1993). Mesh sizes are gradually reduced and fish are retained in latter portions of the net by preventing fish from physically passing through the mesh.

Herding behavior is critical to the efficiency of midwater trawls, and is likely to be size-dependent due to the reduced sensory and swimming abilities of juvenile fish relative to adults (e.g. Arimoto et al., 1991; Zhang and Arimoto, 1993). Size-dependent herding ability may be the primary factor linking fish behavior and net selectivity. Despite its importance, stimuli that control fish herding and resulting behavior responses are not well understood for midwater trawls. In this study, herding behavior exhibited by walleye pollock (*Theragra chalcogramma* hereafter pollock) is examined in a midwater trawl used to sample fish during an acoustic trawl abundance survey. A more complete view of fish behavior is achieved by combining sampling with measurements from optical and acoustic instruments. The results provide a quantitative measure of behavioral patterns underlying trawl selectivity for pollock, which can be applied to other pelagic or semi-demersal species and future trawl development for fisheries surveys and commercial applications.

3.2. MATERIALS AND METHODS

This study simultaneously deployed recapture nets, termed pocket nets, a still-image stereo-camera system, and imaging sonar (dual-frequency identification sonar,

DIDSON). Data were analyzed using a diversity of techniques to provide different insight into fish behavior in a midwater trawl.

3.2.1. Data collection

Pollock behavior observations were collected from six trawls taken July 2007 in the Eastern Bering Sea aboard the NOAA fisheries RV Oscar Dyson. Hauls were made using an Aleutian wing trawl (AWT; Fig. 3.1), which is a scaled-down version of a commercial pollock midwater trawl with a 1.3 cm liner placed in the codend. When fishing, the AWT has a vertical opening of 25 m, a horizontal opening of 35 m, and spans ~ 160 m from the wings to the codend. The trawl was instrumented with a net sounder (FS70, Simrad), a depth and temperature logger (SBE 39, Sea-bird electronics), and a light meter (mk9 archival tag, Wildlife Computers). Each trawl catch was sorted to species and approximately 300 pollock from the codend were measured for fork length to the nearest cm.

3.2.2. Pocket nets

Fish escapement from the AWT was quantified using pocket nets mounted to the outside of the trawl. Previous experiments (Chapter 2) in the EBS found that the majority of escapement occurred in the aft quarter of the trawl. To explore escapement behavior at higher resolution, pocket nets were arranged only over the aft section where escapement was expected to be highest. A total of 12 pocket nets were attached to the trawl on all 4

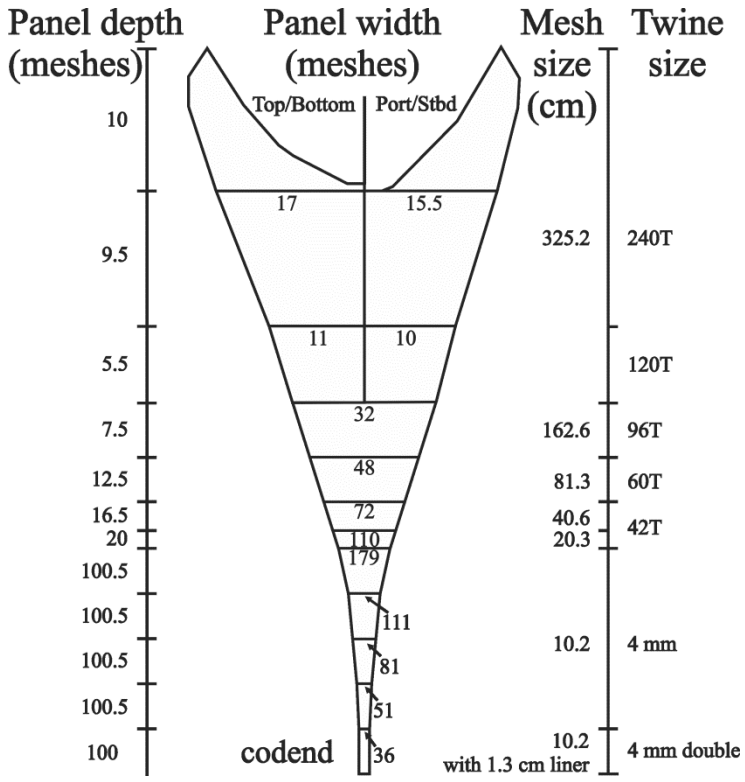

Figure 3.1. Aleutian Wing Trawl (AWT) design. The AWT is used during acoustic surveys of walleye pollock to sample fish aggregations. Net panels with mesh size >10.2 cm are constructed with nylon twine, and 10.2 cm mesh panel is constructed with polyethylene twine.

trawl panels (top, bottom, and sides) in 3 locations along the trawl axis, with each pocket net covering approximately 4 m^2 area of the trawl surface during fishing (Fig. 3.2). The pocket nets were not detached from the trawl between hauls; only the individual pocket net catches were removed and processed. The pocket nets were constructed of 19 mm stretch mesh clear monofilament gill net material, providing low visibility and drag making it less likely that fish may avoid the pocket nets. The results of the catch were compared using a Three-way ANOVA, with pocket net samples grouped by day vs. night, trawl section, and trawl panels.

3.2.3. Stereo-camera

System description

The stereo-camera system consisted of two Canon Digital Rebel XT digital cameras and a strobe fitted in underwater housings (Fig. 3.3 A,B). Attached to the cameras were Cannon EF 20 mm lenses providing a 24 by 36 degree view after passing through the planar viewports in the housings. The housings were fixed to a sled and calibrated (see below for description) before data collection. Images were downloaded after each deployment without removing the cameras from the housings to ensure that inter-camera geometry remained fixed during data collection. A microcontroller was used to simultaneously trigger both cameras and strobe at 5 sec intervals. The camera system was also equipped with a pressure switch, which turned on the system after a depth of 20 m was reached.

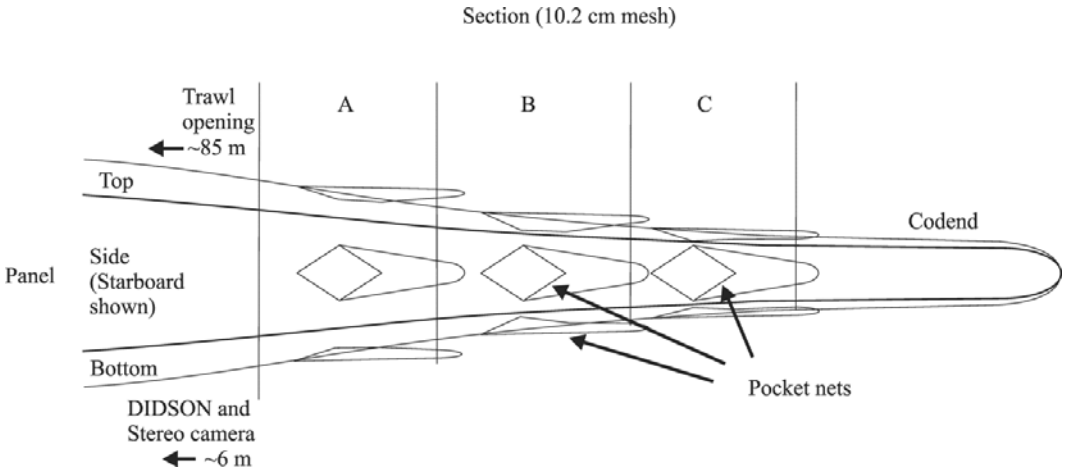

Figure 3.2. Pocket net placement used in the study of pollock behavior in AWT.

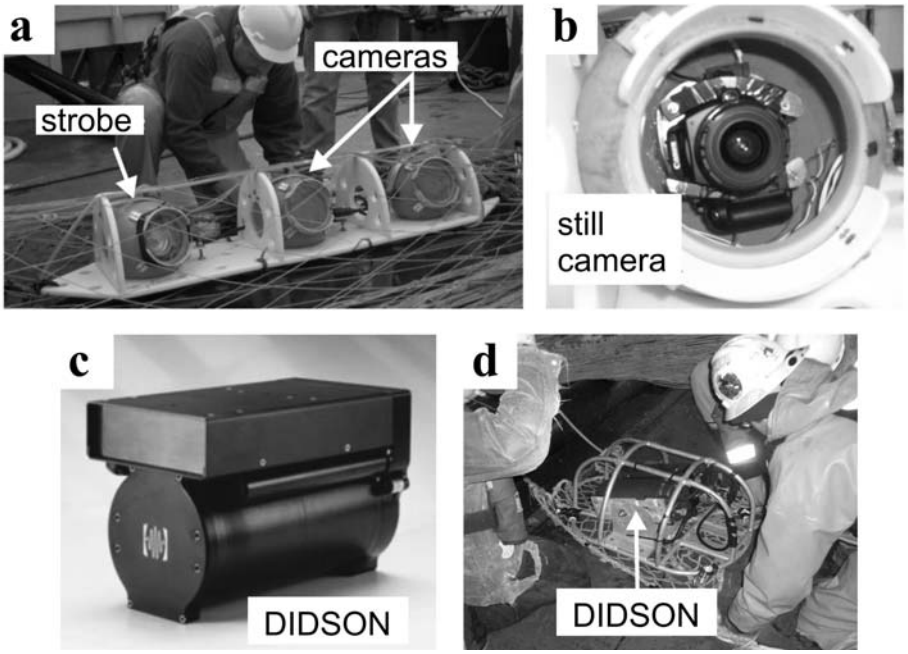

Figure 3.3. Stereo-camera system and the Dual frequency identification sonar (DIDSON) used to assess pollock behavior in a midwater trawl. Upper panels show the attachment of the cameras in the midwater trawl (a), and the individual digital still camera unit in its housing (b). Lower panels show the DIDSON unit(c) and the mounting approach into the trawl(d).

Stereo camera calibration

The cameras were calibrated in a 3 m circular tank prior to data collection. Underwater images from a variety of angles and ranges were taken of one side of a target plate with a printed 10 × 10 square checkerboard pattern, with each square measuring 100 mm. Approximately 20 paired images where the target checkerboard was visible in both cameras were selected for analysis. Calibration parameters were estimated using calibration software written for Matlab software (Mathworks, Inc.; Bouget, 2008). For each image pair, the position of corner points of the checkerboard pattern were identified by clicking on the images. The checkerboard pattern allowed the software to automatically pinpoint exact corner locations based on the contrast of the square boundaries, making the precision of the initial manual corner selection less critical. The calibration software then used the relative location of these points to determine the intrinsic parameters for each camera. Intrinsic parameters were used to correct individual images for optical distortion resulting from the camera lenses (Bouget, 2008). The checkerboard corners had to be identified in the same order in each of the synchronous image pairs to correctly match up analogous points. These points, once corrected for optical distortion in individual cameras, were then used to compute the epipolar geometry, which consisted of iteratively solving for the translation and rotation vectors that describe the relationship between the coordinate systems of the two cameras (Xu and Zhang, 1996). Once these matrices were estimated by the software, the three-dimensional position of a point viewed in both cameras could be determined using a triangulation function supplied by the camera calibration toolbox.

Image data collection

During deployment, images were taken at five second intervals to insure adequate re-sampling of individual fish and to minimize effects of the strobe flash. The sled was fastened inside the trawl at the 40 cm mesh section (Fig. 3.4), with the cameras facing across the trawl, orthogonal to the main trawl axis. The cameras were aimed at the bottom panel to overlap with the area insonified by an imaging sonar (dual-frequency identification sonar DIDSON, Sound metrics) that was also deployed in the net.

Stereo-camera analysis

Fish length measurements were obtained by identifying the coordinates of corresponding pixel locations in the left and right camera still frames of a fish's snout and tail (Fig. 3.5), which were then used to solve for the three-dimensional coordinates. Once the three-dimensional coordinates of the snout and tail were obtained, total length was estimated by computing the Euclidian distance between the points in Cartesian space:

$$l = \sqrt{(x_s - x_t)^2 + (y_s - y_t)^2 + (z_s - z_t)^2} \tag{3.1}$$

where x, y, and z are the real space coordinates for the snout and tail. This measurement method underestimates the length of any fish whose body is curved. In the current study, few fish were observed in a curved posture, and those individuals were not measured. Image processing analysis is illustrated in Figure 3.6. The three-dimensional coordinates

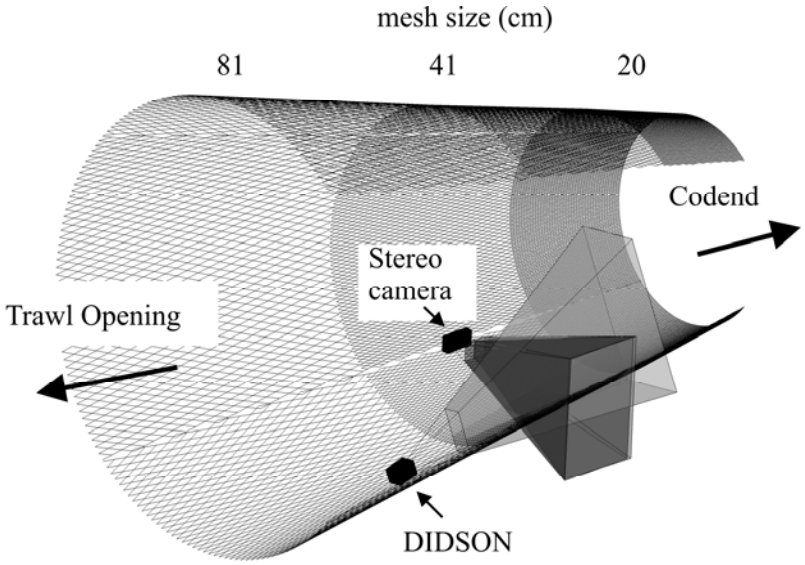

Figure 3.4. The placement of the stereo-camera and DIDSON imaging sonar within a midwater trawl to observe walleye pollock behavior.

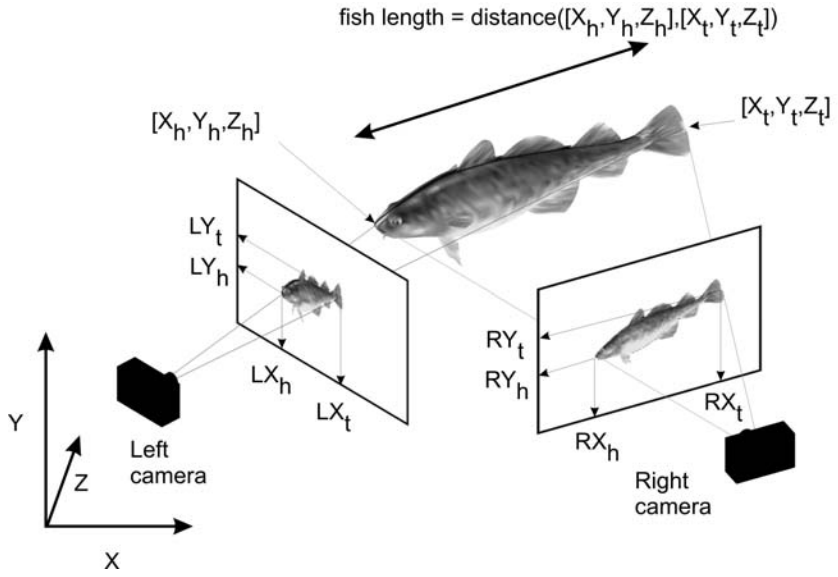

Figure 3.5. Method for determining fish length measurements using stereo images. The three-dimensional coordinates of the fish head and tail (X_h,Y_h,Z_h; X_t,Y_t,Z_t) are determined by stereo-triangulation using the image-based coordinates from the image pairs (i.e., LX_h,LY_h; RX_h,RY_h). Fish length is estimated as the Euclidian distance between the three-dimensional points of the head and tail.

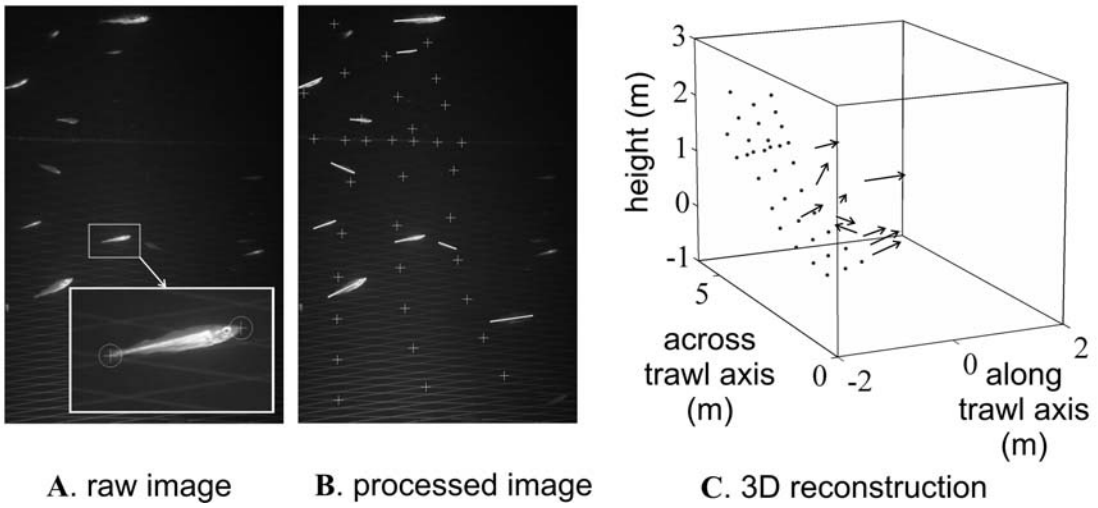

Figure 3.6. Stereo processing of still-frame stereo-camera images of walleye pollock (*Theragra chalcogramma*) in a midwater trawl. (A) Fish lengths were measured by enlarging the image of a fish and selecting the pixel coordinates (shown as circles) associated with the snout and tail in both right and left raw images (only the left image is shown above). (B) The chosen fish endpoints are overlaid on the image as lines. In addition to estimates of fish length, stereo-processing allows the position of fish relative to the trawl to be estimated. Additional points in the images can be determined by finding corresponding left-right image pixel coordinates (B, shown as crosses). (C) Following stereo-triangulation, a three-dimensional plot shows the fish targets as arrows and trawl mesh knots as dots.

extracted from the still-frame images also provided data on the position and orientation of walleye pollock relative to the trawl by calculating distances of pollock targets to trawl components and fish tilt (i.e. deviation of snout-tail axis from horizontal) and yaw (i.e. fish heading in the horizontal plane) angles.

3.2.4. DIDSON

System description

The DIDSON a produces an "image" by combining backscatter from an array of 96 beams, with equivalent beam angles of 0.3^{o} by 12^{o} each. This array of beams is assembled into a sector along the narrow dimension of the beams to constitute a 29^{o} X 12^{o} field of view. The data are structured in a polar coordinate system, where the location of each cell is defined by its beam identity (i.e. angle deviation relative to the central axis of the transducer) and the range along that beam. The range is sub-sampled into 256 equal range bins, resulting in a frame resolution of 96 X 256. Because the beams are arranged in a line, fish movement in the axis orthogonal to the multi-beam "fan" is undetectable. The backscatter display provides the illusion of three dimensions when viewed, due to its high resolution and the effect of shadowing. This feature can aid in gross identification of fish, but cannot be used when tracking individual animals, limiting the analysis to two dimensions.

Trawl deployments

The DIDSON was mounted to the outside of the trawl bottom panel facing aft with the narrow dimension of beam oriented vertically. This orientation enabled the interaction between fish targets and the bottom trawl panel to be observed (Fig. 3.7 A). The system was set up to record data to an internal hard disk, with power provided by a separate battery housing. The DIDSON was placed on the trawl at the panel with 40 cm meshes. Observations were collected at a frequency of 1.8 MHz, a sample rate of 8 frames sec^{-1} and the range set from 3 to 11 meters.

Data Analysis

DIDSON observation data were used to estimate fish movement by tracking the trajectories of individual fish targets (Fig. 3.7 B). Tracking was accomplished using a tracking application described in Handegard and Williams (2008). Before the tracking algorithm was applied, data was pre-processed to remove the trawl panel using a background subtraction based on a moving average of 40 frames. The tracking algorithm associates individual targets into tracks by predicting future target positions based on past target velocities. The resulting tracks, consisting of associated individual target positions across frames, were then smoothed using spline fitting to reduce errors due to target position estimation. Target positions from the smoothed tracks were normalized relative to the estimate of the trawl panel location from each data frame. An estimate of the angle of the trawl mesh relative to the central axis of the trawl (i.e. the narrowing angle) was 10.8^{o} based on a computer model of the trawl geometry. Track data were rotated by this

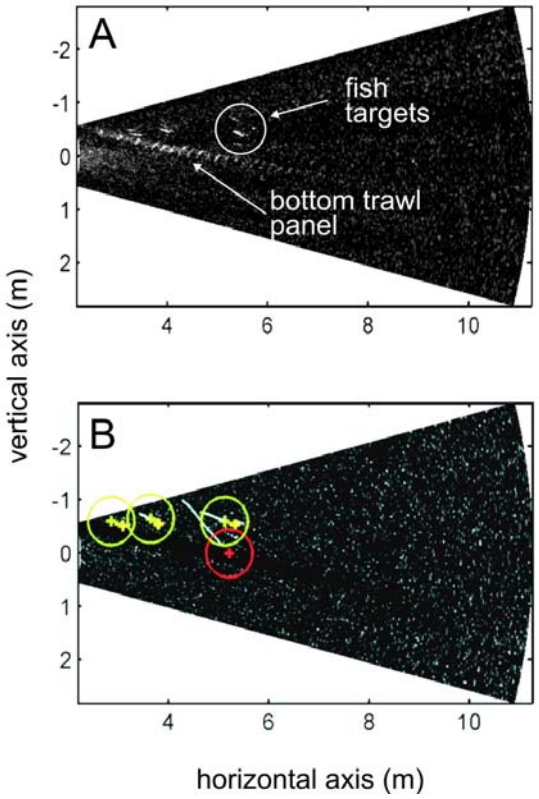

Figure 3.7. Walleye pollock observation in a midwater trawl using a dual-frequency identification sonar (DIDSON). The image represents a single acoustic ping, showing the trawl panel and individual fish targets.

angle so that a heading of 0^o indicated a trajectory parallel to the main trawl axis toward the codend and 90 indicates upward vertical movement orthogonal to the main trawl axis.

For each target detection along a track, the velocity was estimated by taking a derivative of the fitted spline function at each time-step along a track. The velocity vectors were decomposed into polar equivalents, resulting in a target direction *d* and range *r* for each tracked target and frame. Target speed *s* was simply calculated as the change in range between time steps divided by the time step interval (1/8 sec). These velocity values were then averaged by track to represent mean target direction ($\bar{d}$) and mean target speed ($\bar{s}$). For targets that passed through the trawl panel, only the portion of the track within the net was averaged, as the behavior of fish outside of the trawl was not of primary interest. Only tracks consisting of four or more target detections were used for this analysis. The change in direction Δd from previous time-step was computed as:

$$\Delta d = d_{t+1} - d_t \tag{3.2}$$

and averaged by track ($\Delta\bar{d}$), which was used as an indication of how often the fish changed its trajectory while being observed. Water velocity was not subtracted from trajectory speed, so these values do not represent actual swimming speed of the fish. Tracks were classified into three response categories based on their final trajectories, which were determined by averaging the target detection *d* for the last three detections in the track (Fig. 3.8). Targets passing through the panel were classified as escaping while targets whose final trajectory indicated they would not come in contact with the trawl netting were classed as herding. Targets that were not observed to have escaped, but whose trajectory indicated they would encounter the trawl panel were categorized as

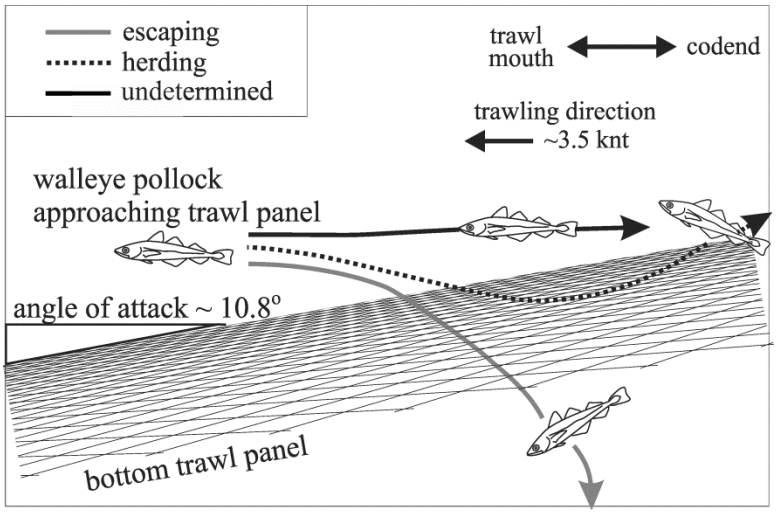

Figure 3.8. Classification of DIDSON tracks into three response types. Fish classed as escaping have been observed to pass though the trawl panel, herding fish have a last trajectory greater than the angle of attack, and undetermined targets are not observed to react to the panel during the observation period.

undetermined, since the outcome of their encounter with the panel could result in either herding or escapement.

A second objective of the study was to investigate the possibility of matching DIDSON and stereo-camera targets. A small metal target intended to be visible to the DIDSON and in the stereo-camera images was attached to the trawl to facilitate target matching. To ensure accurate indexing of all data, computer clocks were synchronized between the vessel computer network, the cameras, and the DIDSON.

3.3. RESULTS

3.3.1. Trawl samples

Haul data are given in Table 3.1. The six hauls were conducted in succession, taking place over an 18 h period. Fishing durations were varied in an attempt to standardize the amount of catch between hauls. Haul durations ranged from 8 to 20 min, yielding catches of 248 to 869 kg. On average, pollock comprised 99.5 % of the catch by weight. Hauls 1-3 occurred during the day and hauls 4-6 at night. The camera system did not operate correctly for hauls 1-3, while the DIDSON failed to collect data on haul 2.

3.3.2. Pocket net results

Pocket net catch data provide the relative distribution of escapement from the trawl, and a method to identify escaping targets observed as trajectories in the DIDSON data. The

Table 3.1. Results of six hauls taken to evaluate pollock behavior in midwater trawls.

haul		1	2	3	4	5	6
parameter	units						
start tow time	GMT	00:02:44	03:06:11	05:58:54	09:22:06	12:01:45	14:02:31
duration	min	12.57	10.53	21	7.97	6.48	10.07
distance fished	nmi	0.66	0.51	1.01	0.45	0.38	0.54
bottom depth	m	139	140	140	140	140	140
footrope depth	m	136	135.4	134.5	129.8	128.9	131.4
surface temperature	oC	10.9	10.5	10.9	10.6	10.5	10.4
gear temperature	oC	2.2	1.9	1.9	1.9	1.9	1.9
catch weight	kg	435.5	868.6	379.6	547.4	248	376.6
average length	cm	31.14	27.68	26.33	21.8	18.72	22.66
pocket catch	num.	6	31	65	120	248	105
pocket avg. length	cm	14.0	22.2	14.2	15.3	13.9	14.1
DIDSON targets	num.	117	24	NA	80	124	63
Stereo camera targets	num.	NA	NA	NA	52	209	99
light level	μE m^{-2} s^{-1}	4.71E-02	2.64E-02	6.62E-03	5.68E-06	2.24E-06	5.30E-06

pocket net catches were dominated by pollock (88.5%), the majority of which were age-1 (92 %) ranging from 10 – 20 cm (Fig. 3.9). In contrast, age-1 pollock made up 41.1 % of the codend catch by number.

For the comparative analysis, pocket net catches were expressed as a percentage relative to the number of age-1 fish caught in the codend for each haul sample, and normalized by the coverage area of each pocket net (m^2). For the ANOVA, haul 2 was excluded because the length distribution of fish in the catch was markedly different than those of the other five hauls, with predominant component of the catch being age-2 pollock. Due to the *a priori* expectation of lower escapement of age-2 relative to age-1 pollock, this haul sample was not directly comparable to the other five samples in terms of escapement or mean length. Significantly more fish escaped from trawls conducted al lower ambient light levels ($p = 0.05$, Table 3.2). Escapement rate differed significantly among panels ($p > 0.01$), but did not differ between sections of the trawl ($p = 0.09$). Comparisons of mean length of fish caught in pocket nets detected significant ($p < 0.01$) differences among trawl sections (Table 3.3). A multiple comparison of mean length across sections showed larger fish (Table 3.4) tended to escape from the forward-most section of the trawl, and escapement rates through the bottom panel differed significantly from the other panels, which had similar rates. A comparison of escapement rates showed variability between hauls (Fig. 3.10a), which could be attributed to the different length distributions encountered among trawls and different ambient light levels.

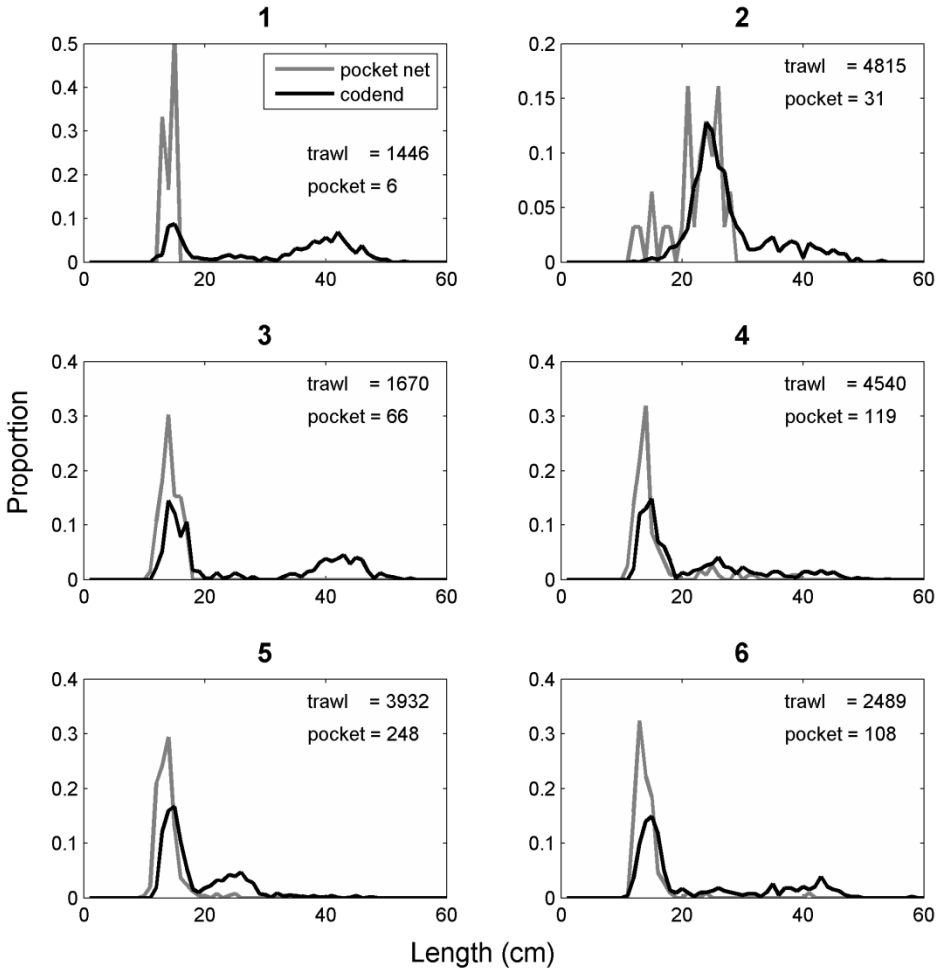

Figure 3.9. Length frequency distributions of Walleye Pollock from combined pocket net catches compared with the codend. Age-1 pollock (10-20 cm) comprised a higher proportion in the pocket nets than in the catch, indicating that these fish were under-represented in the trawl codend catch.

Table 3.2. Three-way ANOVA table for mean pocket net escapement rate, expressed as # of escaping fish per m^2 per h. A total of six hauls were taken with pocket nets mounted on three sections (forward, mid, and aft), and on four panels (top, port, stbd, and bottom).

Source	Sum Sq.	d.f.	Mean Sq.	F	Prob>F
Light level	0.16	1	0.16	4.71	0.034
Section	0.17	2	0.09	2.56	0.087
Panel	0.48	3	0.16	4.78	0.005
Error	1.77	53	0.03		
Total	2.58	59			

Table 3.3. Three-way ANOVA table for mean pocket net fish lengths, in cm. A total of five hauls with pocket nets mounted on three sections (forward, mid, and aft), and on four panels (top, port, stbd, and bottom) were compared.

Source	Sum Sq.	d.f.	Mean Sq.	F	Prob>F
Light level	0.09	1	0.09	0.045	0.833
Section	20.14	2	10.07	4.796	0.014
Panel	7.06	3	2.35	1.12	0.354
Error	75.59	36	2.1		
Total	102.88	42			

Table 3.4. Comparison of mean lengths of escaping pollock among three sections and mean escape rate among four sides of a midwater trawl. Variables with different letters in the third column are significantly different from each other.

Comparison of fish lengths (cm)			
Section	Mean length	Standard error	Significance comparison
Forward	16.1	0.60	a
Mid	13.7	0.44	b
Aft	14.0	0.41	b

Comparison of escape rates (relative % esc/m2)			
Section	Mean rate	Standard error	Significance comparison
Bottom	0.27	0.296	a
Starboard	0.12	0.174	b
Port	0.07	0.084	b
Top	0.08	0.134	b

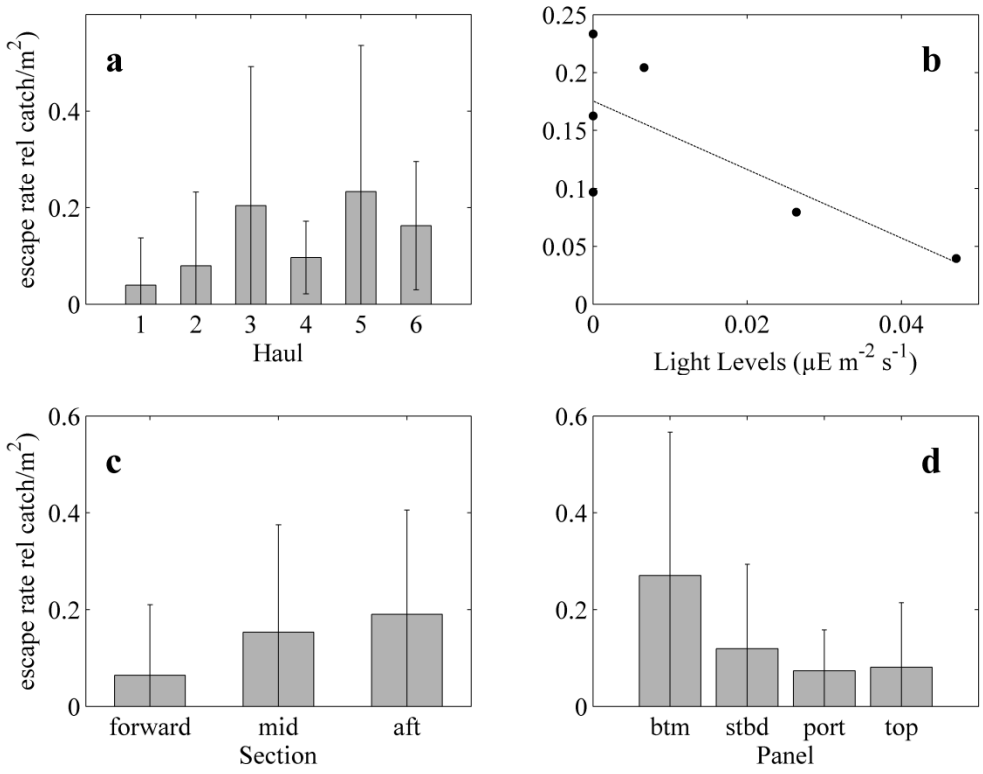

Figure 3.10. Escape pattern observed from the pocket net data. Escapement rate is number of fish caught in pocket nets expressed as a percentage of same size fish caught in the codend. Vertical lines represent the standard deviation across pocket net groupings. Highest escapement of walleye pollock was observed in hauls taken at night (a, 4-6), as shown by plotting escape rate as a function of ambient light levels (b). Dotted line represents a linear fit of escapement rate to light level. Escapement was similar along the different trawl sections (c), while pollock appeared to preferentially escape out of the bottom panel (d).

3.3.3. Stereo-camera observations

The camera system provided adequate lighting and resolution for age-1 pollock to be identified to species and measured at distances up to 4.5 m. The long interval between images (5 sec), necessary for recharging the strobe, resulted in a relatively low number of targets for analysis (Table 3.1). Based on image-derived estimates of fish length and position within the trawl, distributions of individual distance to the trawl panel did not differ significantly among juvenile ($\leq$ 20 cm, n = 291) and larger fish (> 20 cm, n= 69, Kolmogorof- Smirnov test, p = 0.11), and both groups had maximum densities at a distance of 0.5 to 1.5 m (Fig. 3.11). A comparison of tilt and yaw estimates yielded similar patterns for the two size groups. The tilt distribution was wide, ranging from -50^{o} to 50^{o}, with the highest tilt densities observed between 0^{o} and 15^{o}. Tilt measurements reflect the angular tilt relative to the camera platform and not an absolute estimate, although the camera mounting was essentially parallel to the main trawl axis and therefore close to horizontal. Yaw estimates showed a bimodal pattern with most (70.0 %) fish facing toward the trawl mouth and the remainder heading into the codend. No fish were observed in orientations parallel to the camera view axis (90^{o} & 270^{o}), or orthogonal to the main trawl axis.

Classifying the data into range bins revealed a pattern of increasing diversity of lengths closer to the trawl surface (Fig. 3.12). The median tilt value did not appear to change significantly with approach to the trawl, but the proportion of fish that were orienting toward the codend increased with approach to the trawl.

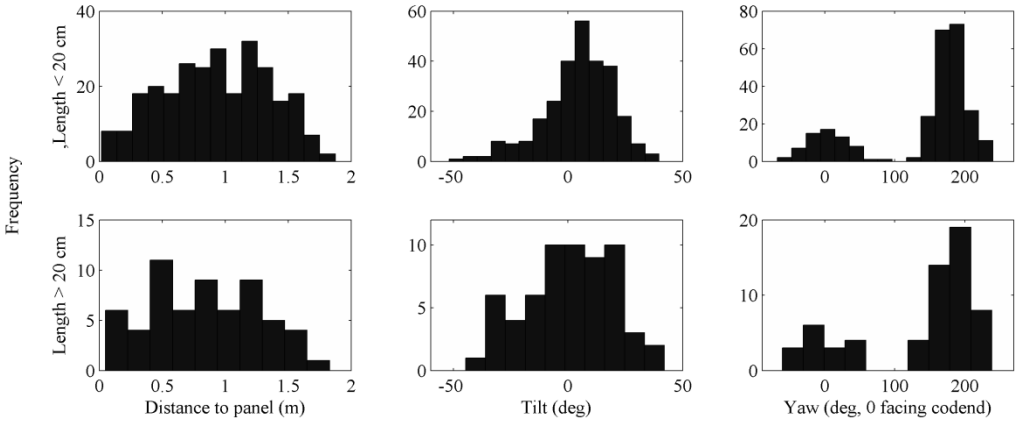

Figure 3.11. Position and orientation of walleye pollock in the midwater trawl as determined from stereo-camera images. Tilt angles indicate heading in the vertical plane with 0 degrees parallel to the main trawl axis. Yaw angles indicate the heading in the horizontal plane with 0 degrees facing the codend, 180 degrees facing the trawl mouth.

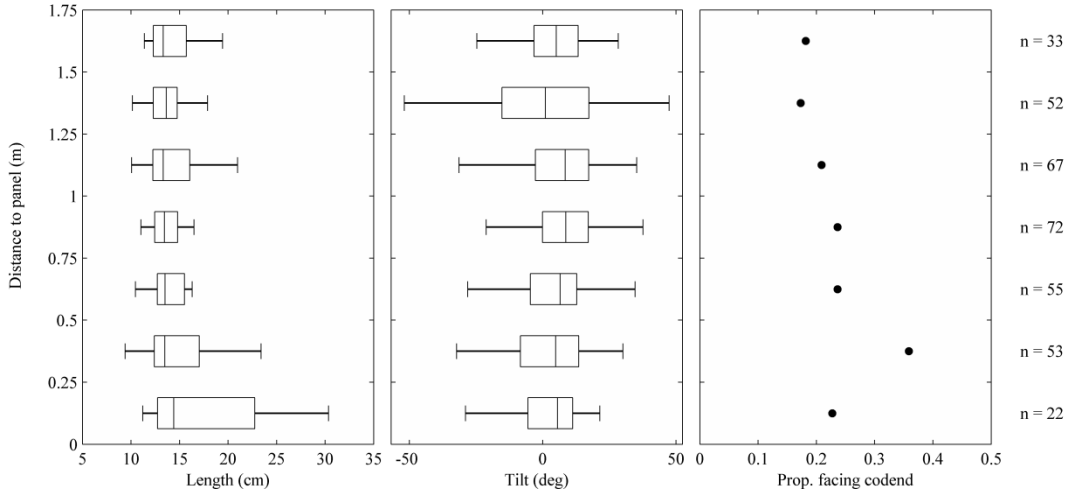

Figure 3.12. Patterns of walleye pollock orientation and length relative to proximity to the midwater trawl netting panel, determined from stereo-camera images.

3.3.4. Fish tracking using the DIDSON

Speed (*s*) and direction (*d*) at each target detection were grouped into range intervals and summarized (Fig. 3.13). Target speeds towards the center the trawl were fairly uniform at ~ 1.3 m sec^{-1}, which is comparable to the expected water flow through the observed section of the trawl (Craig Rose, NOAA/NMFS/RACE, Seattle, WA, personal comm.). As fish approached the panel, median values of *d* transitioned from moving straight towards the codend to nearly parallel to the estimated angle of the trawl panel. The expected heading for fish herding back into the net would be parallel to or greater than the trawl panel angle estimated at 10.8^{o}. Most animals did not appear to avoid the panel until they were within 0.5 m of the trawl meshes. This pattern was accompanied by a decrease in median value of *s* and an increase in variability with approach to the panel. Pollock appeared unable to maintain stationary position relative to the panel. Once a fish passed through the panel out of the trawl, their direction was highly variable, but on average indicated a heading away from the trawl.

Four-hundred and eight tracks were analyzed, with a mean track length of 9.01 detections and a mean duration of 1.125 sec, equivalent to 9 DIDSON frames. Using the target classification scheme, a majority of tracks (> 74 %) were "undetermined" (Fig. 3.14), providing no insight into the ultimate retention or escapement of the target. For many of these tracks, the end point appeared to be in close proximity to the trawl panel. It is possible that an encounter with the trawl surface would invoke lateral movement, which would remove the target from the horizontally compressed sampling volume of the DIDSON.

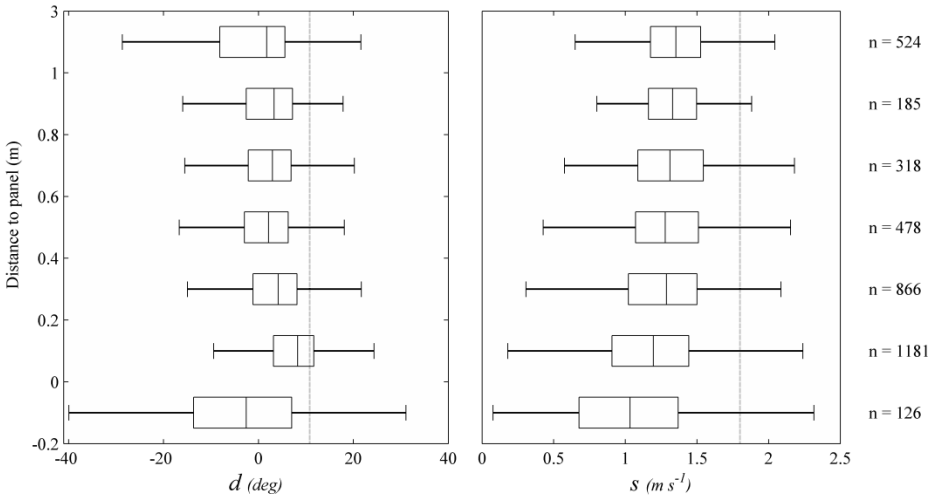

Figure 3.13. Changes in walleye pollock trajectory (*d*) and speed relative to the trawl (*s*) as they get closer to the netting panel of a midwater trawl. Values < 0 in the vertical axis indicate the position is outside of the trawl. Vertical line in left panel indicates the attach angle of the trawl panel relative to the main trawl axis, and the vertical line in the right panel indicated mean speed of the trawl though the water. Results are based on DIDSON target tracking analysis.

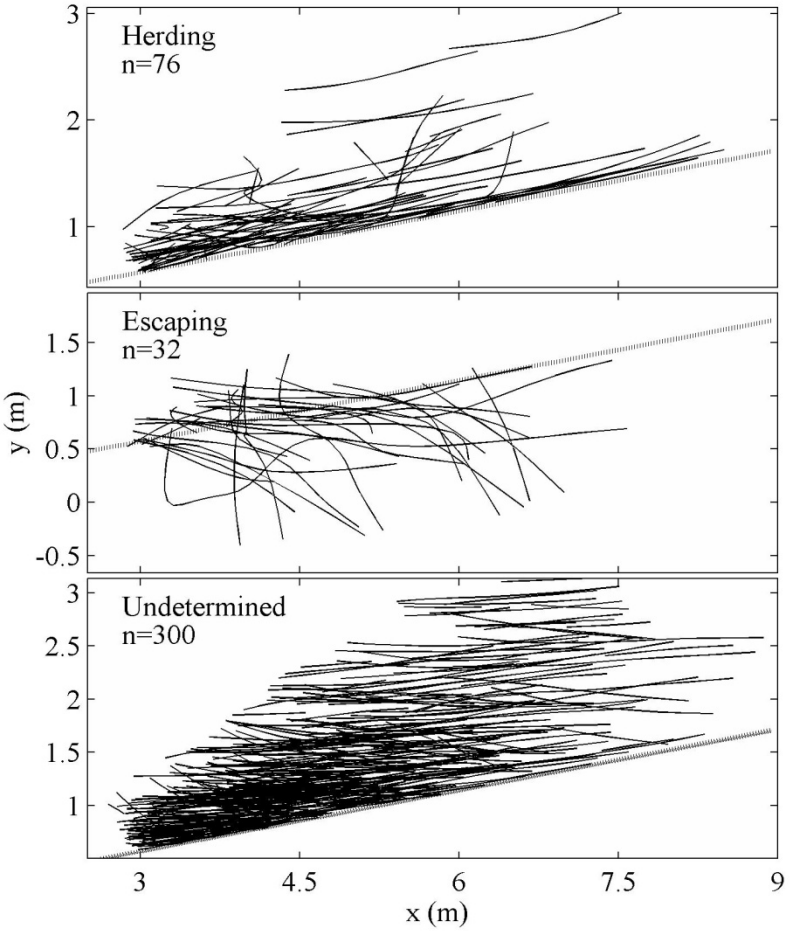

Figure 3.14. Tracking traces of walleye pollock targets observed by the DIDSON. Tracks are classified into herding, escaping, and undetermined classes based on their reaction to the bottom panel of a midwater trawl (shown as a dotted line).

More fish escaped in the last three trawls (Table 3.5), corresponding to higher catch rates in pocket nets during the night. Targets differed in their nearest approach distance to the trawl panel between day and night hauls (Fig. 3.15), suggesting that increased escapement coincided with greater densities of fish closer to the trawl panels.

When comparing track metrics among the three different trajectory categories, the mean heading reflected the criteria used to classify the responses, with herding fish averaging a positive heading (into the trawl), escaping fish displaying a higher variability in heading that was negative on average, and the undetermined response tracks on average following the water flow direction in the trawl (Fig. 3.16). Averaged values of the change in direction ($\Delta\bar{d}$) showed the "undetermined" class of tracks characterized by approximately straight-line movement, which contrasts to a more variable response in the herding fish, and especially escaping fish. Target speed in herding and escaping fish averaged lower than targets classed as undetermined, suggesting that fish interacting with the panel exhibited some effort to swim against the water flow in the trawl.

The potential influence of the stereo-camera strobe lighting on DIDSON track data was investigated using spectral analysis methods. It was assumed that fish reactions to the strobe light could be observed in track data as changes in Δd at the frequency of strobe events (Fig. 3.17a). Values of Δd were averaged in each frame where multiple targets occurred to produce a time series of movement change for the duration of the trawl event ($\Delta\bar{d}_f$). For DIDSON frames that did not contain any targets, the time series was filled with the mean value of Δd over the entire deployment. Spectral analysis of the $\Delta\bar{d}_f$ time series did not show any increased power at or near the frequencies of the strobe (0.2 Hz)

Table 3.5. Frequency of pollock behavior response classes in a midwater trawl determined by analysis of DIDSON tracks.

Class	Haul				
	1	2	4	5	6
escaping	1	2	11	9	9
herding	17	6	19	25	9
undetermined	99	16	50	90	45

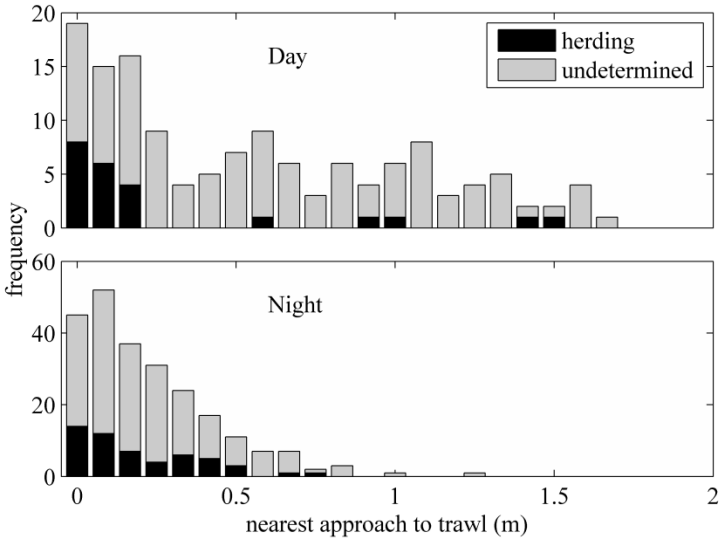

Figure 3.15. A comparison of day and night distributions of nearest distances of walleye pollock targets to trawl panel netting observed by the DIDSON.

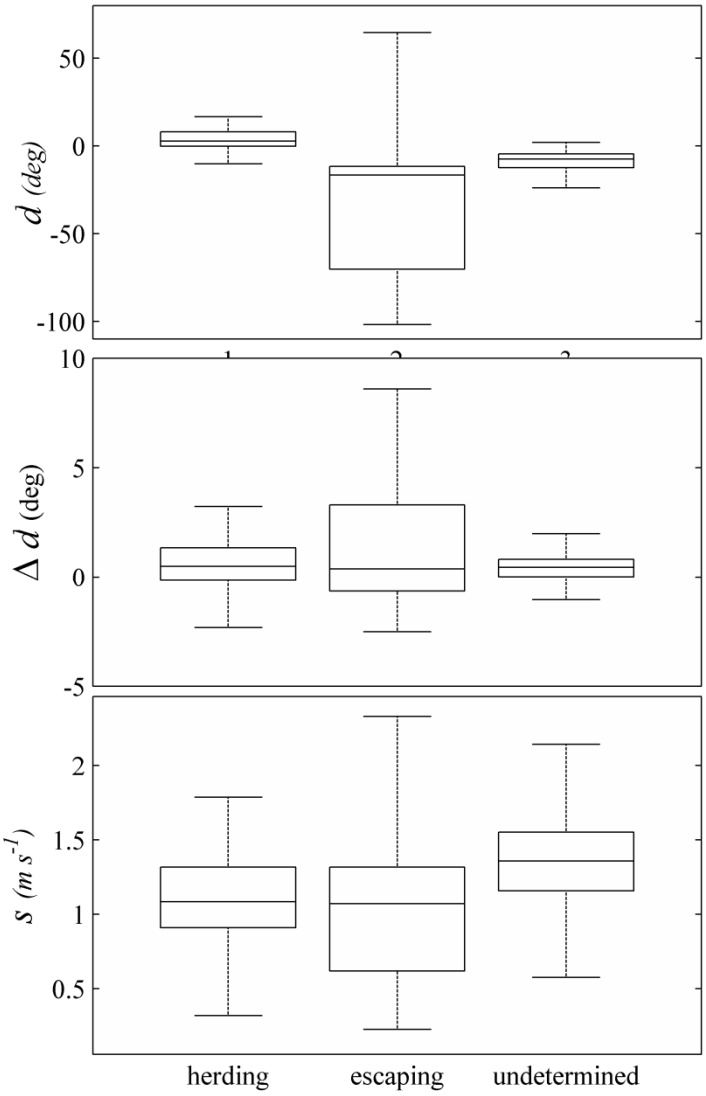

Figure 3.16. A comparison of mean direction, mean change in direction, and mean speed of individual tracks of walleye pollock in a midwater trawl derived from DIDSON data. Only portions of the track inside the trawl were used.

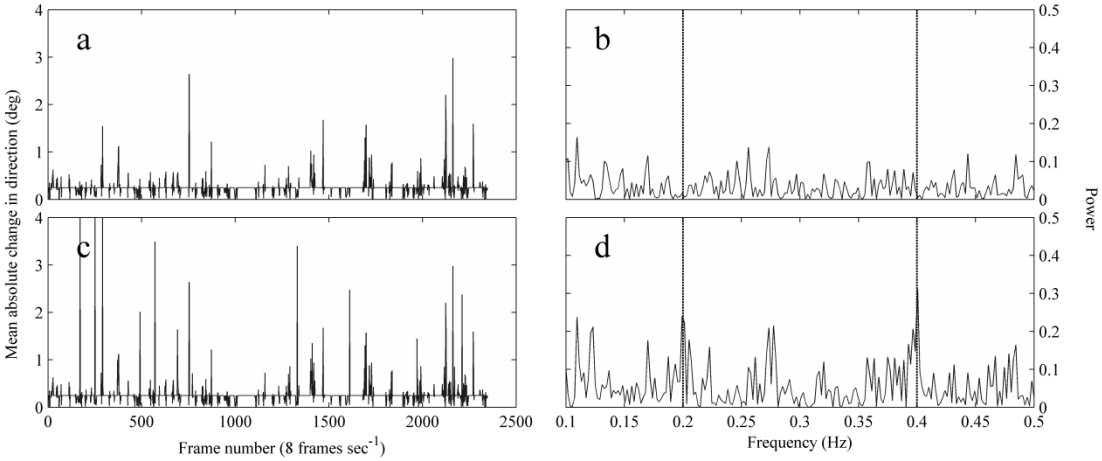

Figure 3.17. Exploring the potential effect of artificial strobing light on walleye pollock behavior inside a midwater trawl. Panel (a) represents the average change in direction in fish targets from the previous DIDSON time frame, derived from individual fish tracks. A spectral analysis of the mean absolute change in direction shows no pattern at the strobing frequency (b, 0.2 Hz), and the next harmonic frequency (0.4 Hz). A simulated data set with a periodic random error $e \sim N(0,2)$ added at the strobing frequency (c) shows detectable peaks at 0.2 and 0.4 Hz (d).

or the nearest harmonic (0.4 Hz), as might be expected if the strobe caused the fish to suddenly change their trajectory in response to the light stimulus. A test data set (Fig. 3.17b) into which a periodic value of $\Delta\overline{d}_f$ was inserted at the frequency corresponding to the strobe cycle showed the expected result of an increase in spectral density at the frequency of the strobe lights.

The common sampling volume where a target could be seen by both the cameras and the DIDSON was small (~ 2.95 m^3), resulting in few targets that could be matched. This was accentuated, in part, by the low image acquisition rate of the cameras. The trawl portion viewed by the cameras corresponded to the 5 to 7 m range in the DIDSON data, meaning that only larger (>25 cm) pollock remained visible. Overall, 19 pollock targets could be reliably matched between the data sets, all of which exceeded 25 cm in length. The small number of targets and the possibility of length bias precluded the use of matching targets for further analysis.

3.4. DISCUSSION

Trawls have often been described as "blunt" tools for collecting ecological data and conducting fisheries assessments. This is partially due to the mechanism by which fish are captured in trawls. Trawls function by evoking instinctual predator avoidance behavior to herd fish into the codend (Ferno, 1993; Ryer, 2008). This process is dependent on a combination of behavioral characteristics and environmental influences (e.g. light, temperature, see Glass and Wardle, 1989; Ryer, 2008), resulting in more effective capture of some species under specific conditions (Suuronen et al., 1997). The

ability to accurately reconstruct species and length compositions of fish populations in the environment from survey trawl catches may be limited without knowledge of how species or length-specific behaviors influence trawl retention.

The main objective of this study was to quantitatively examine pollock behavior in a midwater trawl to understand why selective retention occurs. The mesh size in the portion of the trawl observed by the DIDSON and cameras was 40 cm, a mesh size that would not restrict any fish from escaping. Fish were only retained in the net at this section because of their reluctance to pass through meshes. This behavioral retention has been shown to be length-dependent (Chapter 2), suggesting that there are ontogenetic factors that influence how fish react to trawl netting. Quantifying fish reactions to the trawl net requires a selection of metrics that adequately describe behavioral responses, which are in turn limited by the instruments used to observe behavior. An ideal observation tool would unobtrusively provide information on target species, length, orientation, and motion relative to the trawl. Optical instruments often require artificial light at depths where fish are found, potentially biasing behavioral observations (Stoner et. al., 2008). High resolution sonar devices, such as the DIDSON, provide unobtrusive observation without lights, but generally do not provide adequate resolution to identify targets to species and length when both targets and the instrument platform are not stationary. This shortcoming reduces their value in studies of selectivity where fish length is a critical measure. In this study, we attempted to combine the strengths of these two approaches by directly matching targets between a DIDSON and a stereo-camera. Matching targets was problematic due to the non-rigid arrangement between the instruments, which added uncertainty to the spatial reconstruction of the common

sampling space. The resulting low number of matched targets (n = 19) prevented quantitative analysis. Due to the high potential value of finding corresponding DIDSON and optical targets, this approach should be pursued further.

Interpretation of pollock behavior in a midwater trawl was based on the integration of multiple data sources used to reconstruct behavioral patterns. Fish observed by the DIDSON could not be measured for length, but pocket net catches indicated that fish seen escaping in the DIDSON were likely to be age-1 individuals (length: 10 to 20 cm). Similarly, greater than 75% of the DIDSON tracks indicated straight-line movement along the primary axis of the trawl at approximately the speed of the water flow. Seventy-five percent of fish seen in the cameras had tilt angles within 15 degrees of horizontal and faced the trawl opening. Combined, these patterns indicate that typical pollock trawl behavior can be generalized as passively moving with the water flow while oriented into the perceived flow direction.

Given the importance of light to fish behavior in trawls, it was expected that some behavioral patterns may be influenced by the amount of ambient light at fishing depth. A plausible expectation of length-dependent herding behavior would be that larger pollock would detect the netting panel from a greater distance and then maintain a greater separation from the panel, or a stronger herding reaction, consistent with the greater retention of adults compared to juveniles by the trawl (c.f. Chapter 2). The stereo-image data, collected at night, did not support this hypothesis. There was a weak pattern of larger fish approaching the panel more readily. Based on retinal tissue development studies, pollock visual acuity is length-dependent (Zhang and Arimoto, 1993). But this potential difference in length-dependent detection ability did not translate to a difference

in net avoidance behavior at night, perhaps due to the night light levels being close to the visual threshold for pollock. (5×10^{-7} $\mu E\ s^{-1}\ m^{-1}$, Ryer & Olla, 1999; this study night average 5.6×10^{-6} $\mu E\ s^{-1}\ m^{-1}$).

Laboratory studies using walleye pollock reported that juvenile fish decreased their distance from a trawl panel as light levels decreased (Ryer and Olla, 2000). This observation is consistent with DIDSON tracking observations from the midwater trawl. Track data showed increased density of targets closer to the trawl panel during night tows relative to those that were conducted during the day. This trend was not confirmed by stereo-camera observations, where the peak density was seen at approximately 1 m from the trawl. This contradictory result may be due to artifacts in this metric from differences in geometries of the imaging volumes between the two instruments. Neither device sampled the entire cross sectional volume of the net, and both had a disproportionate amount of sampling volume at the trawl panel (i.e. the further away from the panel a fish went, the less likely it was to be sampled).

Another laboratory study showed that haddock (*Melanogrammus aeglefinus*) preferentially passed through meshes that were less visible or had lower contrast compared to the background (Glass et al., 1993). In reduced light more fish would be expected to pass through the mesh simply as a function of visual stimulus. Based on pocket net catches of pollock, only smaller fish ($\leq$ 20 cm) passed through the meshes, and at increased rates during night. Although all lengths of pollock may not see the meshes in low light, larger fish are still herded by some other mechanism toward the codend of the trawl, such as contact with the mesh.

When observed by infrared light or strobe cameras, the orientation of walleye pollock and other gadoids in trawls at low light levels has been described as chaotic or disorganized (Olla et. al, 2000, Glass and Wardle, 1989). In this study, pollock observed at night were primarily oriented toward the trawl opening or the codend, parallel to the main trawl axis. The tilt distribution was comparable to pollock observations in captivity (Horne, 2003) and not much different than what might be expected based on other *in situ* or *ex situ* observations of gadoids (e.g Pacific whiting, Henderson et al., 2008). Unfortunately, the lack of daytime stereo-camera data prevents a direct comparison in light-dependent orientation of walleye pollock.

Tracking data provided unique, individual-based insight into fish movements relative to the trawl panel. Across all tracking measures, escaping fish had the highest variability among individuals, suggesting that escapement lacked predictable movement and cannot be generalized. One consistent pattern observed was that within-trawl trajectories of escaping fish were, on average, steeper relative to the trawl panel than the main water flow, suggesting that some fish were swimming toward the panel before contact rather than passively encountering the panel and being carried out of the trawl with the water flow. Herding fish and those whose response was categorized as undetermined had less variable metrics than those that escaped, but mean values differed, illustrating that herding fish headed away from the trawl at a slower speed, as might be expected of fish that perceived the trawl panel. Undetermined response fish moved in a straight line at the greatest speed, directly toward the codend, and represent 'typical' targets based on the current set of data.

The pocket net data provided information on pollock trawl behavior at a coarser resolution compared to observations by the stereo-cameras and the acoustic camera. The difference in mean length in pocket net catches between the forward-most section and the latter two sections of the trawl was not observed in previous pocket net experiments, and although the difference is small (2.1 – 2.4 cm), it indicates a potential gradient in length selectivity as fish approach the codend. All three sections contained the same size of mesh (10 cm), but the amount that the meshes are open may vary, presenting larger fish with an easier escape path further forward in the trawl. The directivity of escapement seen in the pocket net data suggests a tendency for pollock to move downward when disturbed, which was also seen in the Gulf of Alaska experiments described in Chapter 2. Diving pollock schools in front of a trawl have been observed on many occasions during trawling, and may be a common response by semi-demersal gadoids such as cod and haddock (Wardle, 1993). A major cause for this reaction is probably radiated vessel noise, as fish diving after a vessel passes has been demonstrated for pollock (De Robertis and Wilson, 2006). It is interesting that this diving reaction may continue within the trawl, which may reflect an innate bottom-orienting tendency in pelagic aggregations that are located 10's of meters above the sea floor.

Fish behavior in trawls is an important element to both commercial fishing where bycatch reduction is important (Maclennan, 1992), and in fisheries surveys where length selectivity may produce biased assessments of fish abundance (Nakashima, 1990; Godo and Sunnana, 1992). The results of this study provide a starting point for new designs or modifications of survey trawl gear, which may reduce trawl selectivity and increase accuracy of trawl catch compositions relative to the population of interest. To illustrate

by example, high visibility material could be used to enhance retention of smaller fish by providing a stronger visual stimulus. Smaller mesh material could be used in bottom panels of midwater trawls to reduce length selectivity due to the prevailing downward direction of escapement. Increased escapement at night suggests that trawling at night should be minimized during abundance estimate surveys. Results from this and similar studies of fish behavior in trawls can also be applied to commercial trawling operations, where reduced catches of juvenile fish is a desirable outcome.

This study provided a more complete insight into small-scale fish behavior within trawls by integrating several technologies to observe and quantify fish behavior in trawls. While this approach presented some unique challenges in logistics, it allowed for an analysis framework where ambiguities in one method could be compensated by another, thus allowing more confident inferences to be made. We hope this approach will be more widely used in future fish behavior studies.

CHAPTER 4. EXAMINING INFLUENCES OF ENVIRONMENTAL, TRAWL GEAR, AND FISH POPULATION FACTORS ON MIDWATER TRAWL PERFORMANCE USING ACOUSTIC METHODS

4.1. INTRODUCTION

Trawls are used as scientific tools in fishery-independent surveys of fish abundance and demographic structure. The value of trawl sampling depends on knowing its ability to provide accurate data. For example, acoustic trawl (AT) surveys rely predominantly on midwater trawl catches to interpret acoustic backscatter and scale it to abundance. Fish behavior during trawl capture can bias trawl samples, and these biases are propagated into abundance estimates. Critical parameters of trawl performance are efficiency for capturing target species, and selectivity in retaining different sizes and species of fish that enter the trawl (Hilborn and Walters, 1992).

Trawl efficiency is also termed catchability, although this term is typically used when fitting trawl data to stock assessment models (Arreguín-Sánchez, 1996), and represents differences between survey and model estimates of abundance (Loth et al., 2004). In this context, catchability is usually estimated by comparing trawl catch per unit effort with model estimates of abundance. This method only addresses systematic, relative differences between catch and model-derived abundance. It does not incorporate inter-annual changes in trawl performance due to environmental or other influences (Francis et al., 2003). To estimate efficiency and selectivity of a survey trawl on a local scale (e.g. not on the survey level), and thus evaluate changes in trawl performance due to

environmental influences, fish state, or survey methodology, an independent measurement of fish density is needed. Acoustic estimates of density have been used for this purpose for bottom trawl catches (Aglen, 1996, Hjellviket al., 2003, Kotwicki, et al. in press), primarily to estimate how much fish is in the near bottom acoustic "dead zone", and to evaluate vertical downward herding into the trawl. Both of these concepts are specific to bottom trawls.

Trawl efficiency is less important for acoustic surveys if the catch is representative of the true population, because abundance is calculated using acoustic data (Simmonds & MacLennan, 2005). In contrast, trawl efficiency is a critical factor for abundance estimates based on catch-per-unit-effort. Biases in trawl catch lengths and species compositions (i.e. selectivity), due to differences in catch rates are a primary concern for both types of surveys, as they result in a misrepresentation of fish population length structure, and can cause substantial errors in biomass estimated for acoustic surveys (Chapter 5). By examining environmental influences on trawl efficiency and selectivity, information on fish behavior relative to trawl capture is increased, which may contribute to efforts to op timize harvest while minimizing impacts of commercial trawling (Valdemarsen & Suuronen, 2001).

In this study we evaluate midwater trawl performance for use in acoustic surveys of walleye pollock (*Theragra chalcogramma*; hereafter pollock), an important commercial fish species in the North Pacific. We use acoustic data collected during trawling to provide independent density estimates against which trawl catch-based density, and by extension, fish reactions to trawl capture, can be compared. The approach presented here is an extension of methods described in Somerton et al. (2011) to assess efficiency,

selectivity, and potential environmental, physiological, and methodological influences on these variables.

4.2. MATERIALS AND METHODS

4.2.1. Acoustic and catch data

Acoustic surveys for pollock from 1995 – 2010 conducted in the eastern Bering Sea and Gulf of Alaska were included in this study. Surveys from 1995 – 2007 were conducted using the NOAA ship Miller Freeman (MF), and 2008 – 2010 using the NOAA ship Oscar Dyson (DY). The latter vessel (DY) was specifically designed for low underwater radiated noise levels to reduce potential vessel avoidance by fish (De Robertis & Wilson, 2010). Acoustic data, consisting of the volume backscatter coefficient S_V (m^2 m^{-3}, MacLennan et al., 2002) measured at 38 kHz, were collected during AT survey trawling operations, along with trawl position and trawl mouth opening dimensions. Trawl positions during fishing were used to estimate fish density using acoustic data within the path of the trawl. This was done by integrating acoustic returns from a layer starting at the measured headrope depth and extending to the footrope of the trawl (Fig. 4.1). Because acoustic data were collected on the ship's echosounder, there is a depth-dependent temporal offset between backscatter received from fish targets under the vessel and when those fish encounter the trawl. To adjust for this offset, the start and end points for the integrated region representing the trawl path were translated by calculating the distance between the trawl and the vessel's echosounders, and then multiplying by the

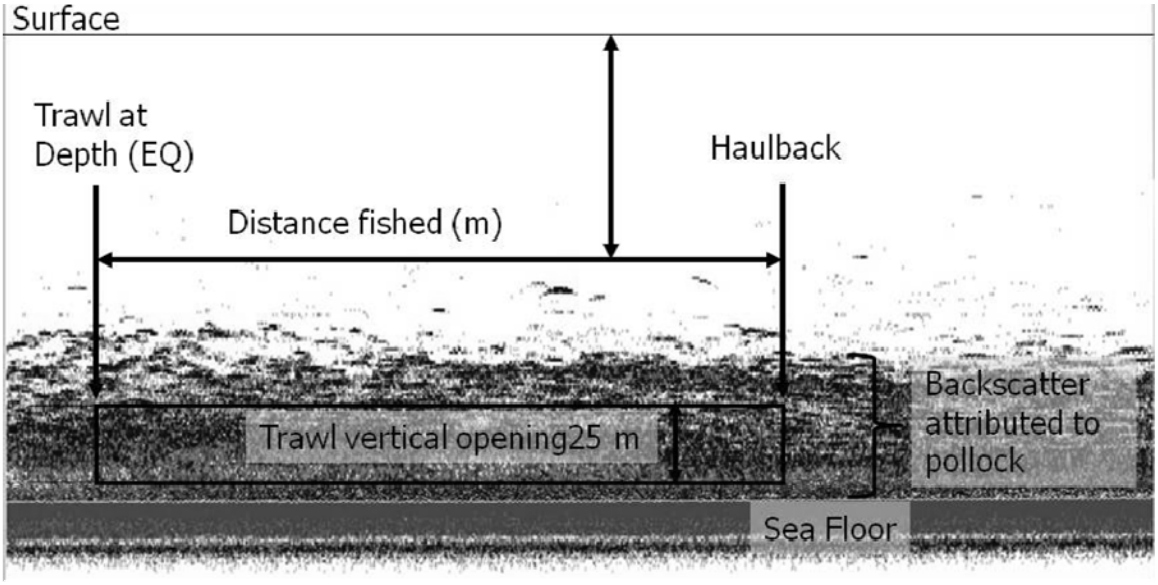

Figure 4.1. Estimating mean acoustic backscatter of pollock within the path of the midwater trawl. Background image represents an echogram at 38 kHz.

vessel speed to covert this distance to an offset time. Analyses were performed using Echoview (Myriax Software PLT, Version 4.9) in scripting mode.

The AT survey used an Aleutian wing trawl (AWT, Net systems, Bainbridge Island, Washington) for catch sampling during the study period. The AWT has nominal vertical and horizontal trawl opening dimensions of 25 m and 45 m. The mesh size in the forward portion of the trawl is ~ 3 m and is gradually reduced to 10 cm in the codend. The codend contains a small mesh liner which varied by survey between 3.2 cm (1.25”) and 1.3 cm (0.5”).

Trawl catches were sorted by species and ~300 pollock were measured for length to the nearest cm. When juvenile pollock co-occurred with adult pollock in the catch, and the juvenile length mode was distinct from the adults, juveniles were sampled separately and then merged with adult measurements to increase the precision of the length frequency estimate. Depth and water temperature at the trawl headrope were measured during deployment using an SBE-39 (Sea-bird Electronics, Bellevue, Washington) bathythermograph. Only catches of at least 500 kg, and a pollock content of > 95% by weight were included in the analysis. A total of 547 hauls were analyzed from all surveyed areas and years.

4.2.2. Model relating acoustic backscatter and catch

The objective of the modeling effort was to compare observed acoustic density along the path of the trawl with estimates of fish density based on trawl catch. The modeling effort

consisted of a series of increasingly complex models seeking to explain variability between acoustic measurements and trawl catch of pollock. In the null model (M0), the expected acoustic density $\hat{S}_V$ is

$$\hat{S}_V = 10 \log_{10} \left(\frac{\sum_l N_l \sigma_{bs,l}}{V} \right) \quad 4.1$$

where N_l is the number of fish caught at length l (cm), $\sigma_{bs,l}$ is the length-dependent backscattering cross-section (MacLennan et al., 2002), V is the volume sampled by the trawl. The backscattering cross-section is the linear equivalent of acoustic target strength (*TS*), which for pollock has been estimated using *in situ* measurements of individual fish targets followed by trawling to confirm target species and length composition (Traynor, 1996). Based on this work, the TS of pollock was found to be

$$TS_l = 20 log_{10}(l) - 66 \quad 4.2$$

And converted to linear equivalent by

$$\sigma_{bs,l} = 10^{TS_l/10} \quad 4.3$$

V was estimated as

$$V = \frac{vh}{2} \pi d \quad 4.4$$

where v and h are the mean measured vertical and horizontal net opening in m and d is the distance fished in m, computed as the Cartesian distance between coordinate points of when the trawl reached fishing depth and the point at which it was hauled back (Fig. 4.1). To estimate trawl efficiency and selectivity, the base model was expanded to include

trawl efficiency (i.e., herding or avoidance) and selectivity (i.e. escapement of juvenile fish from the trawl), by including additional parameters. This model (M1) was specified as

$$\hat{S}_V = 10\log_{10}\left(\left[e^g \sum_{l=1}^{l=f} N_l \sigma_{bs\,l} + \sum_{l=f+1}^{l=80} N_l\, \sigma_{bs\,l}\right][Ve^k]^{-1}\right) \quad (4.5)$$

where g is the natural logarithm of the probability of retention for juvenile fish, f defines the length below which fish were considered juveniles, and k is the natural logarithm of the efficiency parameter q. Values of g were converted to proportion of juvenile fish retained by the trawl p by

$$p = \exp\,(g)^{-1} \quad (4.6)$$

which is comparable to standard measures of trawl selectivity. The logarithmic transforms of the parameters of interest (p, q) assured that negative scaling factors did not occur.

4.2.3. Including efficiency, selectivity, and covariates in model structure

To examine potential environmental, survey-related, and fish population effects on trawl efficiency and selectivity, the model was expanded to include covariates, representing conditions of each haul sample. Covariates were selected based on published studies examining influences of external factors on fish behavior during trawl capture. Environmental factors included water temperature at the trawl (GT), surface water temperature (ST), trawl headrope depth (HD), and depth off bottom (DB). Survey-

related factors consisted of the time from solar noon when haul was taken (TN), Julian day (JD), survey vessel (MF and DY) used (SH), and the size of the codend liner (CL). Descriptors of the sampled fish populations included average condition factor (CD), and proportion of adults spawning (SP). The condition factor was computed using

$$CF = 100\frac{W}{L^3} \tag{4.7}$$

where W is the fish weight in grams and L is the length in cm (Fulton, 1904).

Covariates were included in the model by defining k and g as a function of parameters β and covariates x using a linear equation (k shown)

$$k = \beta_0 + \beta_1 x_1 + \beta_2 x_2 + .. \beta_n x_n \tag{4.8}$$

4.2.4. Model fitting and evaluation

Parameter estimates were found using maximum likelihood. Preliminary analysis assuming normally distributed errors for the null model revealed that the residual distribution was leptokurtic (Fig. 4.2), therefore a normal error model was inappropriate for this data set. An alternative error distribution is the location scale t-distribution, which is a generalization of the student's t-distribution specified by a scale parameter (τ), in addition to the mean μ and degrees of freedom (ν). The residual distribution when fitting the null model was symmetrical, suggesting that fitting the model to logarithmic backscatter terms was appropriate, as linear units would likely produce a skewed error

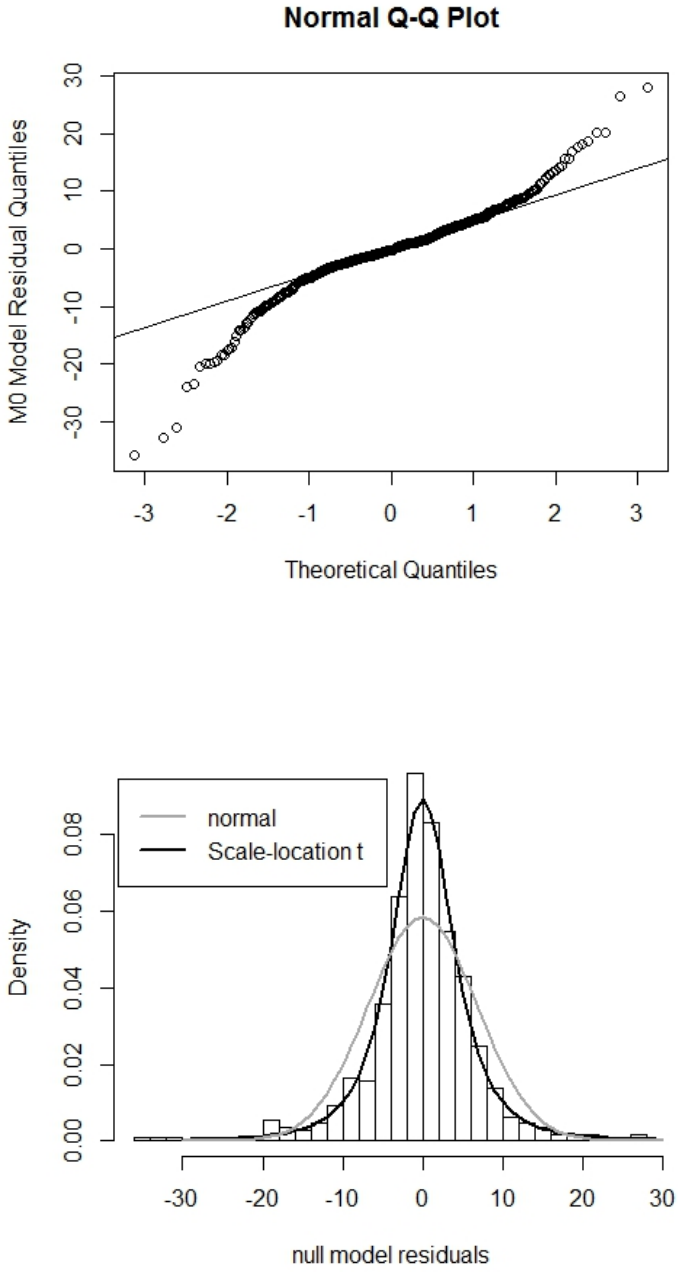

Figure 4.2. Residual pattern from the fit of the null model. Upper panel shows deviation of residuals from theoretical quantiles for a normal distribution, including a reduced density in the upper and lower tails relative to the normal distribution. Lower panel shows a histogram of model residuals. A better fit for this distribution was achieved using the scale-location t-distribution.

distribution. The negative log likelihood (-log$L$) function for location scale t-distribution is

$$-\log L = \sum\left(-\log\left(\frac{\Gamma\left(\frac{\nu+1}{2}\right)}{\Gamma\left(\frac{\nu}{2}\right)}\sqrt{\frac{\tau}{\nu\pi}}\left(1+\left(\frac{\tau(S_V-\hat{S}_V)^2}{\nu}\right)^{\frac{-(\nu+1)}{2}}\right)\right)\right) \quad (4.9)$$

The distribution parameters (ν,τ) were estimated during model fitting. All models were fit using the *mle* (maximum likelihood estimation) function in R statistical package (Version 2.12.1; R development core team, 2010) to minimize -log$L$. Model convergence was assessed by varying the starting values for the parameters. Model fits were evaluated by examining residuals and using quantile-quantile (i.e. Q-Q) plots. For models with covariates, the potential for multicollinearity was examined using correlation plots and by calculating variance inflation factors (VIF; Kutner et al., 2004) for each covariate. Model selection was performed using the Akaike information criterion (Akaike, 1974), incorporating a correction for finite sample sizes (AICc; Hurvich & Tsai, 1989). AICc is defined as

$$AICc = 2c + 2(-\log L) + \frac{2c(c+1)}{n-c-1} \quad (4.10)$$

where c is the number of parameters in the model, -log$L$ is the negative log likelihood (Equation 4.9), and n is the number of data points used. Covariates were evaluated in a forward stepwise manner by retaining the combination of covariates with the lowest AICc score at each stepwise increase in the model terms. Covariates were added to k first, followed by g, because catchability scaled the entire length component of the catch whereas selectivity only impacted the juveniles.

4.3. RESULTS

4.3.1. Model selection

Large reduction in AICC values relative to the null model showed that inclusion of selectivity and efficiency parameters improved model fit (Table 4.1). Model M1 with both terms resulted in lower AICc than intermediate models including either efficiency and selectivity independently, meaning that both processes are important descriptors of midwater trawl performance when sampling pollock. The nested arrangement of g and k in the model reduced the likelihood of poor model convergence due to confounding of these two parameters. Examination of the parameter covariance matrix confirmed a low covariance between g and k (5.8×10^{-3}).

Further expansion of model M1 by adding covariates to both terms further improved model fit by a greater reduction in AICc relative to the comparison of M0 and M1.

4.3.2. Model with covariates (M2)

Of the nine covariates evaluated, six were retained in the linear function for k, and two were retained for g (Table 4.1). Inclusion of the covariates resulted in an AICc reduction of 28 units relative to model M1, indicating the importance of covariates in explaining the data. Plots of residuals against covariates, including those not retained in the final model, did not indicate evidence for non-linear relationships between the

Table 4.1. Model fits and parameter estimates for 3 models relating measured acoustic backscatter to trawl catch. Parameter *k* represents the natural logarithm of trawl efficiency, while *g* is the fitted variable representing proportion of juvenile pollock retained by the trawl (*p*). Covariates included in the model were (symbols and units given in parentheses) spawning proportion (SP) gear temperature (GT, C°), Time from solar noon (TN, h), condition factor (CD), and survey vessel (SH: MF = 0, DY = 1).

Model	Parameter estimates	Number of parameters	Δ AICc (from previous model)
null (M0)	ν = 2.65 τ = 0.06	2	-
selectivity added (M1)	ν = 2.49 τ = 0.07 *k* = 0.09, exp(k) = 1.10 g = 2.51, p = 0.08 f = 14 (fixed)	4	-22.23
Covariates for k and *g* added (M2)	ν = 2.41 τ = 0.07 *k* = 0.62 - 0.49×SP - 0.06×GT - 0.03×TN g = -6.09+ 11.83×CD – 1.20×SH f = 14 (fixed)	9	-28.03

covariates and the response variable (retained covariates shown in Fig. 4.3 a-e). Residual analysis showed some evidence that the residual variance is a function of the proportion of spawning fish (Fig. 4.3 a). A Q-Q plot contrasting residual quantiles with the theoretical quantiles defined by the error model (Equation 4.9) showed good agreement (Fig. 4.3 f), validating the distribution used for the likelihood function. VIFs for the six covariates in the model ranged from 1.02-1.54 , reducing the possibility of a strong bias due to multicollinearity, which is usually associated with VIF values >5 (Kutner et al., 2004).

The initial model runs were performed at f = 18 cm, as the length range of 1-18 cm appeared to encapsulate the age-1 pollock length mode (Fig. 4.4). A likelihood profile of f using model M2 found the maximum likelihood estimate for f within the range examined (10-20 cm) to be 14 cm. The final model was specified with f = 14. Estimates of k ranged from 0.6 - 1.8 among hauls and were symmetrically distributed around the median value of 1.15 (Fig 4.5 a). The median estimate of the proportion of juvenile pollock (p) retained by the trawl was 0.11 (Fig. 4.5 b), suggesting that substantial under-sampling of juveniles occurred. To compare p to experimental estimates of selectivity of the same trawl (Chapter 2), an equivalent juvenile retention rate was calculated by integrating logistic selectivity curves derived by the experiments over the length interval 1 – 14 cm and dividing the integral by the number of length classes in the interval (14). Retention rates from the three experiments were 0.147, 0.021, and 0.124, indicating that the acoustic model provided estimates within the range of experimental values.

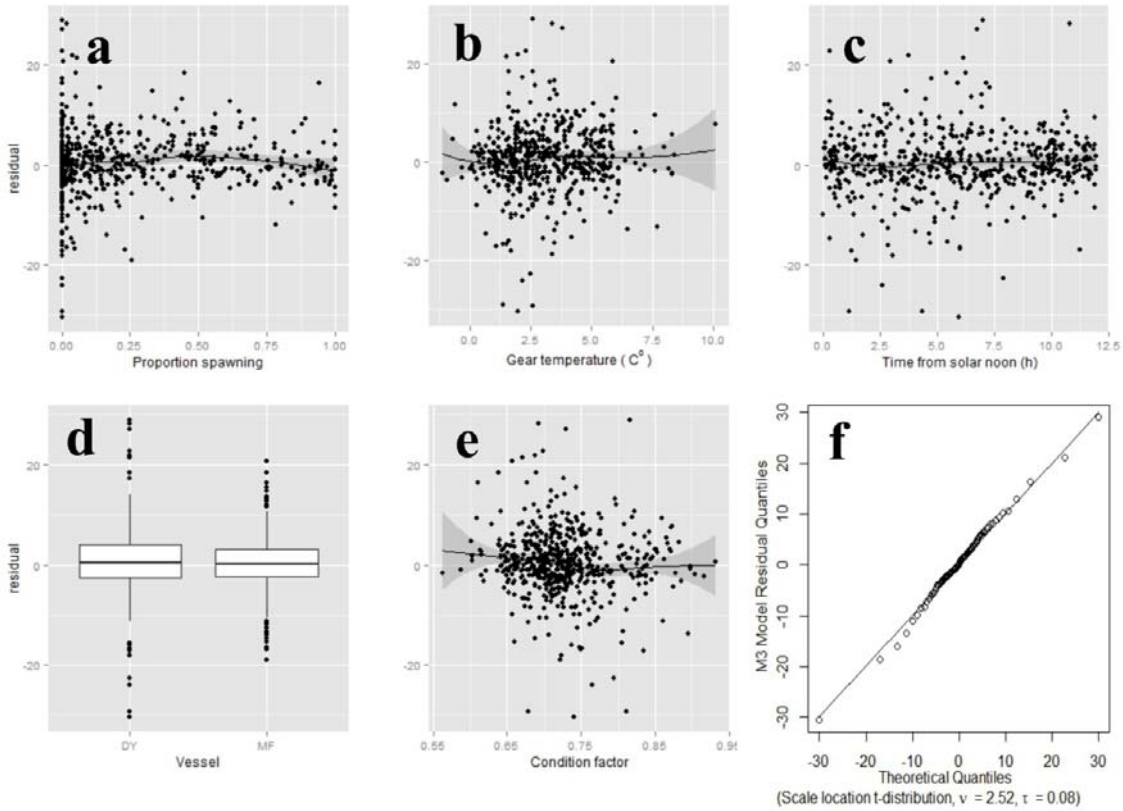

Figure 4.3. Residuals from model fits of measured backscatter and estimates of backscatter based on trawl catch (dB S_V), plotted against covariates used in the model consisting of: a) proportion of spawning fish in the haul catch, b) water temperature at the trawling gear, c) difference in haul time from solar noon, d) survey vessel used for towing, and e) mean condition factor of fish in haul. A locally weighted scatterplot smoothing function (LOWESS) is shown to visualize trends in residuals. For the survey vessel covariate, residual distributions by vessel are shown using boxplots. Plot f shows quantile-quantile plot for the residuals based on a scale-location t-distribution.

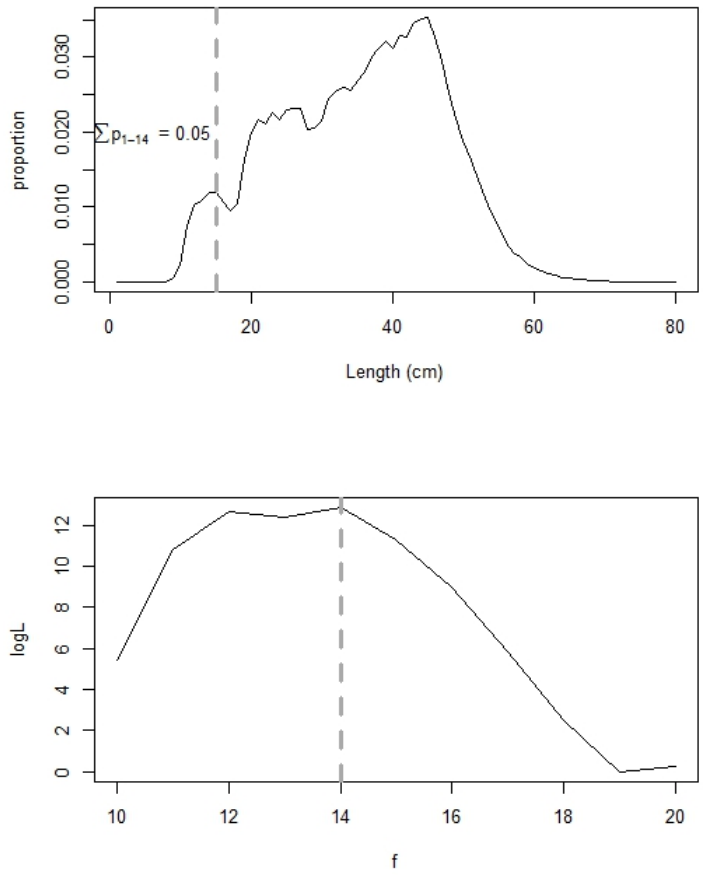

Figure 4.4. Defining juvenile breakpoint selection for the model. Upper panel shows the normalized aggregate length frequency distribution of the catch data to illustrate juvenile length structure and relative abundance of fish ≤ 14 cm. Lower panel shows the likelihood profile for juvenile length breakpoint f within the range 10-20 cm based on model M2. Dashed grey line shows the fixed value of f =14 used in models M1 and M2.

4.3.3. Covariate effects

The stepwise improvement in fit by adding covariate terms is shown in Table 4.2. The improvement in AICc increased by smaller margins with each added covariate, with the strongest improvement resulting from the inclusion of the proportion of fish in spawning condition as a covariate for *k*. Effects of all efficiency covariates are shown in Figure 4.6. To enhance interpretation, effects were plotted relative to efficiency (q), or e^k. As q is a scalar for the trawl mouth opening, values < 1 indicate that fish are avoiding the trawl as $S_V > \hat{S}_V$. By extension, the effective fishing area is greater than the trawl mouth when $e^k > 1$, suggesting potential herding by trawl doors, warps, or the vessel. Covariate effects on *k* were similar in magnitude and direction, with estimates of q ranging from 0.8 – 1.4 at the extremes of the covariate range. A strong effect of condition factor on selectivity was found, with juvenile pollock retention rates ranging from 1 to 80 %, and higher retention rates associated with low condition factors (CD < 0.6). Higher retention rates were also estimated for hauls taken by the Oscar Dyson compared to the Miller Freeman ($\tilde{p}_{DY} = 0.25, \tilde{p}_{MF} = 0.09$). Of covariates evaluated for trawl selectivity, only condition factor and survey vessel reduced AICc. Only hauls containing juvenile fish (n = 207, 37.7 %) were affected by these covariates, and of these hauls, juveniles composed an average of 11.4 % of the total number caught. The improvement of model fit when adding covariates to selectivity was modest (Δ AICc = -2.39) when compared to herding effects (Table 4.2.).

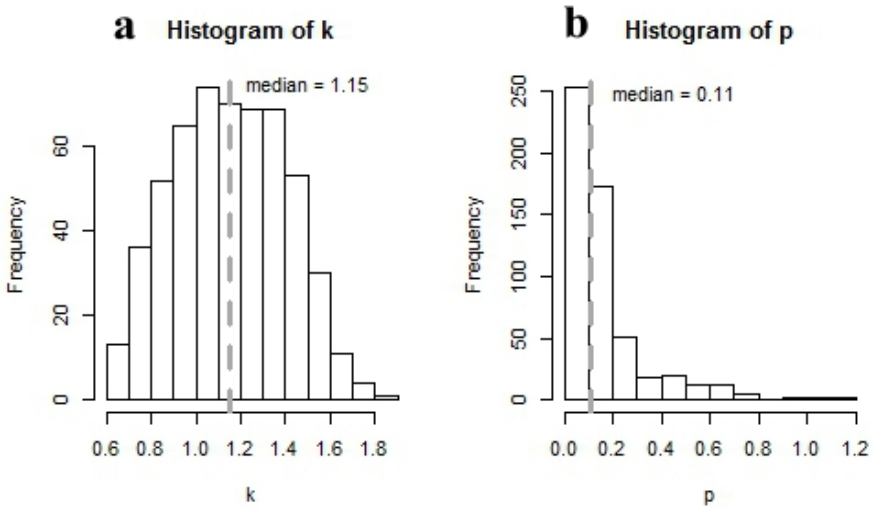

Figure 4.5. Distributions for a) trawl efficiency (k = scalar for measured trawl mouth opening) and b) selectivity (p = retention proportion of pollock <14 cm) from model M2. Dashed grey line indicates the median value.

Table 4.2. Covariate selection using stepwise change in AICc for a model relating acoustic and midwater trawl catch-based fish density. k and g represent trawl efficiency and selectivity. Covariates included in the model were (units if available and symbols given in parentheses) spawning proportion (SP) gear temperature (C°, GT), time from solar noon (h, TN), survey vessel (MF = 0, DY = 1, SH), and condition factor (CH).

Formulation	k = *f*(SP)	*k* = *f* (SP,TN)	*k* =*f*(SP,TN,GT)	*k* =*f*(SP,TN,GT) *g* = *f*(CD)	*k* =*f*(SP,TN,GT) *g* = *f*(CD,SH)
Δ AICc	-	-5.42	-3.79	-0.95	-1.44

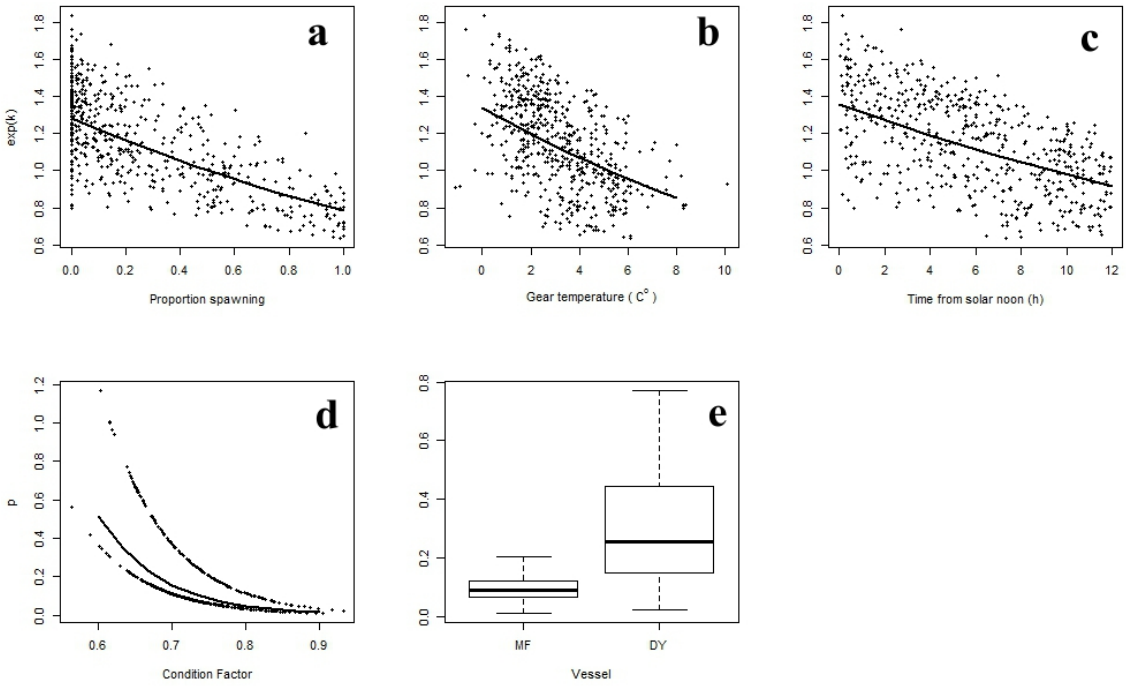

Figure 4.6. Covariate effects on trawl efficiency and selectivity. Plots a-c show partial effects of a) proportion of spawning fish in haul catch, b) water temperature of the trawling gear, c) difference in haul time from solar noon. Points represent e^k for 547 hauls estimated using a linear function of haul-specific covariates and model estimated slope and intercept parameters, and lines represent the effect of each individual factor when all the other factors are evaluated at their means. Values of e^k >1 indicate greater herding into the net, while values <1 indicate potential trawl avoidance. Plots d and e show mean condition factor and vessel effect on the proportion of juvenile pollock (p) retained by the trawl. Vessel effect was evaluated using boxplots of p grouped by the vessel.

4.4. DISCUSSION

4.4.1. General modeling results

This study demonstrates the potential for using acoustic backscatter data to assess midwater trawl performance and fish behavior. A large historical trawl dataset spanning 15 years of pollock surveys provided sufficient contrast in variables examined to assess their effects. Despite the large sample size, the relationship between modeled and observed values of S_V was characterized by high variability and low agreement, illustrated by low correlation between the two variables (M0: $r^2 = 0.07$). Upper and lower quartile values (CFD [0.25,0.75]) for the model residuals were -2.92 and 3.26 dB, which in linear terms equates to a range of ~ ½ to > 2 times the mean. For half the observations the difference between acoustic-derived and catch-derived density was greater than two-fold, suggesting that for pollock, midwater trawl catch is an imprecise predictor of acoustic density in the trawl path. While the model r^2 increased from 0.09 with the null model to 0.14 with the addition of selectivity and covariates, it was low compared to similar studies with bottom trawls (e.g. $r^2 = 0.67$ for haddock, Aglen, 1996; $r^2 = 0.34$, Hjellvik et al., 2003). The primary source of this variability could be attributed to estimating the trawl path in the water column, which relies on correct estimates of trawl offset from the vessel during fishing. It is possible to include an aggregation of fish in the estimated path of the trawl on the echogram that is not encountered by the trawl, or the opposite, when the small scale (~ 100 m) horizontal spatial variability of S_v is high (i.e. patchy fish distribution). Trawl path estimation is less critical when fish form horizontally uniform layers. The trawl may be located to either side of the vessel trajectory (e.g. “crabbing”), such that there is no direct way to sample aggregations

observed in the vessel path, increasing the potential for a mismatch between acoustic- and catch-density estimates. The validity of using backscatter in the trawl path rests on the assumption that density differences caused by any mismatch is random across parameters of interest, the covariates used in the model, and the samples used to estimate to fit the model.

4.4.2. Inclusion of catchability and selectivity in the model

In the model specification, q is equivalent to catchability in bottom trawl surveys, with volume being equivalent to the two-dimensional ”area swept” used in bottom trawl abundance estimates. Functionally, q provides a scalar for the catch-per-unit-effort (CPUE) based estimate of fish density, accounting for systematic, behavior-induced bias in the estimate of volume filtered by the trawl. In this study, the median value for q for hauls in the dataset was 1.15 (Fig. 4.5), suggesting that herding by the vessel, trawl doors, and bridles is not strong for pollock in midwater trawls, and primary herding is by the trawl mouth. Similar behavior is thought to occur for pollock being fished with bottom trawls (Somerton, 2004). The g parameter allowed for a length dependence to be added to catchability allowing length-dependent retention, or selectivity to be evaluated. Similar to Somerton et al. (2011), the addition of efficiency and selectivity resulted in a reduction in AICc (22.23 log-likelihood units), indicating that these factors should be included in comparisons of acoustic- and catch-derived estimates of density due to fish behavior.

4.4.3. Covariate effects on catchability

The interpretation of catchability or efficiency is two-fold, with values >1 indicating herding into the trawl, and values <1 indicating avoidance of the trawl or potentially escapement from the trawl. These responses are dependent on locomotive and sensory ability, which are in turn influenced by the environment and by the physiological state of the fish. Understanding the potential mechanisms through which covariates influence behavior can be challenging without direct observations of individual fish responses. For example, ambient water temperature has been shown to influence swimming ability in a closely related species, Atlantic cod (*Gadus morhua*; He, 1991). In this study, water temperature was inversely proportional to catchability (Fig 6b), suggesting that fish are more effectively captured when their swimming ability is reduced, or are more able to avoid the trawl when they can swim faster. However, herding into the trawl mouth should also be more effective when fish can swim faster, suggesting that other mechanisms may be at play. The influence of time of day on capture is more easily interpreted as being related to differences in pollock aggregation patterns between night and day (e.g. DeRobertis et al., 2008, their Fig. 3), as well as the use of visual cues for herding (Glass & Wardle, 1989). Fish in spawning condition were less susceptible to capture, which may be due to reduced ability of fish to respond to herding stimuli, or a heightened ability to evade or escape from the trawl. The former interpretation is more consistent with observations of captive spawning pollock, which did not feed and were preoccupied with spawning behavior (Baird & Olla, 1991). It is also possible that the spawning state may change the TS of pollock (Ona, 1990), which would influence any model that relies on TS to convert catch to backscatter.

4.4.4. Covariate effects on Selectivity

Similar to catchability, trawl selectivity has been shown to be influenced by conditions during capture, such as seasonality (Ozbilgin, 2006) and light levels (Chapter 2). The effect of condition factor on juvenile escapement may be best interpreted by distinguishing trawl escapement as either active or passive. *In situ* observations of pollock escaping the trawl partially support active escapement (Chapter 3), while recapture experiments have shown greatest escapement when light falls below visual thresholds, suggesting that passive escapement is responsible for loss of fish from the trawl body (Chapter 2). Condition is positively correlated with an increased activity state and therefore increased locomotive ability (Lapointe et al., 2006), which could enable a greater rate of active escapement, similar to the expected effect of temperature. More experimentation is needed to confirm this hypothesis, with potentially important outcomes on interpretation of survey data given the importance of trawl selectivity in acoustic surveys of pollock (Chapter 5).

In addition to general agreement between experimental measurements of selectivity (Chapter 2) and the current study, the vessel effect on selectivity also parallels experimental results. The OD conducted two experiments resulting in a mean juvenile (1-14 cm) retention rate of 0.136. The third experiment was conducted with the MF, resulting in a juvenile retention rate of 0.02. The median juvenile retention estimated by the model for the DY was 0.254 and the MF at 0.091. The rates were higher for model estimates, but the general pattern was consistent. The reason for the higher retention of

juvenile fish in the trawl when using a noise-quieted vessel is not known, but may be related to the increased fish diving behavior observed in reaction to the passing of the noisier MF (De Robertis & Wilson, 2010), especially on shallow fish aggregations that are usually composed of juveniles (Guttormsen et al., 2010). Codend liner mesh size did not improve model fit, which is interesting primarily because the motivation for incorporating a liner in the codend was to increase retention of juvenile pollock. No paired catch comparison studies were made when changing from larger to smaller mesh liners. This study suggests that the liner effect may not be a large factor in trawl selectivity for pollock.

4.4.5. Conclusions

Catchability has been found to vary with environmental factors in bottom trawls used to estimate fish abundance (Kotwicki et al, *in press*, Addison et. al, 2003, Aglen, 1996, Michaelsen et al., 1996), but pelagic survey trawls have not been studied. In contrast to surveys where catch is used as a direct measure of density, the efficiency of the midwater trawl may not have as strong an effect on acoustic survey estimates, as long as the catch-derived length composition is representative of the population. For this reason, ambient temperature, and spawning proportion may not be of critical importance, while the effects of fish condition and survey vessel on selectivity may be more important. The diel effect was not found to be significant for selectivity. This model result contrasts with recapture experiments where escapement was greater during the night (Chapters 1,2). Results of this study may encourage further research on vessel effect in selectivity,

because selectivity has been shown to have large impacts on acoustic-based survey results of pollock populations in the GOA (Chapter 5).

This study applies a novel method of using acoustics and catch data to model trawl performance and fish behavior. Acoustic data were used to provide an independent density measurement against which to measure fish behavior during trawl capture. Due to the indirect assessment of fish behavior using acoustics, study results are indicative of the magnitude and directivity of covariate effects, rather than estimates of changes in efficiency or selectivity. The study also highlights potential risks when using trawl catch to define fish distribution in relation to environmental or other covariates, because it may be difficult to distinguish between true patterns in fish abundance and biases in the trawl data caused by the same variables.

CHAPTER 5. EFFECT OF TRAWL SELECTIVITY ON THE ACOUSTIC SURVEY AND ASSESSMENT OF GULF OF ALASKA WALLEYE POLLOCK (*THERAGRA CHALCOGRAMMA*).

5.1. INTRODUCTION

Acoustic-based abundance estimates of fish populations require trawl samples to estimate fish lengths and species compositions of acoustic backscatter measurements. Fish length frequencies are used to convert backscatter into fish abundance, as acoustic reflectivity of individual fish is length-dependent. Inaccuracies in length composition derived from catch are propagated into abundance estimates (Simmons & MacLennan, 2005), with their effect being further magnified by the scaling of the catch data across all backscatter represented by the trawl catch. For this reason, sources of error in trawl samples should be investigated when assessing uncertainty of survey abundance estimates.

Trawls are selective samplers (Wileman *et al*., 1996), resulting from unequal vulnerability of fish sizes and species to the trawl gear. Trawl selectivity, trawl avoidance, and vessel avoidance during trawling can potentially result in a difference between species and size compositions observed in the catch and those in the acoustically observed population (Bethke *et al*., 2010). Length selectivity, caused by size-dependent probability of being retained by a trawl, can cause biased estimates of fish population length structure when trawl catches are used as representative population samples (Nakashima, 1990; Godo & Sunnana, 1992). In most cases, trawl selectivity results in the

under-retention of smaller fishes due to higher levels of escapement through the trawl meshes.

When assessing the role of trawl selectivity in a stock assessment, it is important to scrutinize the survey analysis as well as the treatment of survey data in the stock assessment. If trawl selectivity is assumed to result in a constant bias, it will result in a smaller impact on population assessments as survey time series are treated as relative abundance indexes in stock assessment models (Rose *et al*., 2000; Walters & Martell, 2004). The reduced accuracy of the estimate may affect other uses of the data where the population is not modeled, such as ecological studies. If the constant selectivity assumption cannot be met, and trawl selectivity-induced error varies from year to year, then the accuracy of stock assessments will be reduced due to increased uncertainty in the size and composition of the population. Of greatest concern is the potential for multi-year patterns in selectivity-induced error, which could lead to trends in the data that differ from those in the true population.

Trawl selectivity impacts acoustic-trawl (AT) surveys in different ways than in surveys where abundance is assessed using catch-per-unit effort (CPUE). In the latter case, selectivity of the survey gear can be estimated in the stock assessment model, as it represents a constant relationship between survey observations and modeled populations (Somerton *et al*., 1999). In contrast, acoustic surveys estimate abundance using backscatter (i.e. reflected acoustic energy), and trawl catches are used to convert acoustic density estimates to fish abundance. Effects of trawl selectivity on acoustic survey results could vary across years even if trawl performance is assumed constant across the

survey time series, a common assumption in resource surveys where efforts are made to standardize trawl gear configuration and its operation (Walsh, 1996).

The effect of selectivity can be explored by evaluating the sensitivity of the AT survey abundance estimate to biased catch data. Incorporating trawl selectivity into abundance estimation requires a re-analysis of the AT survey data using length-frequency data that are modified to correct for underestimated abundance. Uncertainty in trawl selectivity estimates also needs to be propagated through the re-analysis of survey data, ensuring that this error is included in the overall estimate of survey uncertainty.

By extension, the effects of selectivity should be evaluated for stock assessment models which are fitted to survey data. A common assumption when modeling populations is that survey-based estimates of demographic structure are biased (Walters & Martell, 2004. To address this bias, models incorporate selection functions for surveys. It is expected that these functions adjust for survey trawl selectivity. However, this may not be a valid expectation for acoustic surveys due to the distinct effect of trawl selectivity on survey abundance estimates. As population models are often the primary quantitative tool for deriving harvest recommendations, it is important to assess the sensitivity of model outputs such as spawning stock biomass (SSB), recruitment (R) and fishing mortality (F) to trawl-selectivity. To examine model sensitivity, the stock assessment model has to be re-run with selectivity-adjusted abundance estimates, followed by a comparison of model outputs to original results.

This study investigates effects of length-selectivity of midwater trawls used in acoustic surveys for walleye pollock (*Theragra chalcogramma*; hereafter referred to as pollock) in the Gulf of Alaska (GOA) on the survey abundance estimates and the stock assessment model outputs. The pollock stock in the GOA is assessed using a statistical catch-at-age model fitted to data from the commercial fishery, and the research bottom trawl and acoustic-trawl surveys (Dorn *et al*., 2009). The AT survey provides abundance estimates for younger age classes which are mostly pelagic (Karp & Walters, 1994), and are not available to the bottom trawl survey or caught by the commercial fishery. AT surveys are conducted annually during the spawning season (Feb – Mar) when large spawning aggregations of pollock are found in Shelikof Strait (SS; Guttormsen *et al*., 2010), which is used as an abundance index for the entire GOA pollock population. At this time of the year, large numbers of juvenile pollock (<3 years old) are also encountered in SS. In some areas, juvenile and adult pollock occur in mixed aggregations, and trawl-catch samples of these aggregations have the greatest potential for selectivity bias as a large length range of fish is present in each catch. Trawl length selectivity was experimentally determined in SS in 2007 and 2008 (Williams *et al.,* 2011) using recapture nets to estimate escapement of fish from the entire trawl. The resulting selectivity estimates, and their uncertainty, are used in the current study to modify AT survey abundance estimates for SS, which were then used to fit the GOA pollock stock assessment model.

5.2. MATERIALS AND METHODS

5.2.1. Computation of abundance based on acoustic survey data

Acoustic-trawl surveys of pollock combine several sources of data to produce estimates of length- specific abundance in the surveyed area. The primary data source is the reflected acoustic energy, or backscatter, from animals measured by scientific echosounders. Backscatter from fish aggregations is integrated over depth intervals to quantify acoustic density per unit area (s_A m^2/nmi^2; Simmonds & MacLennan, 2005). When processing acoustic data, backscatter judged to be from pollock is integrated over the water column and averaged within 0.5 nmi horizontal bins along each survey transect (Honkalehto et al., 2008).

The second component of the AT survey data is biological sampling of pollock using survey trawls. Pollock are semi-demersal, with a large component of the population occurring in midwater aggregations, and are therefore sampled using a midwater trawl. In the SS survey, the midwater trawl used is an Aleutian wing trawl (AWT), with a vertical opening of 25 m and a horizontal opening of 45 m when fishing. Trawling is conducted opportunistically following established protocols (Honkalehto et al., 2008) intended to optimize effort by disproportionately sampling areas with higher fish density. Trawl catches are processed to provide species composition, length frequency, and other biological data.

Backscatter is converted into fish density by dividing s_A by the mean acoustic reflectivity of individual targets (i.e. backscattering cross-section or target strength [*TS*]*;* Simmonds & MacLennan, 2005). The *TS* for pollock is length-dependent (Traynor, 1996), so the average *TS* for an aggregation of pollock is obtained from the length composition of the trawl catch thought to represent the aggregation. In this process, hauls with similar length frequency distributions are pooled to reduce the influence of any individual haul. Fish

density estimates are scaled to total abundance for the survey area and then converted into biomass using a length-weight relationship computed from individual fish weight measurements collected during the survey. The survey analysis is illustrated graphically in Figure 5.1, and demonstrates how the length-specific abundance is directly linked to estimates of the length composition of pollock from trawl data. Details of the acoustic conversion computations as they pertain to the pollock acoustic surveys are given in the Appendix A5.1.

5.2.2. Theoretical effects of trawl selectivity on acoustic survey results

A simulated data set was used to illustrate how trawl selectivity influences acoustic-based density estimates. Three cases were examined; juvenile pollock (mean = 13 +/- 3 cm), adult pollock (40 +/- 10 cm), and a mixed population of adults and juveniles. The previously described process was used to convert pollock acoustic backscatter to abundance-at-length. If these populations were selectively sampled using trawls, and the resulting catch-based length frequency was used to convert acoustic backscatter (s_A) to abundance, then the resulting estimates would be biased in terms of population abundance, biomass, and length composition. To quantify how theoretical expectations may influence survey data, a mixing index *d* was computed as

$$d = 1 - abs\left(p_{juvenile} - p_{adult}\right) \quad (5.1)$$

where $p_{juvenile}$ is the proportion of fish under 20 cm and p_{adult} is ≥ 20 cm. Greater than 90 % of age-1 pollock in SS in the winter are below 20 cm, and > 90 % of age 2+ pollock

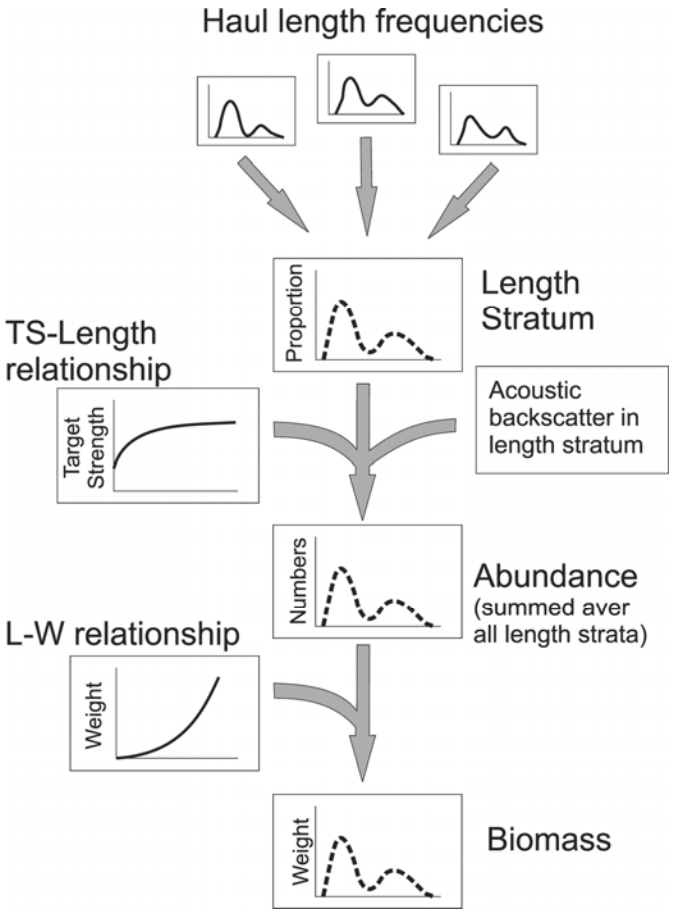

Figure 5.1. Flow chart illustrating walleye pollock acoustic-trawl survey abundance estimation, representing a single length stratum, several of which are combined for total survey biomass estimates. This process combines measured acoustic density (water-column integrated backscatter) with trawl catch data to estimate fish abundance and biomass.

exceed 20 cm (Guttormsen et al, 2010), allowing length to be used as a proxy for age. A *d* value near 0 indicates a homogeneous juvenile or adult population, while a *d* value near 1 represents a balanced mix of adults and juveniles in the same haul.

5.2.3. Implementing a trawl selectivity correction in survey abundance computation

Two experimental sets of hauls were taken in SS in 2008 (C1) and 2007 (C2) to estimate selectivity of a midwater trawl (Chapter 2). The latter experimental set had higher estimates of L_{50}, defined as the length at which 50% of the fish are retained (Fig. 5.2). In Chapter 2, a hierarchical Bayesian model was used to estimate selectivity, providing an estimate of the posterior predictive distribution for selectivity parameters L_{50} and selection range (*SR*) for each trawl set. *SR* is the length range between 25% and 75% retention points on the selection curve. These distributions represent the values of selectivity parameters for an unknown haul using the same trawl gear in SS.

A Monte Carlo re-sampling method was used to propagate uncertainty in selectivity parameters estimated from experiments. First, for each haul sample, random selectivity parameter values (L_{50} and *SR)* were drawn from the posterior predictive distributions derived from a hierarchical Bayesian model as described in Chapter 2. These values were used to estimate trawl selectivity *S* at length class *l* as:

$$S_l = \left(1 + e^{\left(\frac{k(L_{50}-l)}{SR}\right)}\right)^{-1} \quad (5.2)$$

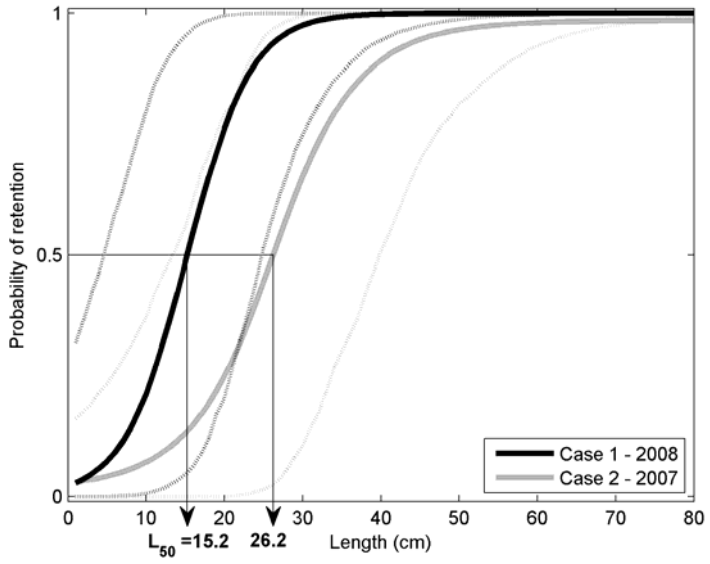

Figure 5.2. Trawl-selectivity curves with 95% credibility intervals for a midwater trawl used to sample walleye pollock in Shelikof Strait, Alaska. The two curves represent two separate experiments conducted in 2007 and 2008 (for details see Chapter 2).

where k = 2*log(3) (Wileman et al., 1996). The estimate of the true length composition in the population (g_l) for each haul was then computed as

$$g_l = {f_l}/{s_l} \tag{5.3}$$

where f_l is the measured catch-at-length. g_l was then used in place of f_l to estimate the abundance-at-length for the survey, following the methods described in the Appendix A5.1. The assignment of hauls to length strata was not changed when re-computing the abundance estimation; it is assumed that the pooling of hauls into length strata is unaffected by the selectivity correction. The correction process was repeated 500 times to determine the coefficient of variation (CV) and the mean values for abundance estimates. These estimates were then compared to original estimates derived using the uncorrected data. Surveys conducted in 1993 to 2010 were used for the correction, because this is when the AWT midwater trawl was used as the trawling gear, and the acoustic data necessary for reanalysis of the survey abundance estimates were not available for years prior to 1992.

A cohort-based analysis was performed to compare original cohort depletion rates with those resulting from the selectivity correction of the survey results. All 1992-2001 pollock cohorts (e.g. 1992 year class appearing in the 1993 survey as age 1 pollock) were normalized by the overall cohort abundance through age 8, yielding proportions at ages 1-8. Cohort proportions-at-age were averaged across year classes using an arithmetic mean to examine cohort depletion.

5.2.4. The Gulf of Alaska Pollock stock assessment model

The GOA pollock assessment model is fitted to data from the commercial fishery and six resource survey indexes, two of which result from the AT survey conducted annually in SS (Dorn et al., 2009). The survey provides a biomass index, consisting of the total estimated pollock biomass for ages ≥ 2, and a demographic index consisting of the numbers-at-age for ages 2 through 10, with the age 10 group containing all fish aged 10 and above. The model age structure is constrained to age 2+ due to the high uncertainty in survey estimates of age 1 pollock, and assumed high variability in survival of pollock from age 1 to age 2. The AT survey abundance estimate of age-1 pollock is used as a separate index of year class strength.

Survey data are used for assessment model parameter estimation through maximum likelihood, which defines the probability of observing the survey data given the model parameters. For the AT survey, the likelihood (L) consists of two components. The first is total survey biomass is modeled under the assumption that it is log-normally distributed:

$$\log L = -\sum_i \frac{[\log(B_i) - \log(\hat{B}_i)]^2}{2\sigma_i^2} \tag{5.4}$$

where B_i is the survey biomass, σ is the standard deviation of the logarithm of the biomass, and $\hat{B}_i$ is the model-predicted survey biomass in year i:

$$\hat{B}_i = q \sum_j w_{i,j} s_j N_{i,j} e^{-\phi_i Z_{i,j}} \quad (5.5)$$

where q is the survey catchability coefficient, $w_{i,j}$ is the mean weight-at-age j in year i, s_j is the survey selectivity for age j, $Z_{i,j}$ is the total mortality on animals of age j during year i, and ϕ_t is the proportion of the year elapsed when the survey was conducted (for further details on the assessment model, see Dorn *et al*., 2009).

Equation 5.5 shows that the model abundance is not directly compared to survey estimates, because the survey is assumed to be a relative index of abundance. Two terms are used to scale the model population to the expected survey index value: the catchability coefficient q which determines the relationship between the survey-estimated biomass and the model derived biomass, and survey selectivity s which defines the bias between observed and modeled population demographics.

The AT survey time series is separated into three time periods because of changes in acoustic technology, each with its own estimate of q. The first period is associated with the Biosonics echosounder used from 1981 to 1992, the second represents the change to the Simrad EK500 echosounder (1993 – 2007), and the third reflects the change in the survey vessel from the Miller Freeman to the Oscar Dyson (2008 – 2011) and also includes a switch to the Simrad EK60 echosounder. The Oscar Dyson was specifically designed to reduce underwater radiated vessel noise and therefore reduce fish avoidance reactions during surveys (i.e., increase catchability, De Robertis & Handegard, 2012). In trawl-based surveys, q is thought to be primarily a function of trawl gear performance, but in the pollock AT survey the acoustic instrumentation is considered more important

in defining q, exemplified by not including separate q values corresponding to when the midwater trawl was changed over the time series.

Survey selectivity consists of a vector of probabilities by age. The form of the selectivity function was determined by examining systematic differences between age distributions observed in the AT survey data and those in the assessment model. Survey selectivity essentially indicates the availability of each age class to the AT survey. For the GOA pollock assessment, AT survey selectivity is defined as an inverse logistic function

$$s_j = 1 - \left(1 + e^{(-b(j-a))}\right)^{-1} \tag{5.6}$$

where a and b are (estimable) selectivity parameters and j is the age class from 2 to 10. For this study, selection was re-scaled to s at age 2, such that $s_2 = 1$. Scaling s prevented poorly determined fits due to confounding of q estimates with survey selectivity.

The second component of the likelihood function was used to include survey estimates of age composition in the assessment:

$$\log L = \sum_i m_i \sum_j \pi_{i,j} \log\left(\frac{\hat{\pi}_{i,j}}{\pi_{i,j}}\right) \tag{5.7}$$

where m is the number of age samples, and the expected proportions at-age in the survey $\hat{\pi}$ are calculated as

$$\hat{\pi}_{i,j} = \frac{s_j N_{i,j} e^{-\phi_i Z_{i,j}}}{\sum_j s_j N_{i,j} e^{-\phi_i Z_{i,j}}} \quad (5.8)$$

Note that σ^2 from Equation 5.4 and m represent the amount of expected variance in estimates and are pre-specified, with σ^2 being approximated by the estimate of survey CV. These estimates ranged from 12 to 35 % for the first catchability period (1981 – 1992), and were fixed at 20 % for the latter two catchability phases of the time series (Dorn et al., 2009).

Age-1 abundance from the AT survey (termed the McKelvey Index; Mckelvey, 1996) is used as an index of recruitment of age 2 fish in the year following the survey. The model is fitted to this index using the same assumptions and structure (Equation 3) as in fitting the AT survey biomass, but using survey abundance (N, in billions) instead. The expected index value $\hat{I}$ is:

$$\hat{I}_i = q_m N_{i+1,2} \quad (5.9)$$

such that the number of age 2 fish in year i is expected to be proportional to the number of age-1 fish observed in the survey the previous year I_{i-1}, with q_m being a year-invariant proportionality factor rather than the true "catchability" of age 1 fish. The McKelvey index is heavily down-weighted in the model fitting due to large uncertainties in age 1 abundance as estimated by the AT survey (Dorn, personal comm.).

Parameters pertaining to the AT survey estimated by the assessment model are catchability (q) for the three survey periods, two selection parameters (a,b), and q_m. The

model was fitted to the original survey data, and data sets created by applying the two trawl-selectivity cases (C1 and C2), and a final data set where (for C2) the AT survey coefficient of variation (CV) was increased by adding the CV from the survey correction process described above (C2 + CV). Model fitting was performed using AD Model builder software (Fournier *et al*., 2011).

5.3. RESULTS

5.3.1. Simulation results

Theoretical changes to biomass estimates due to selectivity depended on the length compositions of the three test cases (Fig. 5.3). As expected, the smallest effect was seen with adult fish, as the majority of the length distribution was fully retained by the gear (i.e. selectivity = 1). The largest selectivity-induced change in length frequency was seen when the population was mixed. The mixed population case resulted in an 82 % underestimate of juvenile biomass when abundance-at-length was converted to abundance-at-weight using a representative length-weight relation for Gulf of Alaska pollock (Guttormsen *et al*., 2010). Interestingly, there was a 9 % overestimate in juvenile biomass when there were only juvenile fish, because the post-selection length composition was increased by ~2 cm compared to the actual frequency distribution. Even though the increase in length resulted in a higher average *TS*, and therefore fewer individuals per unit of s_A , the greater rate of increase in individual fish mass resulted in a net increase in total biomass. The greatest potential error was observed in the mixed size populations where a selective trawl sample can simultaneously cause an underestimate of

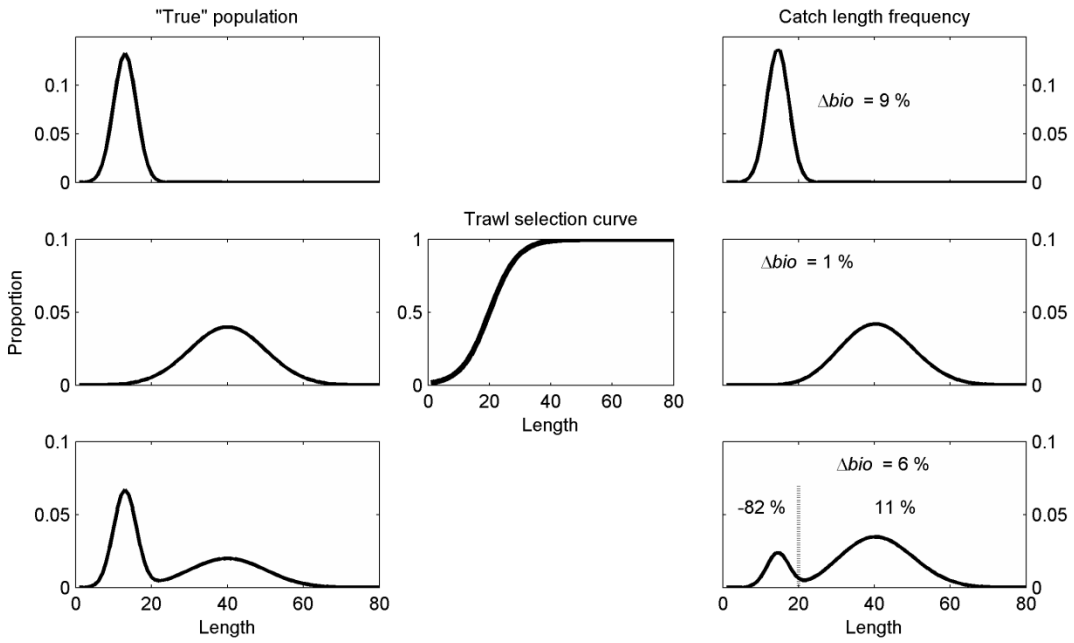

Figure 5.3. Theoretical expectations of how trawl-selectivity might influence acoustically-derived abundance-at-length and -at-biomass estimates. Three cases represent possible effects depending on catch composition and selectivity. *Δb* represents the change in estimated biomass due to trawl selectivity, relative to the "true" biomass.

juvenile biomass and abundance and a overestimate of adult biomass, as acoustic backscatter originating from juvenile fish was erroneously ascribed to adult fish. The effects on juvenile fish in the first test case were also present in the mixed population case, but its effect was overshadowed by the large reduction in juvenile abundance and biomass relative to adult fish.

5.3.2. Changes in acoustic survey time series with selectivity correction

The reanalysis of historical survey data using two selectivity functions resulted in lower biomass estimates for both cases relative to the original biomass (Table 5.1), indicating an overestimate of the biomass as predicted by theoretical computations for mixed-size trawl catches (Fig. 5.3). In general, the selectivity-corrected biomass time series showed a similar pattern of change over time as the original series (Fig. 5.4, top). A closer look at the relative biomass differences, expressed as percentage changes from the original results, (Δb; Fig. 5.4 bottom) showed that the change was proportionally greater in the latter third of the time series (2005-2010).

To examine potential explanatory factors and assess patterns in Δb, correlations were computed with three sets of data descriptors. Δb was correlated (r^2 = 0.69, 0.57 for C1 and C2) with the mean fish length encountered during the survey. Years with higher proportions of juvenile fish were more affected than those dominated by larger fish (Fig. 5.5). A weaker correlation (r^2 = 0.44 in both sets) was observed with the mean mixing index d (averaged over hauls for a given survey). Δb was uncorrelated with overall stock

Table 5.1. Changes to acoustic survey biomass and abundance estimates resulting from trawl selectivity corrections relative to original estimates. Mean changes to survey biomass, CV of survey biomass, and survey abundance averaged over the 1993-2011 time series. Parentheses show the ranges of relative percent deviations across the time series.

Selectivity Correction	Case 1	Case 2
Mean biomass change (%)	-9.3 (-21.5 – -2.7)	-23.3 (-42.5 – -10.6)
Biomass CV	0.06 (0.02 – 0.14)	0.10 (0.04 – 0.21)
Mean change in numbers (%)	49.8 (10.2 – 85.1)	124.5 (31.7 – 234.7)

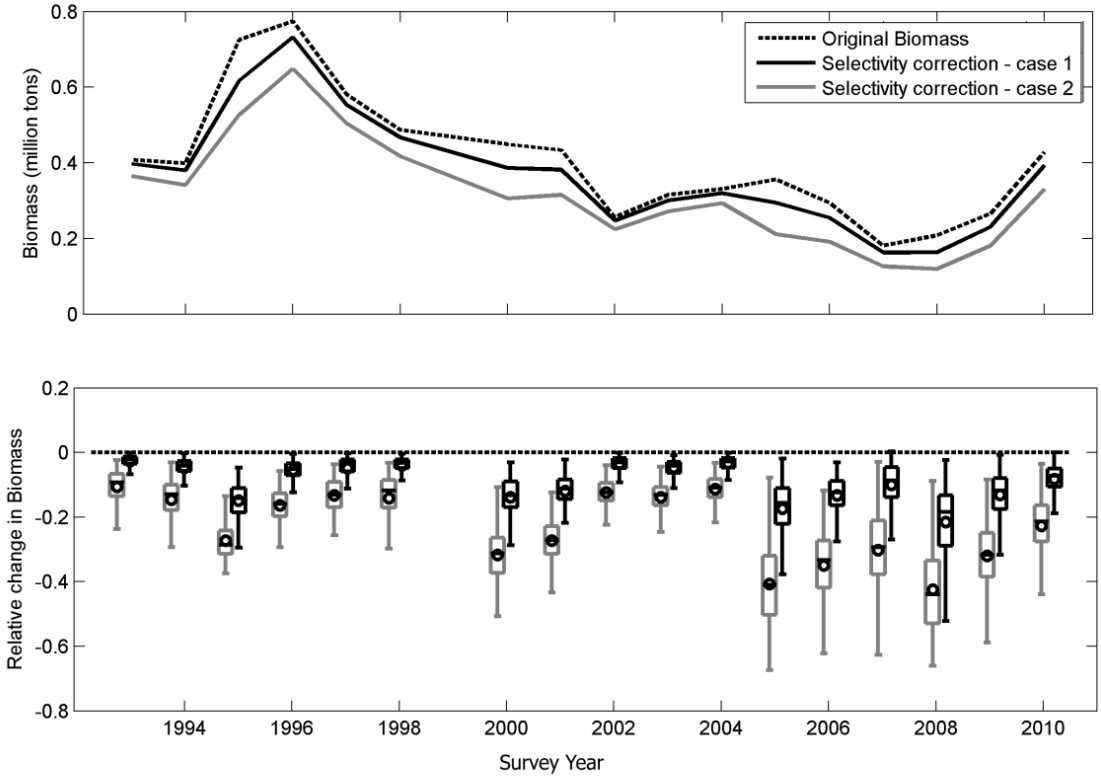

Figure 5.4. Biomass estimates for walleye pollock in Shelikof Strait, Alaska, comparing original estimates with trawl-selectivity corrections based on applying two trawl-selectivity curves (case 1 & case 2; upper panel). Relative changes and trawl-selectivity based uncertainty in biomass estimates are plotted in the lower panel.

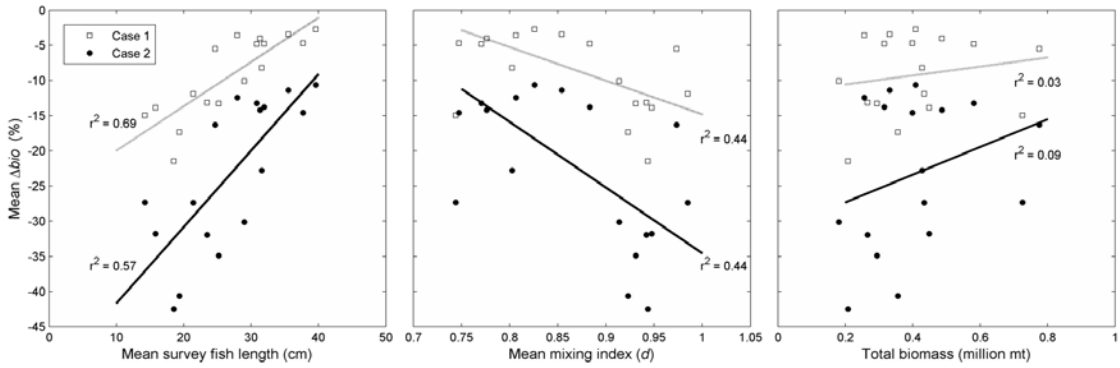

Figure 5.5. Correlations of the relative change in acoustically-derived walleye pollock biomass in Shelikof Strait, Alaska, and mean fish length, mean juvenile-adult mixing ratio, and total survey estimated pollock biomass. Points represent individual survey years.

biomass (r^2 = 0.03, 0.09). This result was not expected given that the latter third of the survey abundance time series (2005-2010) had the highest mean Δb and the lowest mean biomass.

Selectivity-induced error was also evident in survey estimates of population age composition. The original age distribution underestimates abundance of juveniles (age-1 -2), and overestimates the abundance of adult (age 3 +) pollock (Fig. 5.6). This finding is consistent with expectations when hauls contain mixtures of juvenile and adult pollock. The change in estimated age-1 abundance in case 2 was almost 1.5 orders of magnitude (13.6 times the original estimate). While the overall biomass was reduced an average of 23 % for case 2 (Table 5.1), age-1 and age-2 biomass increased 168 %, and adult biomass (age 3+) decreased 35 %.

The selectivity-corrected values show a much steeper cohort depletion curve relative to the original data (Fig. 5.7), which may be more consistent with higher natural mortality at juvenile stages, specifically for age-1 fish. The depletion curves for the two corrected survey time series were less variable across cohorts than the original data, indicating that the correction may explain some of the variation observed in the cohort analysis based on survey abundances.

5.3.3. Changes in Stock Assessment model outputs with selectivity correction

The stock assessment model fitted with corrected AT survey data showed small changes (≤ 5 %, Fig. 5.8) relative to the original data in model-predicted spawning biomass and

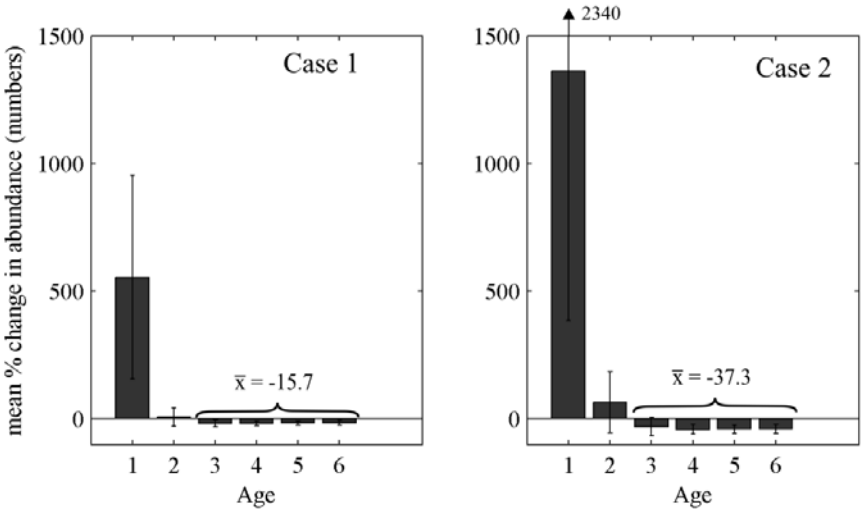

Figure 5.6. Relative changes in numbers-at-age of walleye pollock of two trawl-selectivity corrected time series relative to original abundance for the acoustic-trawl survey of Shelikof Strait, Alaska.

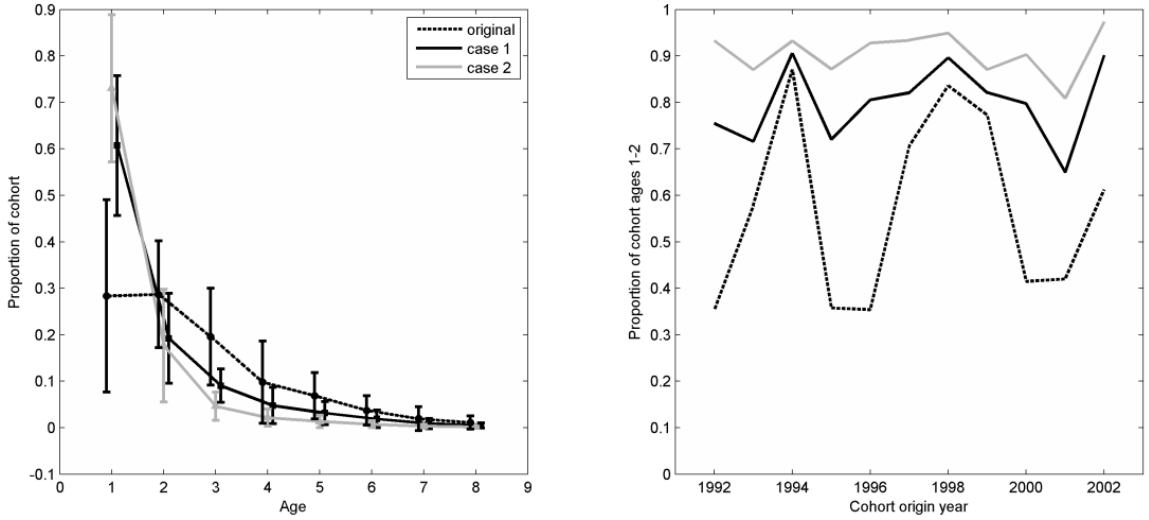

Figure 5.7. Cohort analysis of original and trawl-selectivity-corrected age-composition of walleye pollock in Shelikof Strait, Alaska. Left panel shows normalized cohort depletion averaged over 1992-2001 cohorts. Right panel shows the cohort-specific changes in normalized cohort composition (age 1-2 as a proportion of total).

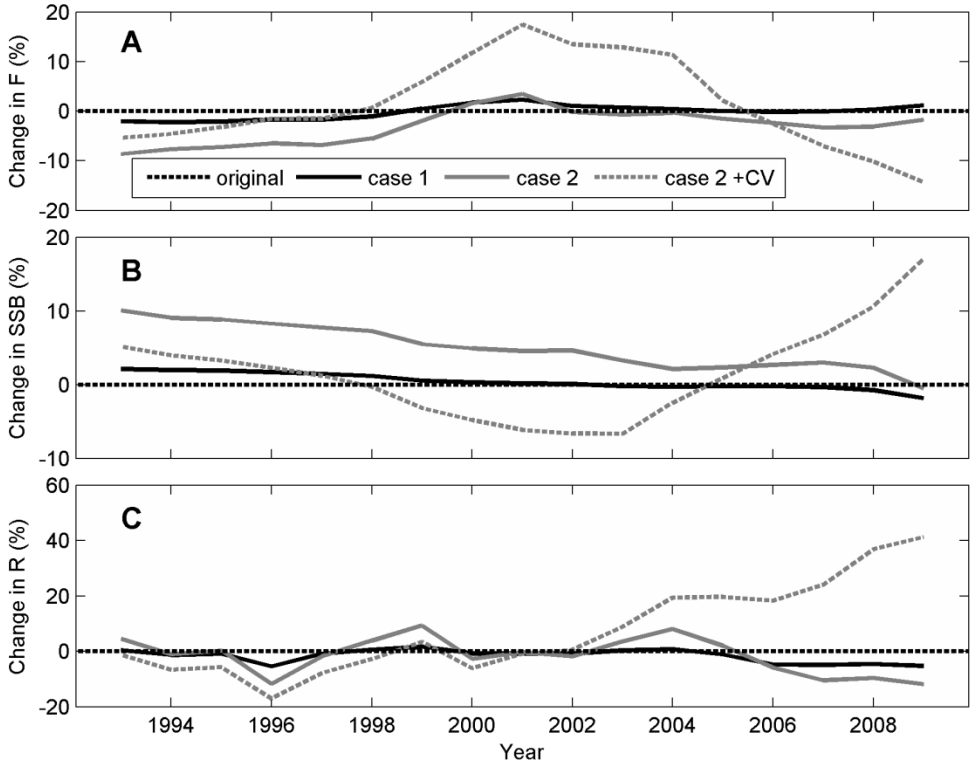

Figure 5.8. Percent changes in GOA walleye pollock stock assessment model outputs of a) Fishing mortality (F), b) spawning stock biomass (SSB), and c) recruitment (R) relative to the original values when the assessment is fitted using two levels of trawl-selectivity corrected data (C1 & C2) and C2 with increased survey CV (C2+CV).

fishing mortality from the pollock trawling fleet, the only directed fishery for pollock in the GOA. The largest change in model outputs was observed in the C2 + CV run, especially in recent years (≥ 2006) where the population appears to have an increased recruitment (~ 41 % in 2009), and higher SSB (~ 17 % in 2009) relative to the original values. The increase in recruitment and SSB with the C2 + CV run were also seen in the model numbers-at-age, with an increase in numbers of 2-5 year old fish relative to the original model state (Fig. 5.9). In the C1 and C2 data sets, minor differences in model age composition were seen between model runs, with the possible exception of age 10+ fish in run C2.

Differences were observed in model estimates of survey selectivity, with a distinct shift towards reduced availability of ages 6-9 when fitting C2 and C2 + CV selectivity-corrected data (Fig. 5.9). The largest change was observed for age-6 fish, where availability to the survey was reduced from 84% in the original data to 45% using the C2 corrected data. An increase in survey uncertainty (i.e. survey CV) did not affect estimates of selectivity parameters relative to C2 data. The substantially different appearance of the selectivity curve in runs C2 and C2 + CV suggest that large changes to the original survey data with these corrections may justify a different functional form for survey selectivity.

Model outputs were also examined for effects of trawl-selectivity on model forecasts of total biomass, survey estimated biomass, exploitation rate and recruitment, which provide critical information for fishery management actions. Forecasts were made using a harvest control rule to reduce the target fishing mortality when the stock biomass is depleted beyond a reference point of $B_{40\%}$ (i.e. 40 % of un-fished level; Dorn et al., 2009). Total

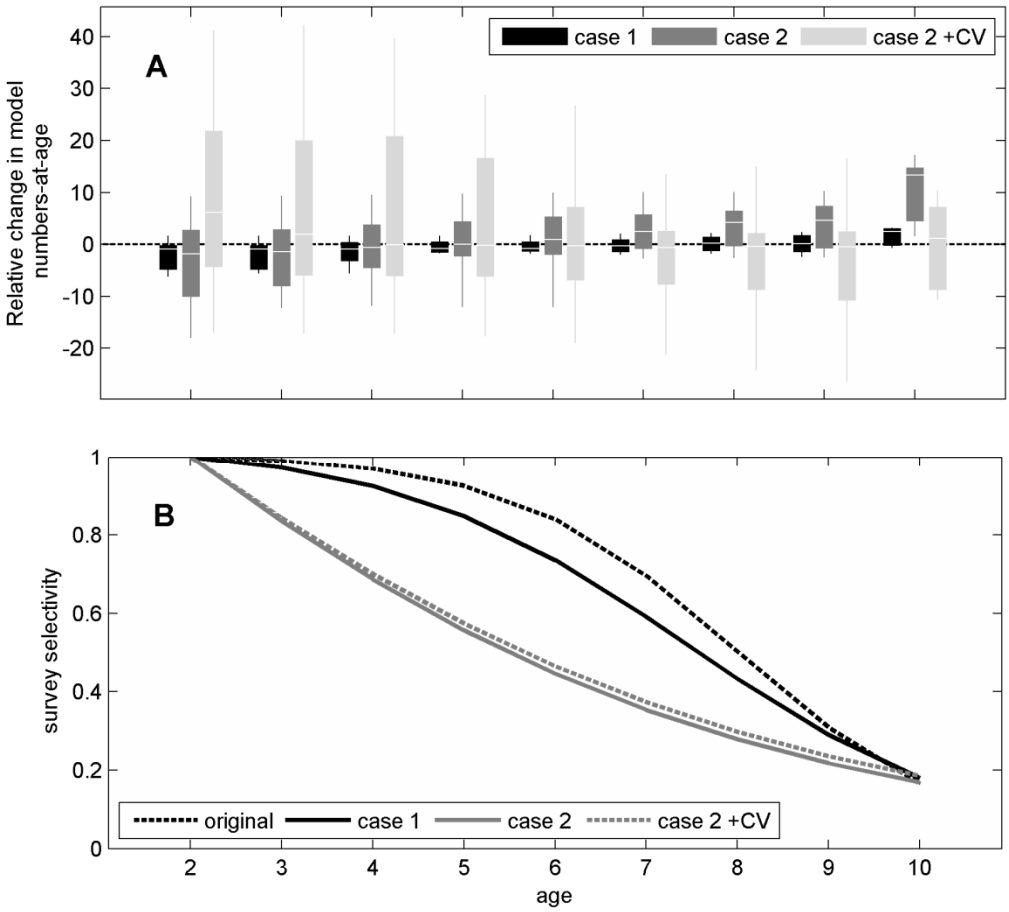

Figure 5.9. Distributions of relative differences in model estimates of numbers-at-age between original data fits and when fitted with two levels of trawl-selectivity corrected data (C1 & C2) and C2 with increased survey CV (C2+CV) (upper panel). Lower panel shows model estimates of survey selectivity (*s*) for each data set used in comparative model runs.

biomass predictions, exploitation rate, and recruitment forecast for 5 years did not change appreciably (< 1%) for C1 and C2 data in terms of parameter estimates (< 1%) and their variance (Table 5.2). More substantial changes occurred in the forecast of survey biomass for these runs. Total biomass increased by 19% when additional uncertainty was added to survey data (C2 + CV), and smaller changes were observed in other parameters continuing trends observed in Figure 5.8. Increased survey CV also doubled the uncertainty in predicted total biomass, and increased uncertainty in survey biomass to a lesser degree. The forecasted fishing mortality was not substantially different between model runs.

The catchability estimates (q) for the three time periods of the AT survey showed little change when model was fit to C1 data. However, fitting C2 data resulted in higher estimates of q in all survey phases, and q values using C2 + CV data diverged even further (~ 20%) in the two more recent periods (Table 5.3). As expected, q_m showed the largest changes as the abundance estimates for age-1 pollock were most affected by trawl selectivity. As model fit was evaluated using likelihood, changes in the log-likelihood of specific components that relate the model to survey data (e.g. age-composition and biomass) were examined to see whether corrected data improved model fit. Log-likelihood decreased when the corrected age structure was used (Equation 5.8), while biomass index values showed slight increases in likelihood using C1 and C2 data (Equation 5.7). Total model log-likelihood increased in cases C1, and C2+CV but was reduced in runs with C2 data (Table 5.3).

Table 5.2. Parameter values and standard deviations of model predictions for a five year horizon for three GOA walleye pollock stock assessment model outputs fitted with two levels of trawl-selectivity corrected data (C1 & C2) and increased survey CV (C2+CV). Percent change relative to original data projections is given in parentheses.

Data set	original		C1		C2		C2 +CV	
Total biomass	1.019	0.043	1.017 (-0.2)	040. 3	1.029 (0.9)	0.044	1.213 (19)	0.101
Survey Estimated biomass	0.634	0.042	0.579 (-8.7)	0.038	0.504 (-20.4)	0.033	0.620 (-2.2)	0.059
Exploitation rate	0.172	0.009	0.172 (0.1)	0.009	0.172 (0.4)	0.009	0.167 (-2.7)	0.008
Recruitment	0.689	0.031	0.692 (0.4)	0.031	0.688 (-0.3)	0.031	0.717 (4.0)	0.033

Table 5.3. Change in catchability estimates and selected likelihood components from GOA walleye pollock stock assessment model runs fitted to data with different levels of trawl-selectivity corrected data (C1 & C2) and increased CV (C2+CV). Changes relative to original data (%) are given in parentheses.

Catchability (q)				
Time period	original	C1	C2	C2 +CV
1981 – 1992 (Biosonics)	0.86	0.90 (5.19)	1.15 (33.91)	1.15 (33.97)
1993-2007 (EK500 – MF)	0.88	0.87 (-1.38)	0.99 (12.60)	1.05 (19.19)
2008-2009 (EK60 – OD)	0.98	0.96 (-1.62)	1.10 (11.90)	1.18 (20.07)
McKelvey Index	0.35	0.95 (171.5)	1.44 (309.9)	1.37 (291.5)
Change in model log-likelihood				
Survey biomass		4.34	15.13	-4.19
Survey age - composition		-9.91	2.92	-9.44
Total		6.43	-14.62	20.87

5.4. DISCUSSION

Trawl selectivity affected pollock abundance estimates in Shelikof Strait, resulting in lower biomass indices, and an increase in estimates of abundance of juvenile fish, especially age-1 pollock. These changes in the survey data resulted in variable affects on stock assessment model estimates when fitted to the different trawl selectivity-modified data sets. Potential impacts on the pollock survey estimates and assessment model outputs demonstrate the importance of correctly determining trawl selectivity for acoustic-trawl surveys.

Midwater trawl selectivity can be determined with reasonable precision for a single location and time as documented in Chapter 2. However, selectivity varied among experimental locations and years. This study applied two estimates of trawl-selectivity to measure the sensitivity of the survey data and subsequent assessment model results to a range of trawl-selectivity values. Estimates of selectivity used to correct survey data in the second case (C2) may represent an extreme situation due to the lower retention of age-1 fish compared to C1, providing a potential upper limit for selectivity-induced errors. A definitive correction of the survey data for stock assessment will require additional estimates of trawl-selectivity, or a method to combine the results from the two selectivity experiments conducted in SS. A combined analysis would provide a single selectivity parameter set, but would likely have higher uncertainty due to differences in selectivity parameter estimates in the two trails.

The largest effect of correcting for trawl selectivity occurred in AT survey abundance estimates for age-1 pollock. This result was expected due to substantial under-sampling

by the midwater trawl. Similar results for trawl selectivity corrections were reported for Barents Sea cod (Aglen & Nakken, 1997). Age-1 pollock are not included in the GOA stock assessment model, partially due to the uncertainty in estimating their abundance. The substantial reduction in the abundance of age 3+ pollock due to the mis-allocation of backscatter shown in this study (Fig. 5.6) demonstrated that trawl selectivity influences acoustic survey results differently from trawl-only surveys. In acoustic surveys, the same principles that resulted in an overestimate of biomass in this study can cause an underestimate when larger, older fish are under-represented in survey trawl catches due to avoidance (e.g., Bauleth-d'Almeida *et al*., 2001).

Among individual cohorts, the corrected data were more consistent with expectations based on population dynamics, for example a log-linear depletion in abundance with age. Many of the cohorts in the original time series appeared to increase in abundance from age-1 - 2, which can be explained by under-retention of age-1 fish by the midwater trawl. In the corrected time series, variability in the depletion curve among cohorts was reduced, suggesting that mortality in the juvenile stages is less variable than would be deduced from the original data. By increasing the precision and accuracy of age-1 abundance estimates, results of this study may support expanding the assessment model structure to include age-1 fish, with potential benefits for forecasting recruitment, population demographics, and determining harvest levels.

Trends in the change in biomass estimates (Δb) over the survey time series due to trawl-selectivity are a specific concern, as the value of the AT survey biomass estimate as an index depends on the index's proportionality to the true abundance. The strong negative correlation of Δb with mean fish length supports the expectation that, when strong year-

classes of juveniles are encountered and the relative abundance of adults is lower, trawl selectivity will decrease accuracy of abundance estimates. Increased Δb in the latter third of the survey time series reflects a greater mixing of adult pollock with juveniles, as the SS pollock winter population shifted from being primarily composed of adult spawning aggregations in the upper strait to mixtures of non-spawning adults and juveniles (Guttormsen *et al.*, 2010) in the central portion of the strait.

The response of assessment model outputs to corrected data sets highlighted model sensitivity to trawl selectivity. Large changes in model state variables (*SSB* and abundance-at-age) and estimates of F and R were evident only when the survey CV was increased. Varying levels of trawl selectivity alone resulted in minimal changes in model output variables. As expected, model parameters used to fit the survey data (q and s) changed in response to the selectivity-induced changes in survey abundance and age composition. Parameters q and s reflect the dissimilarity between the observed and modeled populations due to biases in survey methodology, presenting challenges when interpreting these changes. For example, catchability is more easily interpreted when applied to trawl-only survey data, as fish herding and trawl avoidance are based on fish behavior and are often quantifiable through experimentation and observation (Somerton et al., 1999). In AT surveys, quantifying catchability and survey selectivity are complicated by the presence of the acoustic dead zone, variable target strength, and spatial layout of the survey. In this study, results suggest that catchability has to be jointly interpreted with survey selectivity. This concept is illustrated by the apparent increase in q values for C2 runs. Estimated survey biomass was substantially lower with this correction, which would theoretically result in a lower catchability as the model

attempted to reconcile changes in acoustic survey data with other survey and commercial data inputs. This counter-intuitive result was due to the simultaneous large reduction in the integral of the survey-selectivity (s) curve with the C2 data (Figure 5.9), reducing overall scalar ($q \times s$) values for the acoustic abundance at-age.

Examining survey selectivity estimates identifies future areas of acoustic survey research. Survey-selectivity values estimated by the assessment model suggest that younger age classes (<4 years) are more accurately sampled by the AT survey due to their tendency to form pelagic aggregations, while older age classes may be more unavailable due to inability to sample fish in the acoustic dead zone (Karp and Walters, 1994). The acoustic dead zone consists of the bottom 1-1.5 m of the water column (Simmonds & MacLennan, 2005) and may contain larger pollock, due to relatively larger average lengths observed by bottom trawl surveys conducted in SS (cf. Dorn et. al., 2009). Incorporating trawl selectivity in the AT data amplifies this bias, as the trawl selectivity correction further increases the relative abundance of younger age classes. It is important to note that the interpretation of survey selectivity is based on the assumption that the assessment model represents a more accurate age-composition than that derived from the AT survey. Model age-composition is driven in large part on the assumptions of natural mortality (M), especially for juvenile age classes not yet recruited to the fishery. Underestimates of M are conservative from a management perspective (Clark, 1999; Dorn *et al*., 2009), but may not accurately represent M in the "true" population (Mesnil *et al*., 2009). The well-established confounding of survey-selectivity with natural mortality (Thompson, 1994) makes interpretation of survey-selectivity dependent on the validity of natural mortality assumed in the model. For pollock, independent estimates of juvenile mortality are

higher than that assumed in the GOA assessment model (Hollowed et al., 2000), suggesting that survey selectivity should not be regarded as a deficiency of survey data, but rather a statistical tool when using survey data in assessment models.

The increase in the survey CV had the strongest effect on the assessment model outputs, suggesting that data sources used in the assessment may not be in agreement regarding the population state. Specifically, results indicated that the AT survey data were lowering model abundance estimates and, by extension, increasing fishing mortality estimates. With the increase in survey CV in the third case (C2 + CV), the AT survey became less influential in the assessment model and the estimates of biomass, numbers-at-age, and recruitment increased as fishing mortality was reduced. This response of the model suggests that other data sources, including other surveys and the commercial catch, indicate a different trend in biomass than the AT survey. This apparent data conflict may be independent of trawl selectivity adjustments, and a similar response could be expected by increasing the CV in the original data set. The influence of increased survey CV on the stock assessment results emphasizes the importance of objectively determining survey uncertainty for all data sources and model assumptions.

In this study we quantified survey uncertainty due to trawl selectivity. This approach invites a direct comparison to other sources of uncertainty in AT surveys (e.g. transect layout, haul placements, target strength, performance of acoustic instrumentation). Several studies have attempted to quantify relative magnitudes of acoustic survey errors, but none have included trawl selectivity. The main contributors to error in these studies were acoustic and geo-spatial factors (Rose *et al*., 2000; O'Driscoll, 2004; Loland *et al*., 2007). While trawl selectivity is species- and trawl-specific, surveys targeting semi-

demersal and pelagic gadoid species with large size ranges using a midwater trawl could have similar effects.

In conclusion, results indicate that the assessment model is robust to changes in biomass and abundance of juvenile (pre-recruit) age classes estimated by the acoustic survey. Even changes in survey bias due to selectivity over the data time series (Fig. 5.4) did not affect model outputs, as long as uncertainty due to trawl selectivity estimation was assumed to be contained within the total survey uncertainty specified in the model. Model outputs did change in response to increases in survey CV, however this is more likely caused by differences among data sources used to fit the model and not directly due to trawl selectivity. Studies such as this one also illustrate the need for communication between survey scientists and stock assessment modelers to determine aspects of survey data uncertainty that affect assessment model performance. An important question is whether the acoustic survey data should be corrected for trawl selectivity. In some instances, correcting survey data for trawl selectivity reduced uncertainty in an assessment (Aglen & Nakken, 1999), while other corrections such as diurnal effects resulted in increased uncertainty (Hjellvik *et al*., 2002). The large difference in our estimates of trawl selectivity between two experimental years (Chapter 2) may indicate that selectivity is variable and may increase uncertainty in the assessment derived abundance and population age structure. For this reason, further trawl selectivity work may be required to quantify variability and potential patterns in trawl selectivity. If selectivity-corrected data are to be used as routine inputs into assessment models, then increased accuracy of the age-1 abundance estimate may be sufficient to warrant an extension of the model age structure to include age-1 pollock.

CHAPTER 6. SUMMARY

This dissertation provides a comprehensive evaluation of midwater trawls as scientific instruments when surveying fish populations. Trawls are critically important devices for fisheries surveys, although the degree to which trawl catches represent true species compositions and size structures of fish populations is not typically measured. This lack of scrutiny is partially due to the difficulty of assessing trawl capture efficiency, especially for midwater trawls where escapement is difficult to measure. In trawl based surveys, the influence of biases in trawl-based sampling is minimized by treating catch data as relative indexes of abundance. Given the importance of the topic and the dearth of currently available information, the results of the studies presented here should be of interest to scientists conducting surveys of marine living resources, and to others that rely on survey data for ecological investigations and resource management.

Findings described in this dissertation represent new contributions in several areas in fisheries science. The quantitative assessment of escapement from the midwater trawl body using Bayesian modeling is a new methodological and analytical approach that can be applied to evaluate the selectivity of other survey trawls. Unbiased underwater observations of fish behavior (as described in Chapter 3) are challenging to conduct due to the limitations of remote sensing instruments, such as limited range of optics and the limited resolution of acoustic instruments. The simultaneous use of optic and acoustic instruments combined with pocket net sampling provides a method of partially overcoming instrument limitations, increasing the overall information content of field observations. The use of acoustic backscatter to provide an independent density estimate

to compare to trawl catch-based density estimates (Chapter 4) has not previously been used to estimate trawl selectivity, and has the potential to be applied in any dataset where concurrent remote and direct samples are available to estimate direct sampling selectivity.

In addition to methodological advancements (Chapters 2-4), the results further our understanding of the accuracy and precision of walleye pollock acoustic-based survey abundance estimates. Given the importance and scale of this fishery in terms of the commercial harvests and the ecological role of pollock in the North Pacific, findings in these chapters contribute to better interpretation of survey data, and by extension improvements in the pollock stock assessment that use pollock surveys and other studies that use survey data. Concordance in results among chapters, such as the comparison of juvenile escapement between chapters 2 and 4 and the influence of light seen in both chapters 2 and 3, increase the confidence in the methods and analyses used and the validity of the findings.

The likelihood of selectivity and catchability-induced biases in trawl catch is a valid reason to treat abundance estimates derived by trawls as relative indexes of abundance rather than absolute estimates. The size and variability of this bias can be indirectly estimated by fitting the data to a model of the population, assuming that surveys were conducted using standardized trawl gear and operations over several years. Estimates of bias are dependent on assumptions regarding the dynamics in the population model, such as recruitment and mortality rates of the target species. Independent estimates of selectivity and catchability, as described in this work, can be used to adjust abundance estimates without using the assessment model, resulting in estimates that are more representative of absolute abundance within the surveyed area. This approach provides a

means of testing model assumptions of population characteristics such as natural mortality, which are normally confounded with selectivity in the survey data (Thompson, 1994). In addition, as new areas are surveyed, the length of an abundance estimate time-series is less critical if absolute estimates are available. In the example of walleye pollock in the Gulf of Alaska, the survey selectivity and catchability (Chapter 5) are composite metrics that reflect our ability to determine abundance in Shelikof Strait, as well as the relationship between Shelikof Strait abundance and the entire Gulf of Alaska population. By improving survey methodology to provide estimates of abundance that can be treated as absolute values in the surveyed area, the catchability concept can be reduced to the proportion of the population that is in the surveyed area. As additional areas of the Gulf of Alaska are surveyed on an opportunistic basis, abundance estimates can be incorporated into the model with fewer assumptions and less concern regarding the length or continuity of the survey area time series. As survey data are often used for purposes other than stock assessment, such as ecosystem modeling, providing absolute values can simplify assumptions used in these analyses and improve their accuracy.

The central theme in this work is estimating values and variability of biases in trawl samples due to trawl design and fish behavior during capture. From a scientific standpoint, a more suitable approach would be to design sampling instruments that would remove or reduce these biases. Survey trawls are modified commercial fishing nets, designed with different objectives than those of a scientific abundance survey. As surveys progress into the future, a potential area of development would be to apply scientific scrutiny to the design of survey trawls, resulting in customized trawl-like devices with minimal selectivity and equal catchability across the range of species

present in the environment. This approach is commonly seen in other marine surveying programs, such as biological oceanography. For example, the design of a Bongo net involves consideration of mesh porosity, towing speed, and flow dynamics, resulting in absolute estimates of density of planktonic species. The larger size of midwater and demersal survey trawls and more mobile targets (i.e. fish) make the design process more challenging, but the approach is one that should be considered, and should include experiments that assess the effectiveness of the gear using approaches similar to the those described in this work.

The acceptance of trawl catches as biased samples of reality, and the desire to maintain the stability of trawl survey time series, has minimized innovations in survey trawl design. Acoustic-based surveys are necessarily more dependent on technological advancement in acoustic instrumentation due to the constant change in acoustic instrumentation, but the trawling aspect of these surveys is less technologically driven similar to trawl-based surveys. Applying scientific principles and state-of-the-art technologies to the design of trawls will increase accuracy in sampling, as well as potentially deriving estimates that can be treated as absolute abundances.

In conclusion, this document contains generic methods to inspire similar research, along with specific information on the walleye pollock acoustic survey and effects of trawl sampling errors on estimates of pollock abundance and population structure. The evaluation of trawls as scientific tools will continue, and may evolve into a process of custom survey trawl design, using an objective driven and scientifically based design process.

BIBLIOGRAPHY

Addison, J. T., Lawler, A. R., and Nicholson, M. D. 2003. Adjusting for variable catchability of brown shrimps (*Crangon crangon*) in research surveys. Fisheries Research, 65(1-3): 285-294.

Aglen, A. 1996. Impact of fish distribution and species composition of the relationship between acoustic and swept-area estimates on fish density. ICES Journal of Marine Science, 53:501-505.

Aglen, A. and Nakken, O. 1997. Improving time series of abundance indices applying new knowledge. Fisheries Research, 30:17-26.

Akaike, H. 1974. A new look at the statistical model identification. IEEE Transactions on Automatic Control, 19(6): 716–723

Arimoto, T., Gang, X., and Matsushita, Y. 1991. Muscle-contraction time of captured walleye pollock *Theragra chalcogramma*. Nippon Suisan Gakkaishi, 57: 1225-1228.

Arreguín-Sánchez, F. 1996. Catchability: a key parameter for fish stock assessment. Reviews in Fish Biology and Fisheries, 6(2): 221-242

Askey, P. J., Post, J. R., Parkinson, E. A., Rivot E., Paul A. J., and Biro, P. A. 2007. Estimation of gillnet efficiency and selectivity across multiple sampling units: A hierarchical Bayesian analysis using mark-recapture data. Fisheries Research, 83: 162-174.

Baird, T. A. and Olla, B. L. 1991. Social and reproductive behavior of a captive group of walleye pollock, *Theragra chalcogramma*. Environmental Biology of Fishes, 30:295-301.

Baranoff, T. I. 1918. On the question of the biological basis of fisheries. Institute for Scientific Ichthyological Investigations, Proceedings 1(1) :8l-128.

Bauleth-d'Almeida, G. Krakstad, J-O., and Kanandjembo, A. 2001. Comparison of horse mackerel length frequencies obtained from research vessels and commercial midwater trawlers: implications for biomass estimation. South African Journal of Marine Science, 23: 265–274.

Bethke, E., Gotze, E. and Planque, B. 2010. Estimation of the catchability of redfish and blue whiting for survey trawls in the Norwegian Sea. Journal of Applied Ichthyology 26 (Suppl. 1), 47–53.

Bouguet, J. Y. 2008. Camera calibration toolbox for Matlab [online]. [Available from http://vision.caltech.edu/bouguetj/calib_doc/index.html (accessed September 2008)].

Clark, W. G. 1999. Effects of an erroneous natural mortality rate on a simple age-structured stock assessment. Canadian Journal of Fisheries and Aquatic Science, 56: 1721–1731

De Robertis, A. and Handegard, N. O. 2012. Fish avoidance of research vessels and the efficacy of noise-reduced vessels: a review – ICES Journal of Marine Science In Press

De Robertis, A. and Wilson, C. D. 2006. Walleye pollock respond to trawling vessels. ICES Journal of Marine Science, 63:514-522.

De Robertis, A., and Wilson, C. D. 2010. Silent ships sometimes do encounter more fish: Part II: concurrent echosounder observations from a free-drifting buoy and vessels. ICES Journal of Marine Science, 67:996-1003.

De Robertis, A., Hjellvik, V., Williamson, N. J., and Wilson, C. D. 2008. Silent ships do not always encounter more fish: comparison of acoustic backscatter recorded by a noise-reduced and a conventional research vessel. ICES Journal of Marine Science, 65(4): 623-635.

Dorn, M., Aydin, K., Barbeaux., S., Guttormsen., M., Megrey., B., Spalinger., K., and Wilkins, M. 2009. Assessment of walleye pollock in the Gulf of Alaska . *In* Stock assessment and fisherty evaluation report of the groundfish resources of the Gulf of Alaska. pp. 39-146.

Dremiere, P. Y., Fiorentini, L., Cosimi, G., Leonori, I., Sala, A., and Spagnolo, A. 1999. Escapement from the main body of the bottom trawl used for the Mediterranean international trawl survey (MEDITS). Aquatic Living Resources, 12: 207-217.

Engas, A., and Ona, E. 1990. Day and night fish distribution pattern in the net mouth area of the Norwegian bottom-sampling trawl. Rapports et Procès-Verbaux des Réunions du Conseil International pour l'Exploration de la Mer, 189:123-127.

FAO. 2009. The state of world fisheries and aquaculture 2008, Part 1. World review of fisheries and aquaculture. FAO Fisheries and Aquaculture Department, Rome.

Fernö A. 1993. Advances in understanding of basic behaviour: consequences for fish capture studies. ICES Marine Science Symposia: Fish Behavior in Relation to Fishing Operations, 196: 5-11.

Fournier, D. 2001. An Introduction to AD MODEL BUILDER Version 9.0.0 For Use in Nonlinear Modeling and Statistics. Available from http://admb-project.org.

Francis, R. I. C. C., Hurst, R. J., and Renwick, J. A. 2003. Quantifying annual variation in catchability for commercial and research fishing. Fishery Bulletin, 101: 293–304.

Fryer, R. J. 1991. A model of between haul variation in selectivity. ICES Journal of Marine Science, 48: 281-290.

Fulton, T.W. 1904. The rate of growth of fishes. 22nd Annual Report of the Fishery Board of Scotland 1904, 3:141-241.

Gelman, A., and Rubin, D. B. 1992. Inference from iterative simulation using multiple sequences. Statistical Science, 7: 457-72.

Gelman, A., Carlin, J. B., Stern, H. S., and Rubin, D. B. 2003. Bayesian data analysis, second edition. Chapman and Hall/CRC. Boca Raton, FL. 698 pp.

Glass, C. W., and Wardle, C. S. 1989. Comparison of the reactions of fish to a trawl gear, at high and low light intensities. Fisheries Research, 7: 249-266.

Glass, C. W. and Wardle, C. S. 1995. Studies on the use of visual-stimuli to control fish escape from codends 2: the effect of a black tunnel on the reaction behavior of fish in otter trawl codends. Fisheries Research, 23: 165-174.

Glass, C. W., Wardle, C. S., and Gosden, S. J. 1993. A behavioural study of the principles underlying mesh penetration by fish. Wardle, C. S. and Hollingworth,

C. ICES Marine Science Symposia: Fish Behavior in Relation to Fishing Operations, 196: 92-97.

Godo, O. R. and Sunnana, K. 1992. Size selection during trawl sampling of cod and haddock and its effect on abundance indexes at age. Fisheries Research, 13: 293-310.

Godo, O. R., Karp, W. A., and Totland, A. 1998. Effects of trawl sampling variability on precision of acoustic abundance estimates of gadoids from the Barents sea and the Gulf of Alaska. ICES Journal of Marine Science, 55: 86-94

Graham, N., Jones, E. G., and Reid, D. G. 2004. Review of technological advances for the study of fish behaviour in relation to demersal fishing trawls. ICES Journal of Marine Science, 61: 1036-1043.

Guttormsen, M. A., McCarthy, A., and Jones, D. 2010. Results of the February-March 2009 echo integration-trawl surveys of walleye pollock (*Theragra chalcogramma*) conducted in the Gulf of Alaska, Cruises DY2009-01 and DY2009-04. AFSC Processed Rep. 2010-01, 67 p. Alaska Fish. Sci. Cent., NOAA, Natl. Mar. Fish. Serv., 7600 Sand Point Way NE, Seattle WA 98115

Handegard, N. O. and Williams, K. 2008. Automated tracking of fish in trawls using the DIDSON (Dual frequency IDentification SONar). ICES Journal of Marine Science, 65: 636–644.

Harley, S. J., and Myers, R. A. 2001. Hierarchical Bayesian models of length-specific catchability of research trawl surveys. Canadian Journal of Fisheries and Aquatic Science, 58:1569-1584.

He, P. 1991. Swimming endurance of cod, *Gadus morhua* L. at low temperatures. Fisheries Research, 12: 65-73.

Henderson, M. J., Horne, J. K., and Towler, R. H. 2008. The influence of beam position and swimming direction on fish target strength. ICES Journal of Marine Science, 65: 266-237.

Hilborn, R. and Walters, C. J. 1992. Quantitative fisheries stock assessment: Choice, dynamics and uncertainty. Chapman and Hall, New York. 570 p.

Hjellvik, V., Godø, O. R., and Tjøstheim, D. 2002. Diurnal variation in bottom trawl survey catches: does it pay to adjust? Canadian Journal of Fisheries and Aquatic Science, 59: 33–48.

Hjellvik, V., Michalsen, K., Aglen, A., and Nakken, O. 2003. An attempt at estimating the effective fishing height of the bottom trawl using acoustic survey recordings. ICES Journal of Marine Science, 60: 967–979.

Hollowed, A. B., Ianelli, J. and Livingston, P. 2000. Including predation mortality in stock assessments: a case study for Gulf of Alaska walleye pollock. ICES Journal of Marine Science, 57: 279–29.

Honkalehto, T., Jones, D., McCarthy, A., McKelvey, D., Guttormsen, M., Williams, K., and Williamson, N. 2009. Results of the echo integration-trawl survey of walleye pollock (*Theragra chalcogramma*) on the U.S. and Russian Bering Sea shelf in June and July 2008. U.S. Department of Commerce, NOAA Technical Memorandum NMFS-AFSC-194, 56 p.

Honkalehto, T., Williamson, N., Jones, D., McCarthy, A., and McKelvey, D. 2008. Results of the echo-integration-trawl survey of walleye pollock (*Theragra chalcogramma*) on the U.S. and Russian Bering Sea shelf in June and July 2007. U.S. Dep. Commer., NOAA Tech. Memo. NMFS-AFSC-190, 53 p.

Horne, J. K. 2003. The influence of ontogeny, physiology, and behaviour on the target strength of walleye pollock (*Theragra chalcogramma*). ICES Journal of Marine Science, 60: 1063–107.

Hurvich, C. M., and Tsai, C.-L. 1989. Regression and time series model selection in small samples. Biometrika, 76: 297–307.

Karp, W. A., and Walters G. E. 1994. Survey assessment of semi-pelagic gadoids: the example of walleye pollock, *Theragra chalcogramma*, in the eastern Bering Sea. Marine Fisheries Review, 56: 8-22.

Kim, Y. H. and Wardle, C. S. 2003. Optomotor response and erratic response: quantitative analysis of fish reaction to towed fishing gears. Fisheries Research, 60:455-470.

Kirkwood, G. P., and Walker, T. I. 1986. Gill net selectivities for gummy shark, *Mustelus antarticus* (Gunter), taken in southeastern Australian waters. Australian Journal of Marine and Freshwater Research, 37: 689-697.

Kotwicki, S., De Robertis, A., Ianelli, J., Punt, A. E., and Horne, J. K. In press. Combining bottom trawl and acoustic data to model acoustic dead zone correction and bottom trawl efficiency parameters for semi-pelagic species. Canadian Journal of Fisheries and Aquatic Sciences.

Kotwicki, S., De Robertis, A., von Szalay, P., and Towler, R. 2009. The effect of light intensity on the availability of walleye pollock (*Theragra chalcogramma*) to bottom trawl and acoustic surveys. Canadian Journal of Fisheries and Aquatic Sciences, 66: 983–994.

Kutner, M., Nachtsheim, C., Neter, J., and Li, W. 2004. Applied Linear Statistical Models, McGraw-Hill/Irwin, Homewood, IL, p.701

Lapointe, D., Guderley, H., and Dutil, J. D. 2006. Changes in the condition factor have an impact on metabolic rate and swimming performance relationships in Atlantic cod (*Gadus morhua* L.) Physiological and Biochemical Zoology, 79(1): 109-119.

Lauth, R. R., Ianelli, J., and Wakefield, W. W. 2004. Estimating the size selectivity and catching efficiency of a survey bottom trawl for thornyheads, *Sebastolobus* spp. using a towed video camera sled. Fisheries Research 70: 27–37

Loland, A., Aldrin, M., Ona, E., Hjellvik, V., and Holst, J. C. 2007. Estimating and decomposing total uncertainty for survey-based abundance estimates of Norwegian spring-spawning herring. ICES Journal of Marine Science, 64: 1302–1312.

Mackinson, S. van der Kooij, J., and Neville, S. 2005. The fuzzy relation between acoustic and trawl surveys in the North Sea. ICES Journal of Marine Science, 62: 1556-1575.

Maclennan, D. N. 1992. Fishing gear selectivity - an overview. Fisheries Research, 13: 201-204.

MacLennan, D. N., Fernandes, P. G. and Dalen, J. 2002. A consistent approach to definitions and symbols in fisheries acoustics. ICES Journal of Marine Science, 59:365-369.

Matsushita, Y., Inoue, Y., Shevchenko, A. I., and Norinov, Y. G. 1993. Selectivity in the codend and in the main body of the trawl. ICES Marine Science Symposia: Fish Behavior in Relation to Fishing Operations, 196: 170-177.

McKelvey, D. R. 1996. Juvenile walleye pollock, *Theragra chalcogramma*, distribution and abundance in Shelikof Strait—what can we learn from acoustic surveys. Ecology of Juvenile Walleye Pollock, *Theragra chalcogramma*. NOAA Technical Report NMFS 126, p 25-34.

Mesnil, B., Cotter, J. Fryer, R. J., Needle, C. L., and Trenkel, V. M. 2009. A review of fishery-independent assessment models, and initial evaluation based on simulated data. Aquatic Living Resources, 22, 207–216.

Michalsen, K., Godo, O. R., and Ferno, A. 1996. Diel variation in the catchability of gadoids and its influence on the reliability of abundance indices. ICES Journal of Marine Science, 53(2):389-395.

Millar, R. B. 1992. Estimating the size-selectivity of fishing gear by conditioning on the total catch. Journal of the American Statistical Association, 87: 962-968.

Millar, R. B. 1993. Analysis of trawl selectivity studies (addendum): implementation in SAS. Fisheries Research, 17: 373-377.

Millar, R. B. 1994. Sampling from trawl gears used in size-selectivity experiments. ICES Journal of Marine Science, 51: 293-298.

Millar, R. B., Broadhurst, M. K., and Macbeth, W. G. 2004. Modeling between-haul variability in the size selectivity of trawls. Fisheries Research, 67:171-181.

Nakashima, B. S. 1990. Escapement from a diamond-IX midwater trawl during acoustic surveys for capelin (*Mallotus villosus*) in the Northwest Atlantic. ICES Journal of Marine Science, 47: 76-82.

O'Driscoll, R. L. 2004. Estimating uncertainty associated with acoustic surveys of spawning hoki (*Macruronus novaezelandiae*) in Cook Strait, New Zealand. ICES Journal of Marine Science, 61: 84-97.

Olla, B. L., Davis, M. W., and Rose, C. 2000. Differences in orientation and swimming of walleye pollock *Theragra chalcogramma* in a trawl net under light and dark conditions: concordance between field and laboratory observations. Fisheries Research, 44: 261-266.

Olla, B. L., Davis, M. W., and Schreck, C. B. 1997. Effects of simulated trawling on sablefish and walleye pollock: the role of light intensity, net velocity and towing duration. Journal of Fish Biology, 50: 1181-1194.

Ona, E. 1990. Physiological factors causing natural variations in acoustic target strength of fish. Journal of the Marine Biological Association of the United Kingdom, 70:107-127.

Özbilgin, H., Ferro, R. S. T., Robertson, J. H. B., Holtrop, G., and Kynoch, R. J. 2006. Seasonal variation in trawl codend selection of northern North Sea haddock. ICES Journal of Marine Science, 63:737-748.

Ozbilgin, H., Tosunoglu, Z., Tokac, A., and Metin, G. 2007. Seasonal variation in the trawl codend selectivity of picarel (*Spicare smaris*). ICES Journal of Marine Science, 64: 569-1572.

Polet, H. 2000. Codend and Whole Trawl selectivity of a shrimp beam trawl used in the North Sea. Fisheries Research, 48: 167-183.

Popper, A. N. 2003. Effects of anthropogenic sounds on fish. Fisheries, 28: 24-31

R Development Core Team. 2010. R: A language and environment for statistical computing. R Foundation for Statistical Computing, Vienna, Austria. ISBN 3-900051-07-0, URL http://www.R-project.org.

Rose, G., Gauthier, S., and Lawson, G. 2000. Acoustic surveys in the full monte: simulating uncertainty. Aquatic Living Resources, 13:367−372.

Ryer, C. H. and Olla, B. L. 1999. Light-induced changes in the prey consumption and behavior of two juvenile planktivorous fish. Marine Ecology Progress Series, 181, 41-51.

Ryer, C. H., and Olla, B. L. 2000. Avoidance of an approaching net by juvenile walleye pollock *Theragra chalcogramma* in the laboratory: the influence of light intensity. Fisheries Research, 45:195-199.

Ryer, C.H. 2008. A review of flatfish behavior relative to trawls. Fisheries Research, 90:138-146.

Simmonds, J., MacLennan, D., 2005. Fisheries acoustics: theory and practice. Blackwell Publishers, Oxford. 437 p.

Slotte, A., Skagen, D., and Iversen, S. A. 2007. Size of mackerel in research vessel trawls and commercial purse-seine catches: implications for acoustic estimation of biomass. ICES Journal of Marine Science, 64: 989-994.

Somerton, D. A., Williams, K., von Szalay, P. G., and Rose, C. S. 2011. Using acoustics to estimate the fish-length selectivity of trawl mesh. ICES Journal of Marine Science, 68: 1558–1565.

Somerton, D., Ianelli, J., Walsh, S., Smith, S., Godø, O. R., and Ramm, D. 1999. Incorporating experimentally derived estimates of survey trawl efficiency into the stock assessment process: a discussion. ICES Journal of Marine Science, 56: 200-302.

Somerton, D.A. 2004. Do Pacific Cod (*Gadus Macrocephalus*) and Walleye Pollock (*Theregra Chalcogramma*) lack a herding response to the doors, bridles, and mudclouds of survey trawls? ICES Journal of Marine Science, 61: 1186-1189.

Spiegelhalter, D. J., Best, N. G., Carlin, B. R., and Van der Linde, A. 2002. Bayesian measures of model complexity and fit. Journal of the Royal Statistical Society: Series B, 64: 583-616.

Stoner, A. W., Ryer, C. H., Parker, S. J., Auster, P. J., and Wakefield, W. W. 2008. Evaluating the role of fish behavior in surveys conducted with underwater vehicles. Canadian Journal of Fisheries and Aquatic Science, 65:1230-1243.

Suuronen, P., Lehtonen, E., and Wallace, J. 1997. Avoidance and escape behaviour by herring encountering midwater trawls. Fisheries Research, 29:13-24.

Thompson, G. G. (1994). Confounding of gear selectivity and the natural mortality-rate in cases where the former is a non-monotone function of age. Canadian Journal of Fisheries and Aquatic Science, 51: 2654-2664.

Traynor, J. J. 1996. Target-strength measurements of walleye pollock (*Theragra chalcogramma*) and Pacific whiting (*Merluccius productus*). . ICES Journal of Marine Science, 53:253-258.

Valdemarsen, J. W., and Suuronen, P. 2001. Modifying fishing gear to achieve ecosystem objectives. Reykjavik Conference on Responsible Fisheries in the Marine Ecosystem 3 Reykjavik, Iceland, 1-4 October 2001

Valdemarsen, J. W. 2001. Technological trends in capture fisheries. Ocean & Coastal Management 44, 635-651.

Walsh, S. J. 1996. Efficiency of bottom sampling trawls in deriving survey abundance indices. NAFO Scientific Counsel Studies 1996, 28:9-24.

Walters, C.J. and Martell, S. 2004. Fisheries Ecology and Management. Princeton, New Jersey, Princeton University Press.

Wardle, C. S., 1993. Fish behavior and fishing gear. *In*: Pitcher, T.J. (Ed). Behaviour of teleost fishes. Chapmann & Hall, London. pp. 609-645.

Wileman, D. A., Ferro, R. S. T., Fonteyne, R., and Millar, R. B. 1996. Manual of methods of measuring the selectivity of towed fishing gears. ICES Cooperative Research Report No. 215. Copenhagen. 126 pp.

Williams, K., Punt, A. E., Wilson, C. D., and Horne, J. K. 2011. Length-selective retention of walleye Pollock, *Theragra chalcogramma*, by midwater trawls. ICES Journal of Marine Science, 68:119-129.

Xu G., and Zhang, Z. 1996. Epipolar geometry in stereo, motion, and object recognition: a unified approach. Kluwer Academic Publs., Norwell, MA, 336 p.

Zhang, X. M., and Arimoto, T. 1993.Visual physiology of walleye pollock (*Theragra chalcogramma*) in relation to capture by trawl nets. ICES Marine Science Symposia: Fish Behavior in Relation to Fishing Operations, 196: 113-116.

APPENDIX

A2.1: *Deriving the integral for* μ

The Poisson likelihood of observing a fish of a given length class in each pocket net (m = 1-12) and in the codend sample (m = 13) is

$$L\ (x \mid \mu, F) = \prod_m \frac{(\mu F_m)^{x_m} e^{-\mu F_m}}{x_m!}$$

where x are the observed data, F is the probability of retention by pocket nets and codend and μ is the number of fish at a given length entering the net. This equation can be simplified to yield:

$$L(x \mid \mu, F) = \left(\prod_m \left[\frac{F_m^{x_m}}{x_m!} \right] \right) \mu^{\sum_m x_m} e^{-\mu \sum_m F_m}$$

The next step is to integrate this equation with respect to μ:

$$\widehat{L}(x \mid F) = \int_0^\infty \left(\prod_m \left[\frac{F_m^{x_m}}{x_m!} \right] \right) \mu^{\sum_m x_m} e^{-\mu \sum_m F_m} \, d\mu$$

which yields

$$\widehat{L}(x \mid F) = \left(\prod_m \left[\frac{F_m^{x_m}}{x_m!} \right] \right) \frac{\Gamma\left(\sum_m x_m + 1 \right)}{\left(\sum_m F_m \right)^{\left(\sum_m x_m + 1 \right)}}$$

where Γ is the gamma function and $\hat{L}$ is the integral of the likelihood function. The negative logarithm of $\hat{L}$ which is used in the analysis is proportional to

$$-\log \hat{L}(x \mid \theta) \propto -\sum_m \left(x_m \log[F_m]\right) + \log\left[\sum_m F_m\right]\left[\sum_m x_m + 1\right]$$

after removal of additive constant terms dependent only on the data. This equation summed over all length classes results in Equation 7.

A2.2: *Deviance information criterion (DIC)*

The *DIC* is defined as:

$$DIC = p_D + \overline{D}$$

where p_D is the effective number of parameters and $\overline{D}$ is the mean of the deviance, defined as:

$$D = -2\log(l)$$

with l is the likelihood function (Eq. 9). The effective number of parameters is computed as:

$$p_D = \overline{D} - D(\overline{\theta})$$

where $D(\overline{\theta})$ is the deviance evaluated at the means of the posterior MCMC samples of the model parameters.

A2.3: *Computation of residuals*

The residuals for a given haul were computed as the distance between the model predictions of the pocket net and codend catches, and the observed values where the expected catch in a pocket net, y, is

$$y_{i,j,k} = H_{i,j,k}\mu$$

for a fish of length i in the pocket net located in section j, panel k. The expected codend sample w is

$$w_i = h_i\mu$$

To calculate these quantities, the maximum likelihood estimate for μ was computed as

$$\mu_i = \frac{\sum_j \sum_k x_{i,j,k} + c_i}{\sum_j \sum_k H_{i,j,k} + h}$$

where x and c were the observed catches in the pocket net and codend respectively (Kirkwood and Walker, 1996). H and h were calculated from samples of the posterior distributions of the parameters (L_{50}, SR, π, ρ). This process was repeated for all hauls in a set.

A5.1: *Computation of walleye pollock abundance using acoustic backscatter and trawl catch data*

Acoustic backscatter measured by the ship's echosounders is scrutinized by analysts to identify pollock backscatter, excluding other sources of backscatter such as the sea floor and other organisms in the water column such as macrozooplankton. Pollock backscatter is then integrated vertically over the water column and horizontally over elemental sampling distance units or ESDU's of 0.5 nmi. Integrated backscatter is recorded in units of s_A, or the Nautical area scattering coefficient (MacLennan et al., 2002). Trawl samples are taken opportunistically along the trackline in areas of high backscatter to verify species composition and to obtain length frequency samples. Hauls from adjoining locations with similar length frequency distributions are considered a contiguous pollock aggregation, and are combined into a length stratum as

$$d_l = \frac{\sum_h p_{l,h}}{n}$$

where d_l is the proportion of fish at length l in the stratum, $p_{l,h}$ is the proportion of fish at length l in haul h, and n is the number of hauls in the length strata. ESDU's are assigned to a length stratum based on proximity and characteristics of pollock aggregation.

Pollock backscatter is converted into abundance-at-length (N) for each stratum is computed as

$$N_{l,a} = \frac{\bar{s}_A A}{4\pi\bar{\sigma}_{bs}} p_{l,a}$$

where $\bar{s}_A$ is the mean pollock backscatter in the stratum computed by averaging ESDU's, A is the stratum area computed as the product of trackline length and inter-transect spacing, $\bar{\sigma}_{bs}$ is the length-frequency weighed mean backscattering cross-section of pollock and p_l is the proportion of pollock that are in length class *l* in the length strata *a*. $\bar{\sigma}_{bs}$ is computed by as

$$\bar{\sigma}_{bs} = \sum_{l} \sigma_{bs,l}\, p_l$$

and

$$\sigma_{bs,l} = 10^{TS_l/10}$$

Where *TS* represents the pollock acoustic target strength in dB units relative to 1 μPa at 1 m. Pollock *TS* values were estimated from *in situ* measurements of individual pollock acoustic returns using a method described by Traynor (1996), yielding a *TS* – length relationship of

$$TS_l = 20log_{10}l - 66$$

Total number of pollock in the survey area was computed by summing abundance across length strata. Abundance-at-length was then converted to biomass-at-length by multiplying by the mean weight-at-length computed from individual fish samples taken during the survey.